AD_____

Award Number: W81XWH-07-1-0024

TITLE: Fatty acid synthase inhibitors engage the cell death program through the endoplasmic reticulum

PRINCIPAL INVESTIGATOR: Steven J. Kridel, Ph.D.

CONTRACTING ORGANIZATION: Wake Forest University Health Sciences
Winston-Salem, NC 27157

REPORT DATE: December 2008

TYPE OF REPORT: Annual

PREPARED FOR: U.S. Army Medical Research and Materiel Command
Fort Detrick, Maryland 21702-5012

REPORT DOCUMENTATION PAGE

Form Approved
OMB No. 0704-0188

1. REPORT DATE *(DD-MM-YYYY)*	2. REPORT TYPE	3. DATES COVERED *(From - To)*
31-12-2008	Annual	01 DEC 2007 - 30 NOV 2008

4. TITLE AND SUBTITLE
Fatty acid synthase inhibitors engage the cell death program through the endoplasmic reticulum

5a. CONTRACT NUMBER
W81XWH-07-1-0024

5b. GRANT NUMBER

5c. PROGRAM ELEMENT NUMBER

6. AUTHOR(S)
Steven J. Kridel, Ph.D.

5d. PROJECT NUMBER

5e. TASK NUMBER

5f. WORK UNIT NUMBER

7. PERFORMING ORGANIZATION NAME(S) AND ADDRESS(ES)

Wake Forest University Health Sciences
Medical Center Boulevard
Winston-Salem, NC 27157

8. PERFORMING ORGANIZATION REPORT NUMBER

9. SPONSORING / MONITORING AGENCY NAME(S) AND ADDRESS(ES)
U.S. Army Medical Research
And Materiel Command
Fort Detrick, MD 21702-5012

10. SPONSOR/MONITOR'S ACRONYM(S)

11. SPONSOR/MONITOR'S REPORT NUMBER(S)

12. DISTRIBUTION / AVAILABILITY STATEMENT
Approved for public release; distribution unlimited

13. SUPPLEMENTARY NOTES

14. ABSTRACT
Fatty acid synthase (FAS), the enzyme that synthesizes the 16-carbon fatty acid palmitate, in highly expressed in prostate cancer. Because of a corresponding lack of expression in normal prostate, FAS is an attractive drug target. We have described the endoplasmic stress (ER) response as a critical mediator of the anti-tumor effects of FAS inhibitors. In this report we demonstrate the mechanism that drives the synergy between FASN inhibitors and the FDA-approved proteasome inhibitor bortezomib. Specifically we demonstrate synergy between the inhibitors and illustrate that JNK activation and CHOP expression are required to mediate ER stress-mediated death in prostate tumor cells treated with FASN inhibitors and proteasome inhibitors. We also describe the strategy to target FASN expression using a targeted knockout model in mouse prostate. This platform will be important to elucidate the role of FASN in prostate cancer. These studies will be valuable as FAS inhibitors move toward a clinical setting as a targeted therapeutic in prostate cancer.

15. SUBJECT TERMS
fatty acid synthase, orlistat, endoplasmic reticulum stress, unfolded protein response

16. SECURITY CLASSIFICATION OF:			17. LIMITATION OF ABSTRACT	18. NUMBER OF PAGES	19a. NAME OF RESPONSIBLE PERSON
a. REPORT	b. ABSTRACT	c. THIS PAGE			USAMRMC
U	U	U	UU	58	19b. TELEPHONE NUMBER *(include area code)*

Table of Contents

Introduction

The basic premise of this Idea Award is to determine the mechanism by which FAS inhibitors induce endoplasmic reticulum (ER) stress-dependent cell death in prostate cancer. It is based on our initial findings that FAS inhibitors induce ER stress in tumor cell lines (1). Although FAS-derived fatty acids are primarily used to drive phospholipid synthesis in tumor cells and phospholipid synthesis occurs in the ER, these findings were the first to connect ER function to fatty acid synthase in any capacity. The goal of this proposal was two-fold. One was to determine the mechanism by which the ER might initiate death following FAS inhibition. The second was to determine whether FAS inhibitors can reduce prostate tumor growth in a spontaneous model of prostate cancer and whether ER stress is observed in the treated prostates. A discussion on the progress of these aims is reported in the body below. During the course of the second year funding period we published four papers, three of them directly related to the proposal and the fourth being tangentially related. In addition, the work supported by this award was two presented at a national meetings and at a publically owned pharmaceutical company, each of which are listed in the Reportable Outcomes section to follow.

Body

Specific aim 1. To determine how ER stress initiates cell death when FAS activity is inhibited.

As reported for the previous funding cycle, we identified a novel crosstalk between fatty acid synthase (FASN) and the proteasome. We demonstrated that inhibition of FASN results in accumulation of ubiquitin modified protein and that inhibition of FASN results in increased FASN activity (manuscript #4 in Reportable Outcomes (2)). We hypothesized that the identified crosstalk between FASN and the proteasome would provide a novel strategy to target UPR activation and increase cell death in prostate tumor cells. To test this hypothesis PC-3 and DU145 cells were examined for clonogenic survival after treatment with orlistat or C75 and the proteasome inhibitor bortezomib (Velcade, PS-341). Clonogenic survival of PC-3 and DU-145 cells was reduced by bortezomib treatment in a dose-dependent manner (Figure 1A and B). Sub-optimal concentrations of FASN inhibitors were used to reduce cell killing by any of the single agents (data not shown). Clonogenic survival of PC-3 cells treated with orlistat and C75 was reduced by 60% and 30%, respectively ($P < 0.001$, Figure 1A). In DU145 cells, survival was only reduced by about 20% with each inhibitor. When the FASN inhibitors were combined with bortezomib, clonogenic survival was strikingly diminished compared to cells treated with the single agents ($P \leq 0.005$, Figure 1A and 1B). Although isobologram analyses were inconclusive, an analysis of the combination–index suggests that combining FASN inhibitors with bortezomib results in synergism (3).

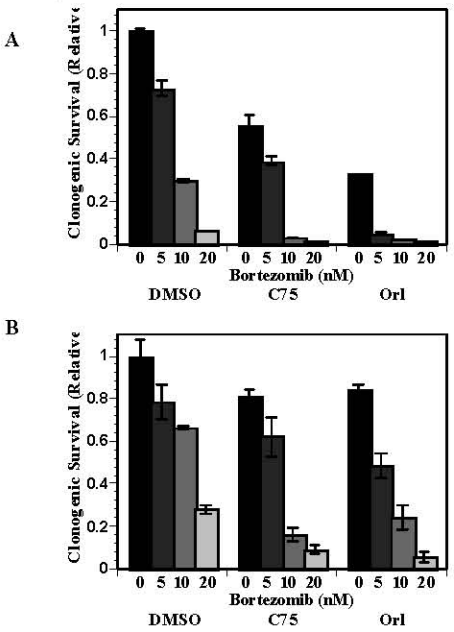

Figure 1. FASN inhibition synergize with bortezomib. PC-3 cells (A) and DU145 cells (B) were treated with 10 μg/ml C75 or 25 μM orlistat and the indicated concentrations of bortezomib for 16 hours. The media was changed and colonies were developed in fresh media. Clonogenic survival was assessed 10-14 days following treatment.

We previously reported that the IRE1 arm of the unfolded protein response (UPR) arm was activated when the FASN-proteasome pathway was disrupted. Specifically JNK activation and CHOP expression were associated with the blocked crosstalk. To test the role of JNK and CHOP two strategies were employed.). A JNK inhibitor was used to verify the role of JNK in mediating CHOP expression. Pharmacological inhibition of JNK blocked the phosphorylation of JNK and c-Jun (Figure 2A). More importantly, inhibition of JNK also reduced CHOP expression and cleavage of caspase-3 and PARP (Figure 2A). Consistent with these findings, trypan-blue exclusion assays also demonstrated that JNK inhibition protected cells from cell death induced by the combination of orlistat and bortezomib ($P < 0.01$, Figure 2B).

We next tested whether CHOP is an effector of JNK signaling that regulates cell death in this scenario. PC-3 cells were transfected with control or *CHOP*-targeted siRNA, and after 48 hours the cells were treated with vehicle, orlistat or with the orlistat-bortezomib combination. The siRNA-mediated knockdown of *CHOP*

had no effect on orlistat or bortezomib induced cell death (not shown). However, siRNA-mediated knockdown of *CHOP* expression protected cells from the effects of the orlistat-bortezomib combination ($P < 0.01$, Figure 2C) at a level that was proportional with the reduction in CHOP levels (Figure 2D). Therefore, it appears that the JNK-CHOP axis is an important mediator of cell death in cells where the UPR is saturated. Collectively, these data demonstrate that blocking crosstalk between FASN and the proteasome shifts UPR balance from adaptation phase to the alarm phase, resulting in increased cell death via JNK-mediated CHOP expression. These data demonstrate a clear role for the UPR in cells treated with FASN inhibitors and suggest a therapeutic strategy to increase apoptosis in prostate cancer by combining tow ER stressing agents.

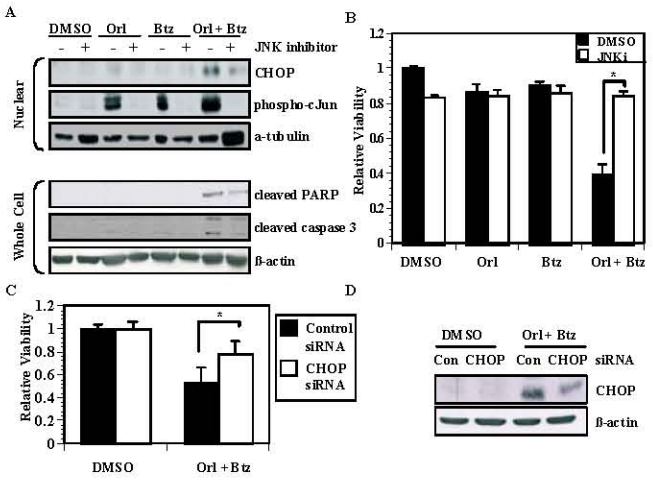

Figure 2. FASN and proteasome inhibitors combine to induce JNK and CHOP dependent cell death. A, CHOP, cleaved-PARP, cleaved caspase-3 and pJNK were evaluated in PC-3 cells treated with orlistat, bortezomib or the combination. B, Cell survival was determined in PC-3 cells treated with orlistat, bortezomib or the combination. C, The survival of PC3 cells was determined following knockdown of CHOP and subsequent treatment with orlistat and bortezomib. D, CHOP expression and knockdown in PC-3 cells treated with orlistat and bortezomib.

Specific Aim 2 Specific Aim 2. <u>To determine the effect of FAS inhibition in a spontaneous model of prostate cancer.</u>

The goal of this aim was to determine whether FASN inhibitors could inhibit the growth of prostate cancer is a genetic mouse model of prostate cancer. The model chosen was the prostate-specific deletion of PTEN using a probasin-driven *Cre* to accomplish loss of PTEN in the prostate. The advantages of this model are: (a) PTEN is the most mutated gene is PCa, so it is clinically relevant, (b) the model mimics the development and progression of human PCa (4), (c) the model is spontaneous and orthotopic and (d) FAS expression is regulated via the PTEN-regulated PI3k-Akt axis(5-7). Accordingly, tumors from $Pten^{-/-}$ mice have significantly elevated FAS expression relative to prostates from wild type mice (not shown). In the previous cycle we initiated these studies. We have also established a more comprehensive approach to study the role of FASN in prostate cancer. We have developed a floxed FASN mouse such that FASN can be knocked out specifically in the prostate. The *FASN* targeting strategy is outline in Figure 3. Briefly, the targeting construct places a Neo cassette following exon 3 and the second flow site after exon 8. We currently have $FASN^{fl/fl}$ mice breeding and are beginning two stratgies. In the first, mice will be crossed with mice expressing a probasin -driven *Cre* to test the role of FASN in prostate development and maintenance. In the second strategy, $FASN^{fl/fl}$ will be crossed into the with $Pten^{-/-}$ mice. The resulting $FASN^{fl/fl}$ $Pten^{-/-}$ mice will be crossed with mice expressing a probasin -driven *Cre* to develop $FASN^{-/-}$ $Pten^{-/-}$. These mice will be compared to $FAS^{+/+}$ $Pten^{-/-}$ to understand the role of FASN in prostate cancer. This strategy will clearly demonstrate whether FASN is a viable target in prostate cancer and provide a platform to better understand the biology of FASN in the prostate and prostate cancer. This model will be the first to accomplish knock out of FASN in a tumor model and will be invaluable to subsequent studies.

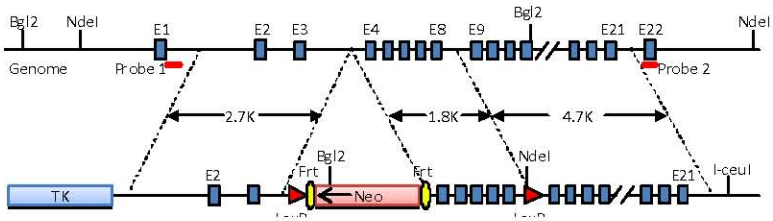

Figure 3. Targeting strategy to develop $FASN^{fl/fl}$ mice.

Key Research Accomplishments:

- Demonstration that 1-^{11}C-acetate can be used as a PET imaging agents for FASN expression in prostate cancer
- FASN inhibitors synergize with bortezomib to kill prostate cancer cell lines

- Combining FASN inhibitors with bortezomib kill cells in a JNK and CHOP-dependent manner
- Generation of *FASN*$^{fl/fl}$ mice for breeding into prostate cancer model.

Reportable Outcomes:
The 2008 funding period was characterized by multiple reportable outcomes. Four manuscripts were published, including an invited book chapter and three original research articles. In addition, the funded work was presented in talks at two venues; the 2008 American Society for Biochemistry and Molecular Biology Annual Meeting and at Infinity Pharmaceuticals. Perhaps most important, the funded work was vital in obtaining two other extramural awards, including a Laboratory-Clinic Transition Award from the Prostate Cancer Research Program. The accomplishments are summarized below.

Manuscripts:
1. Vāvere AL, **Kridel SJ**, Wheeler FB, Lewis JS. 1-^{11}C-Acetate as a PET Radiopharmaceutical for Imaging Fatty Acid Synthase Expression in Prostate Cancer. (2008) *Journal of Nuclear Medicine*, 49:327-334.
2. Little J.L. and **Kridel, S.J.** Fatty Acid Synthase Activity in Tumor Cells. (2008) In *Subcellular Biochemistry: Lipids in Health and Disease,* (PJ Quinn, X Wang, eds.), Springer, 49:169-194.
3. Fels, D.R., Ye, J. Segan, A.T., **Kridel, S.J.**, Spiotto, M., Olson, M., Koong, A.C., and Koumenis, C. Preferential cytotoxicity of bortezomib towards hypoxic cells via over activation of ER stress pathways (2008) *Cancer Research*, 68(22):9323-30.
4. Little, J.L., Wheeler, F.B., Koumenis, C., and **Kridel. S.J.** Disruption of crosstalk between the fatty acid synthesis and proteasome pathways enhances unfolded protein response signaling and cell death. (2008) *Molecular Cancer Therapeutics*, 7(12):3816-3824

Presentations:
1. American Society for Biochemistry and Molecular Biology Annual Meeting, San Diego, CA. April 5-9, 2008, Lipid Signaling and Metabolism, Title: Inhibition of fatty acid synthase activates the unfolded protein response in tumor cells
2. Infinity Pharmaceuticals, August 2008. Title: Regulation of tumor cell function and form by the fatty acid synthesis pathway

Funding received based on this award:

North Carolina Biotechnology Center 7/01/08-6/30/09
Kridel (co-I, 0.6 months) $82,500
Fatty acid synthase inhibitors for cancer therapy

Department of Defense (PCRP) July 2008 03/01/09-12/31/12
Kridel (PI, 2.4 months) $750,000
Inhibitors of Fatty Acid Synthase for Prostate Cancer

Conclusion
The second year of this Idea award resulted in significant progress. We accomplished the goal of Aim to by demonstrating the critical role of ER stress and the unfolded protein response in mediating the response of prostate tumor cells lines to FASN inhibitors. We also provide a blueprint for the rational design of more effective therapeutic options by teaming to ER stressing agents. Such strategies more effectively activate death pathways while suppressing protective pathways. The development of a genetic model of FASN inhibition, a knockout model, is important accomplishment and will provide invaluable data in the near future.

So what does this body of knowledge contribute? This work, as mentioned above, suggest possible strategies for prostate cancer therapy with targeted therapies. Specifically with therapies that activate the UPR. The work

was also the basis for other funding that will be critical for the development and translation of FASN inhibitors into the clinic. This will be important for the development of a new targeted therapy against FASN.

References

1. Little, J. L., Wheeler, F. B., Fels, D. R., Koumenis, C., and Kridel, S. J. Inhibition of Fatty Acid Synthase Induces Endoplasmic Reticulum Stress in Tumor Cells. Cancer Res, *67:* 1262-1269, 2007.
2. Little, J. L., Wheeler, F. B., Koumenis, C., and Kridel, S. J. Disruption of crosstalk between the fatty acid synthesis and proteasome pathways enhances unfolded protein response signaling and cell death. Mol Cancer Ther, *7:* 3816-3824, 2008.
3. Chou, T.-C. and Talalay, P. Quantitative analysis of dose-effect relationships: the combined effects of multiple drugs or enzyme inhibitors. Advances in Enzyme Regulation, *22:* 27-55, 1984.
4. Wang, S., Gao, J., Lei, Q., Rozengurt, N., Pritchard, C., Jiao, J., Thomas, G. V., Li, G., Roy-Burman, P., Nelson, P. S., Liu, X., and Wu, H. Prostate-specific deletion of the murine Pten tumor suppressor gene leads to metastatic prostate cancer. Cancer Cell, *4:* 209-221, 2003.
5. Bandyopadhyay, S., Pai, S. K., Watabe, M., Gross, S. C., Hirota, S., Hosobe, S., Tsukada, T., Miura, K., Saito, K., Markwell, S. J., Wang, Y., Huggenvik, J., Pauza, M. E., Iiizumi, M., and Watabe, K. FAS expression inversely correlates with PTEN level in prostate cancer and a PI 3-kinase inhibitor synergizes with FAS siRNA to induce apoptosis. Oncogene, *24:* 5389-5395, 2005.
6. Wang, H. Q., Altomare, D. A., Skele, K. L., Poulikakos, P. I., Kuhajda, F. P., Di Cristofano, A., and Testa, J. R. Positive feedback regulation between AKT activation and fatty acid synthase expression in ovarian carcinoma cells. Oncogene, *24:* 3574-3582, 2005.
7. Van de Sande, T., De Schrijver, E., Heyns, W., Verhoeven, G., and Swinnen, J. V. Role of the phosphatidylinositol 3'-kinase/PTEN/Akt kinase pathway in the overexpression of fatty acid synthase in LNCaP prostate cancer cells. Cancer Res, *62:* 642-646, 2002.

1-^{11}C-Acetate as a PET Radiopharmaceutical for Imaging Fatty Acid Synthase Expression in Prostate Cancer

Amy L. Vāvere[1], Steven J. Kridel[2], Frances B. Wheeler[2], and Jason S. Lewis[1,3]

[1]*Division of Radiological Sciences, Washington University School of Medicine, St. Louis, Missouri;* [2]*Department of Cancer Biology, Comprehensive Cancer Center, Wake Forest University School of Medicine Winston-Salem, North Carolina; and* [3]*Alvin J. Siteman Cancer Center, Washington University School of Medicine, St. Louis, Missouri*

Although it is accepted that the metabolic fate of 1-^{11}C-acetate is different in tumors than in myocardial tissue because of different clearance patterns, the exact pathway has not been fully elucidated. For decades, fatty acid synthesis has been quantified in vitro by the incubation of cells with ^{14}C-acetate. Fatty acid synthase (FAS) has been found to be overexpressed in prostate carcinomas, as well as other cancers, and it is possible that imaging with 1-^{11}C-acetate could be a marker for its expression. **Methods:** In vitro and in vivo uptake experiments in prostate tumor models with 1-^{11}C-acetate were performed both with and without blocking of fatty acid synthesis with either C75, an inhibitor of FAS, or 5-(tetradecyloxy)-2-furoic acid (TOFA), an inhibitor of acetyl-CoA carboxylase (ACC). FAS levels were measured by Western blot and immunohistochemical techniques for comparison. **Results:** In vitro studies in 3 different prostate tumor models (PC-3, LNCaP, and 22Rv1) demonstrated blocking of 1-^{11}C-acetate accumulation after treatment with both C75 and TOFA. This was further shown in vivo in PC-3 and LNCaP tumor-bearing mice after a single treatment with C75. A positive correlation between 1-^{11}C-acetate uptake into the solid tumors and FAS expression levels was found. **Conclusion:** Extensive involvement of the fatty acid synthesis pathway in 1-^{11}C-acetate uptake in prostate tumors was confirmed, leading to a possible marker for FAS expression in vivo by noninvasive PET.

Key Words: 1-^{11}C-acetate; fatty acid synthase; C75; TOFA

J Nucl Med 2008; 49:327–334
DOI: 10.2967/jnumed.107.046672

The National Cancer Institute estimates that roughly 219,000 new cases of prostate cancer and about 27,000 deaths from this disease will occur in 2007 (*1*). In the early 1990s, early and widespread detection of prostate cancers was made possible by promotion of prostate-specific antigen (PSA) screening in conjunction with digital rectal examination. Elevated PSA levels are quite high in a patient with prostate cancer but, unfortunately, are also caused by benign prostatic hyperplasia and even inflammation or urinary retention (*2*). Transrectal ultrasound is frequently used to assist surgeons in biopsy and for local staging, CT and MRI are commonly used to determine the extent of disease, although structural changes are not always apparent with these modalities (*3*).

^{18}F-FDG PET has become essential in the diagnosis of many malignancies, but it is not ideal in the detection of prostate cancer. Prostate cancer is one of a handful of tumors with low metabolism. and ^{18}F-FDG, being a marker of glucose metabolism, is not highly effective in delineating it from surrounding tissue (*4*). Although ^{18}F-FDG has been shown to be effective in the assessment of high-grade primary tumors and metastatic disease (*5–9*), other obstacles still leave much to be desired for its use with prostate malignancies, especially at early stages. The bladder clearance of ^{18}F-FDG also poses an obstacle as it is in the same anatomic region as the prostate, and, therefore, the primary tumor. Studies have also shown an inability to differentiate benign hyperplasia in the prostate from malignant disease or postoperative scarring from radical prostatectomy (*10,11*).

Because of the problems associated with ^{18}F-FDG imaging in prostate, alternative modalities must be used to image prostate cancer. Clinically, 1-^{11}C-acetate has been shown to be an effective tracer for the delineation of prostate cancer and its metastases with PET in humans (*12–16*). Although it is accepted that the metabolic fate of 1-^{11}C-acetate in tumors differs from that in normal tissue, the exact pathway has not been fully elucidated. Interestingly, fatty acid synthesis has been quantified in vitro by the incubation of cells with ^{14}C-acetate.

Fatty acid synthase (FAS) is a multifunctional enzymatic protein that catalyzes fatty acid biosynthesis (*17*). FAS is overexpressed in prostate carcinomas as well as other cancers (*18–22*). On the other hand, FAS levels are low or absent in most normal tissues. FAS levels are associated with tumor aggressiveness in late-stage prostatic adenocarcinomas as well as a prognostic indicator for overall survival

Received Aug. 23, 2007; revision accepted Oct. 31, 2007.
For correspondence or reprints contact: Jason S. Lewis, PhD, Mallinckrodt Institute of Radiology, Washington University School of Medicine, Campus Box 8225, 510 S. Kingshighway Blvd., St. Louis, MO 63110.
E-mail: j.s.lewis@wustl.edu

(*23*). Previous studies have demonstrated that FAS inhibitors can reduce ^{14}C-acetate incorporation in human tumor cell lines and in human lung xenografts and mouse prostate tumors ex vivo (*24–27*). Because of these facts, we hypothesize that FAS is involved with 1-^{11}C-acetate uptake in prostate cancer. The following reports an examination of the mechanism of 1-^{11}C-acetate uptake in prostate tumor models and its implications for tumor progression and patient survival. Understanding the mechanism of 1-^{11}C-acetate uptake and the relation to FAS expression levels could provide a valuable tool to clinicians for the planning and monitoring of treatments because of the increased mortality with raised levels of this protein in prostate cancer. It could also be used in validating the translation of novel FAS inhibitors, as anticancer agents, into the clinical setting.

MATERIALS AND METHODS

General

All chemicals, unless otherwise stated, were purchased from Sigma-Aldrich Chemical Co., Inc. Radioactive samples were counted in a radioisotope calibrator (Capintec, Inc.) for determination of megabecquerels (millicuries) and an automated well scintillation 8000 γ-counter (Beckman Coulter) for counts per minute. Centrifugation was performed on a Sorvall Superspeed RC-6 Centrifuge (Sorvall, Inc.) refrigerated to 4°C. Male athymic *nu/nu* mice (<20 g; 5- to 6-wk-old) were purchased from the National Cancer Institute. Human prostate carcinoma tumor cell lines PC-3 (androgen receptor negative), LNCaP (androgen responsive), and 22Rv1 (androgen resistant) were obtained from the American Type Culture Collection and maintained by serial passage in cell culture. Both LAPC-4 (androgen responsive) (Dr. Charles Sawyer at UCLA) and CWR22 (androgen responsive) (Bristol Myers Squibb) tumors were implanted and maintained by animal-to-animal passage. ^{11}C-Labeled acetate was prepared by the reaction of ^{11}C-labeled carbon dioxide with a Grignard reagent as described previously (*28*). Radiochemical purity was always ≥99%.

In Vitro Cell Uptake and Inhibition

PC-3, LNCaP, and 22Rv1 prostate cells were plated in 6-well plates (4.5×10^5, 9×10^5, and 1.2×10^6 cells per well, respectively) 24 h before the study was initiated. The cells were grown to ~75% confluence at 37°C and 5% CO_2 in appropriate medium and supplemented with 10% heat-inactivated fetal bovine serum. Eighteen hours before the uptake experiment, C75 (63.5 μg), a FAS inhibitor (*29*), was added to the growth media (5 mL) in each well in a small amount of dimethyl sulfoxide (DMSO) (10 μL) so that the final concentration in each well was 50 μM (controls received DMSO alone). To initiate the study, the culture medium was removed, and cells were rinsed with phosphate-buffered saline (PBS). Approximately 0.37 MBq (10 μCi) of 1-^{11}C-acetate were added to the cells in 1.0 mL fresh media to initiate tracer uptake (including C75 or DMSO alone to maintain inhibitor concentration). Incubation was terminated at various times (15, 30, or 60 min) by removing the radioactive culture medium. Cell monolayers were washed with 2 mL of cold PBS 3 times to remove any excess culture medium from the extracellular spaces. Lysis of the cells was achieved by addition of 1 mL of 0.25% sodium dodecyl sulfate (SDS). Lysis extracts, as well as 1 mL of radioactive culture medium as a standard, were counted in a γ-counter and measured for protein content using a standard copper reduction/bicinchoninic acid assay (BCA; Pierce Biotechnology), with bovine serum albumin as the protein standard. Cellular uptake data for all experiments were normalized for the amount of protein present and calculated as the percentage uptake (cell-associated). A further inhibition study was performed with 5-(tetradecyloxy)-2-furoic acid (TOFA), a potent inhibitor of acetyl-CoA carboxylase (ACC), a key enzyme involved in fatty acid biosynthesis (*30*). Procedures were similar to those stated earlier, with the final concentration of TOFA being 30 μM and the pretreatment occurring 2 h before addition of 1-^{11}C-acetate. The tracer was added directly to the 5 mL of growth media, rather than changing the media, to ensure continued presence of the pretreatment concentration of TOFA.

To compare the abilities of C75 and TOFA to inhibit fatty acid synthesis, PC-3 cells were seeded in 24-well plates at 1×10^5 cells per well. After 48 h the cells were treated with either C75 (0, 10, 20, 30, or 60 μM) to inhibit FAS or TOFA (0, 10, 20, or 30 μM) to inhibit ACC for 2 h, and then 2-^{14}C-acetate (0.037 MBq; 1 μCi) was added for an additional 2 h. An additional study was performed using both PC-3 and LNCaP cells, where cells were seeded in 24-well plates at 1×10^5 cells per well. After 48 h the cells were treated with either C75 (30 μM) to inhibit FAS or TOFA (30 μM) to inhibit ACC for 2 h, and then 2-^{14}C-acetate (0.037 MBq; 1 μCi) was added for an additional 2 h. Control cells received DMSO (0.1%) only. After the labeling period, the cells were collected and washed and lipids were extracted and quantified by scintillation counting as described previously (*31,32*).

To observe the contribution of the tricarboxylic acid (TCA) cycle to 1-^{11}C-acetate cellular uptake, an inhibition study with 3-nitroprionic acid, a known inhibitor of succinate dehydrogenase in the TCA cycle, was performed. PC-3 cells, plated in 6-well plates 24 h before uptake, were treated with 100 μM 3-nitropropionic acid 2 h before radiotracer uptake, whereas control cells received vehicle alone. 1-^{11}C-Acetate (1.11 MBq; 30 μCi) was added to the wells; this was followed by a 25-min incubation. Cells were then washed and collected by trypsin/ethylenediaminetetraacetic acid (EDTA) for counting in the γ-counter and subsequent protein assay for normalization.

Small-Animal PET

All animal experiments were performed in compliance with the Guidelines for the Care and Use of Research Animals established by Washington University's Animal Studies Committee. Single-position, whole-body imaging was performed using small-animal PET (microPET Focus 120 or Focus 220; Siemens Medical Solutions, Inc.) (*33*). Mice were imaged individually or in pairs in a supine position in a specially designed bed. Isoflurane (1%–2%) was used as an inhaled anesthetic to induce and maintain anesthesia during imaging. The bed was placed near the center of the field of view of the PET scanner, where the highest image resolution and sensitivity are available. Imaging was performed, 20-min after injection, with a single 10-min static scan. Images were reconstructed by Fourier rebinning, which was followed by 2-dimensional ordered-subset expectation maximization (OSEM) (*34*).

PET images were evaluated by analysis of the standardized uptake value (SUV) of the tumor and nontarget organ (muscle) using ASIPRO software (Siemens Medical Solutions, Inc.). The average radioactivity concentration within the tumor or tissue was obtained from the average pixel values reported in nanocuries per

milliliter within a volume of interest drawn around the entire tumor or tissue on multiple, consecutive transaxial image slices. SUVs were calculated by dividing this value, the decay-corrected activity per unit volume of tissue (nCi/mL), by the injected activity per unit of body weight (nCi/g). Necrotic tissue was excluded by analysis of the images in comparison with serial slices through the tumor postmortem. Any necrosis in a tumor was noted, and those sections (which also had no uptake) were not included in the overall SUV calculation.

An animal imaging study was performed on 22Rv1, PC-3, CWR22, and LAPC-4 tumor-bearing mice to confirm correlation of uptake of 1-^{11}C-acetate with FAS expression in tumors. Two prostatic carcinoma tumor models were prepared in culture (22Rv1 and PC-3) and then harvested for implant by trypsin/EDTA and injected in a volume of 100 μL into the right flank of intact, male *nu/nu* mice (15–20 g) in the appropriate media at a given concentration (5×10^6 cells in Matrigel [BD Biosciences] for 22Rv1 and 3×10^6 cells in Kaighn's modification of Ham's F12 medium for PC-3). CWR22 and LAPC-4 tumors were obtained from animal-to-animal passage. Tumors were allowed to grow until palpable, and the time varied by model. PET was performed 20 min after intravenous injection of 14.8–18.5 MBq (400–500 μCi) 1-^{11}C-acetate (100 μL) via the tail vein. The 20-min time point after injection was chosen on the basis of the experience of other researchers (*13,14,16*). After imaging, the mice were euthanized, and the tumors were excised and flash frozen to −80°C for subsequent Western blot analysis to determine FAS expression. Images were analyzed for determination of SUV and compared with the Western blots.

Western Blots

Frozen tumors were thawed over ice and homogenized, and the cells were lyzed with 1× cell lysis buffer (Cell Signaling Technology) for determination of protein concentration by BCA protein assay (Pierce). Twenty micrograms of protein of each sample were run using SDS-polyacrylamide gel electrophoresis with a 4%–20% Tris gradient gel. Standard Western blotting was performed with an anti-FAS primary antibody (rabbit; Novus Biologicals) and a goat antirabbit secondary antibody (DyLight 647; Pierce Biotechnology). Final detection was achieved by using the enhanced chemiluminescence system (Amersham Life Sciences) according to the manufacturer's instructions. Prestained standards (Kaleidoscope Prestained Standards 161-0324; Bio-Rad Laboratories) were used on each Western blot for reference. Blots were traced, and intensity and area values were obtained for each band by densitometry using Image J software (National Institutes of Health) to quantify expression.

PET of FAS Inhibition

Male, *nu/nu* mice were injected with either PC-3 (3×10^6 cells/100 μL) ($n = 3$) or LNCaP (1×10^7 cells/100 μL) ($n = 4$) tumor cells subcutaneously in the right flank, which were allowed to grow until palpable. PET was performed 20 min after intravenous injection of 3.7–7.4 MBq (100–200 μCi) 1-^{11}C-acetate (100 μL), which was followed by a low-resolution CT scan for subsequent coregistration and anatomic reference. After imaging, all mice received an intraperitoneal injection of C75 at 30 mg/kg dissolved in DMSO/RPMI 1640 media (<2% DMSO). Eighteen hours after treatment, the mice were imaged again following the same protocol. After imaging, the mice were euthanized, and the tumors were excised and formalin-fixed for staining and immunohistochemical analysis.

Immunohistochemistry

After PET, to observe inhibition of 1-^{11}C-acetate uptake in prostate tumors by blocking of FAS, immunohistochemical techniques were used to demonstrate the extent of protein expression. Tumors from the in vivo inhibition study were formalin-fixed, paraffin-embedded, sliced, and placed on slides for immunohistochemical analysis by the Histology Core at Washington University; 1 slide per section was also stained with hemotoxylin and eosin (H&E) to confirm tissue viability. Slides were baked for 30 min at 60°C and then soaked in xylene, 2 times for 3 min each, hydrated in 2 soaks of 100% ethanol for 2 min each, and soaked 2 times with 95% ethanol for 2 min each, 2 times with 70% ethanol for 2 min each, and 1 time with 50% ethanol for 2 min. Slides were then rinsed in doubly distilled water and placed in 3 washes of PBS before blocking with a protein block (Dako) in a humidified chamber for 30 min at room temperature. After aspiration of the blocking solution, the slides were incubated with the FAS primary antibody (1:1,000; anti-FASN [M] antibody 34-6E7; FASGen, Inc.) overnight in a humidified chamber at 4°C and then rinsed again with PBS. The slides were then incubated with secondary goat anti-mouse antibody labeled with biotin (1:200; ImmunoPure GAM IgG; Pierce) for 30 min and rinsed with PBS, which was followed by incubation for 30 min with ABC Vector Elite (Vector Laboratories) solution diluted in 0.5 M NaCl. The slides were rinsed 3 times in 0.1 M Tris buffer, pH 7.4, and then incubated in 3,3′-diaminobenzidine (DAB) and chromogen (DAB+ Kit; Dako) for 10 min. After repeated rinsing with tap water, the slides were counterstained with Meyer's hematoxylin for 40 s and washed with tap water. The slides were dipped 10 times in Bluing Reagent (YWR International) before they were dehydrated and cover-slipped using Permount (Fisher Scientific). The slides were observed and compared (10×) with the H&E-stained slides under a Nikon Eclipse E600W microscope fitted with a Nikon DXM1200F digital camera. As a result of the protocol, FAS protein should appear brown in color.

Statistical Analysis

Statistically significant differences between mean values were determined using ANOVA coupled to the Scheffé test or, for statistical classification, a Student *t* test was performed.

RESULTS

Inhibition of Fatty Acid Synthesis Reduces 1-^{11}C-Acetate In Vitro Uptake

To confirm the hypothesis that 1-^{11}C-acetate uptake in tumors is related FAS expression, an in vitro blocking study was performed. Cells were pretreated for 18 h with C75, a known inhibitor of FAS, before uptake of 1-^{11}C-acetate to determine if uptake could be blocked. All cells showed a linear increase in uptake over time in both the C75-treated and the control tumor cells. In all cases, the uptake in the control cells was consistently higher throughout the duration of the study. By 30 min, the C75-treated cells showed inhibition of uptake by 26.4% ($P = 0.0005$) in the PC-3 cell line and by 16.7% ($P = 0.0010$) and 26.9% ($P = 0.0007$) for the LNCaP and 22Rv1 cell lines, respectively (Fig. 1A). Cell viability was measured by trypan blue staining. An average of 95% viability was measured for each cell line, with no decrease in overall cell number due to the presence of C75 (data not shown).

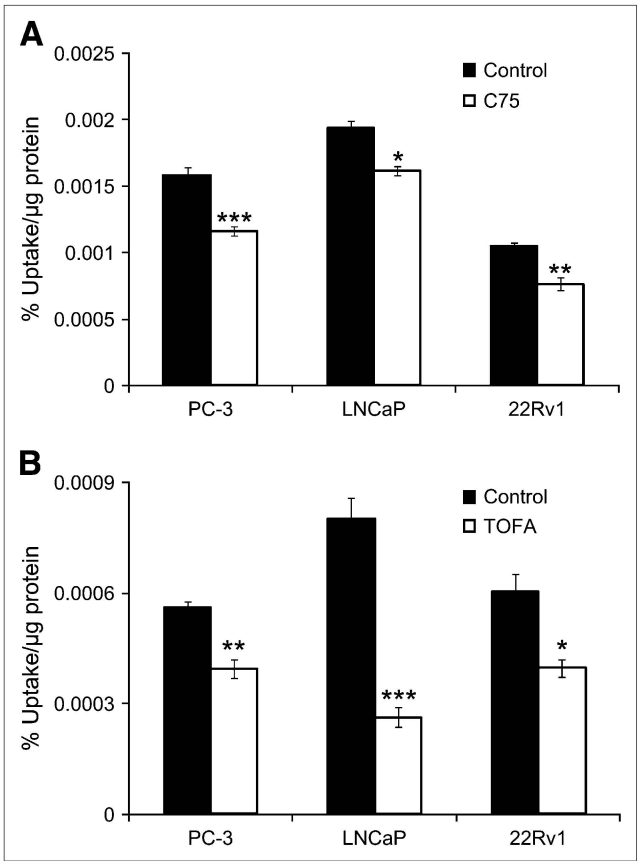

FIGURE 1. (A) In vitro cell association of 1-^{11}C-acetate at 30 min in PC-3, LNCaP, or 22Rv1 prostate cancer cells with and without 18-h prior treatment with C75, a FAS inhibitor. (*P = 0.001; **P = 0.0007; ***P = 0.0005). (B) In vitro cell association of 1-^{11}C-acetate at 30 min in PC-3, LNCaP, or 22Rv1 prostate cancer cells with and without 2-h prior treatment with TOFA, an ACC inhibitor to block the fatty acid synthesis pathway. (*P = 0.0025; **P = 0.0008; ***P = 0.0001). Data are expressed as mean ± SD.

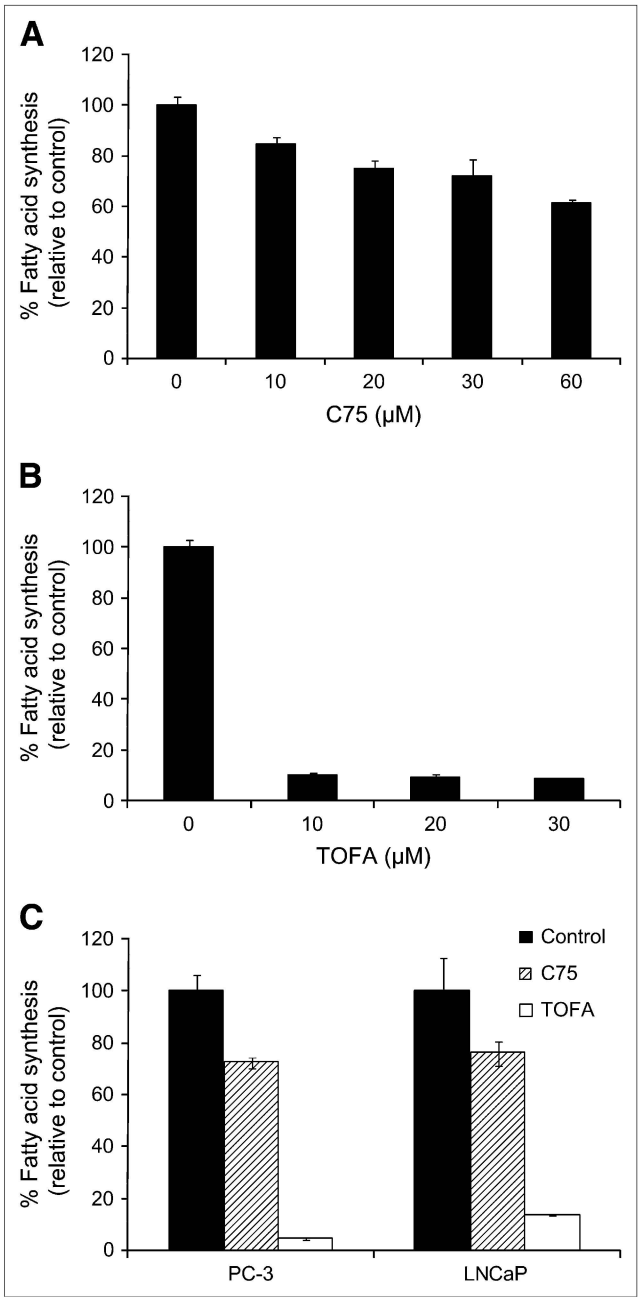

FIGURE 2. Dose–response comparison of relative effects of C75 (A) and TOFA (B) on fatty acid synthesis in PC-3 cells, performed with ^{14}C-acetate. (C) Comparison of fatty acid synthesis inhibition with 30 μM C75 or TOFA in PC-3 and LNCaP cells. Data are expressed as mean ± SD.

The role of ACC in 1-^{11}C-acetate uptake was also determined by treating cells with TOFA, a potent inhibitor of ACC. ACC is the rate-limiting enzyme in the fatty acid synthesis pathway. After pretreatment with TOFA, cell uptake of 1-^{11}C-acetate was significantly reduced, more than with C75 (Fig. 1B). The percentage of blocking increased over time in all cases, with values of 29.8% ± 5.75%, 67.4% ± 9.22%, and 34.7% ± 9.31% for PC-3, LNCaP, and 22Rv1 cell lines, respectively, at 30 min. To demonstrate that TOFA is a more potent inhibitor of fatty acid synthesis than C75, a dose−response comparison between TOFA and C75 in PC-3 cells was performed (Fig. 2A and 2B). It is evident that even at concentrations of 10 μM, TOFA has a significantly more pronounced effect on fatty acid synthesis than C75 (10 μM: 10.7% ± 0.59% vs. 84.9% ± 2.47%). An additional one-point study comparing PC-3 cells with LNCaP cells was undertaken to show that this relationship was observed in more than 1 cell line. It was shown that 30 μM C75 inhibited about 30% of fatty acid activity in both PC-3 and LNCaP cells, whereas TOFA inhibited fatty acid synthesis about 75%–80% (both after a 2-h treatment) (Fig. 2C). These data demonstrate that 1-^{11}C-acetate uptake is directly related to the degree of FAS inhibition in prostate tumor cell lines.

PET Demonstrates In Vivo Correlation Between 1-^{11}C-Acetate Uptake and FAS Expression

To test the hypothesis that 1-^{11}C-acetate may be imaging FAS expression in vivo, an imaging study was performed,

with excision of the tumors after imaging for further analysis of FAS levels by Western blot. 1-^{11}C-Acetate PET of 4 prostate tumor models (PC-3, 22Rv1, CWR22, and LAPC-4) was performed (Figs. 3A–3C). Regions of interest were drawn on the images around the tumors, excluding any necrotic tissue. SUVs at 20 min after injection were calculated to normalize these values (nCi/mL) to the injected activity per animal (nCi) as well as body mass (g). Imaging SUVs were 0.11 ± 0.01 for LAPC-4 (n = 2), 0.26 ± 0.06 for CWR-22 (n = 2), and 0.18 ± 0.02 for 22Rv1 (n = 3). In this case, the PC-3 tumors (n = 2) could not be delineated from the surrounding tissue and, therefore, no SUVs were calculated. Visual inspection of the Western blot results revealed obvious differences in the intensity of the band near 250 kDa (FAS = 267 kDa), with PC-3 showing the lowest levels of expression, 22Rv1 and LAPC-4 with significantly more intensity than PC-3, and CWR22 being the highest of those examined (Fig. 3D). Densitometry analysis confirmed this trend quantitatively. The relative values of expression were averaged for each tumor type, resulting in 2,354.1 ± 22.8, 9,640.9 ± 2,552.3, 11,160 ± 25.0, and 15,798 ± 4,057.6 for PC-3, LAPC-4, 22Rv1, and CWR22, respectively. Comparison of the average SUVs from the PET data with Western blot analysis of the homogenized tumor tissue resulted in a correlation (R^2 = 0.974) between tumor uptake of 1-^{11}C-acetate and FAS expression (Fig. 3E).

Small-Animal PET of FAS Inhibition (C75 Blocks 1-^{11}C-Acetate Uptake In Vivo)

Because the in vitro results confirmed that 1-^{11}C-acetate uptake could be diminished by inhibition of FAS, a similar study was pursued in vivo. PC-3 (as the low-expressing control) and LNCaP tumor-bearing mice were imaged with 1-^{11}C-acetate before and after treatment with C75, so that each mouse would serve as its own control (Fig. 4A). In 6 of the 7 image sets analyzed, tumor uptake of 1-^{11}C-acetate decreased after a single treatment with C75. LNCaP tumors showed an average decrease in uptake of 12.3%, with PC-3 SUVs reduced by an average of 49.4% (Fig. 4B). The reasoning for the significant difference in the effect of FAS inhibition on acetate uptake (P = 0.013) between the 2 tumor types was explored by immunohistochemical analysis of FAS expression (Fig. 4C). Visual inspection of the FAS-stained slides clearly demonstrated a much higher abundance of the protein in the LNCaP tumors compared with that of PC-3 in all cases. H&E stains of all tumor slides confirmed viability of the tissue. The brown staining also colocalized in the same areas as the hemotoxylin stain on subsequent slides, indicating protein-rich portions (data not shown).

DISCUSSION

1-^{11}C-Acetate was first examined as a possible tracer for malignancies by Shreve et al. in 1995 (*35*) and has since been extensively investigated in prostate cancer and its metastases (*12–16*). Direct comparisons by researchers have shown greater sensitivity for detection over the standard use of ^{18}F-FDG (*4,13*). Most recent work has demonstrated 1-^{11}C-acetate as a useful tool for detecting recurrent disease at PSA relapse in many cases (*12,14,15,36*) and even better results when paired with CT and MRI for anatomic reference and observation of structural changes

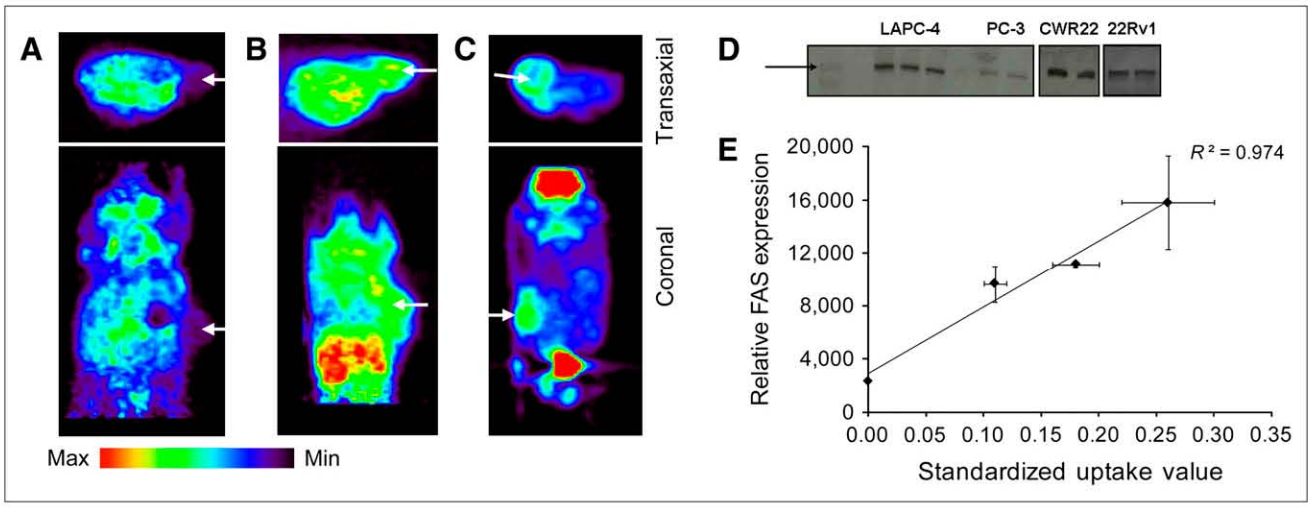

FIGURE 3. Representative transaxial and coronal PET image slices of LAPC-4 (A), CWR22 (B), and 22Rv1 (C) tumor-bearing mice at 20 min after intravenous injection of 14.8–18.5 MBq (400–500 μCi) 1-^{11}C-acetate. Arrows mark tumor location. PC-3 tumors were not visualized. (D) Western blot of tumor lysates shows qualitative levels of FAS expression. Visual inspection of Western blot results revealed obvious differences in intensity of the band near 250 kDa (standard band denoted by black arrow; FAS = 267 kDa), with PC-3 showing relatively nonexistent bands, 22Rv1 and LAPC-4 with significantly more intensity, and CWR22 being the highest of those examined. Multiplication of the area of the band by its intensity (after subtraction of background intensity) gave a relative value of expression for the sample analyzed. (E) SUVs of 1-^{11}C-acetate uptake in prostate tumor models vs. relative FAS expression (by Western blot) of these samples show a direct correlation (R^2 = 0.974). Data are expressed as mean ± SD.

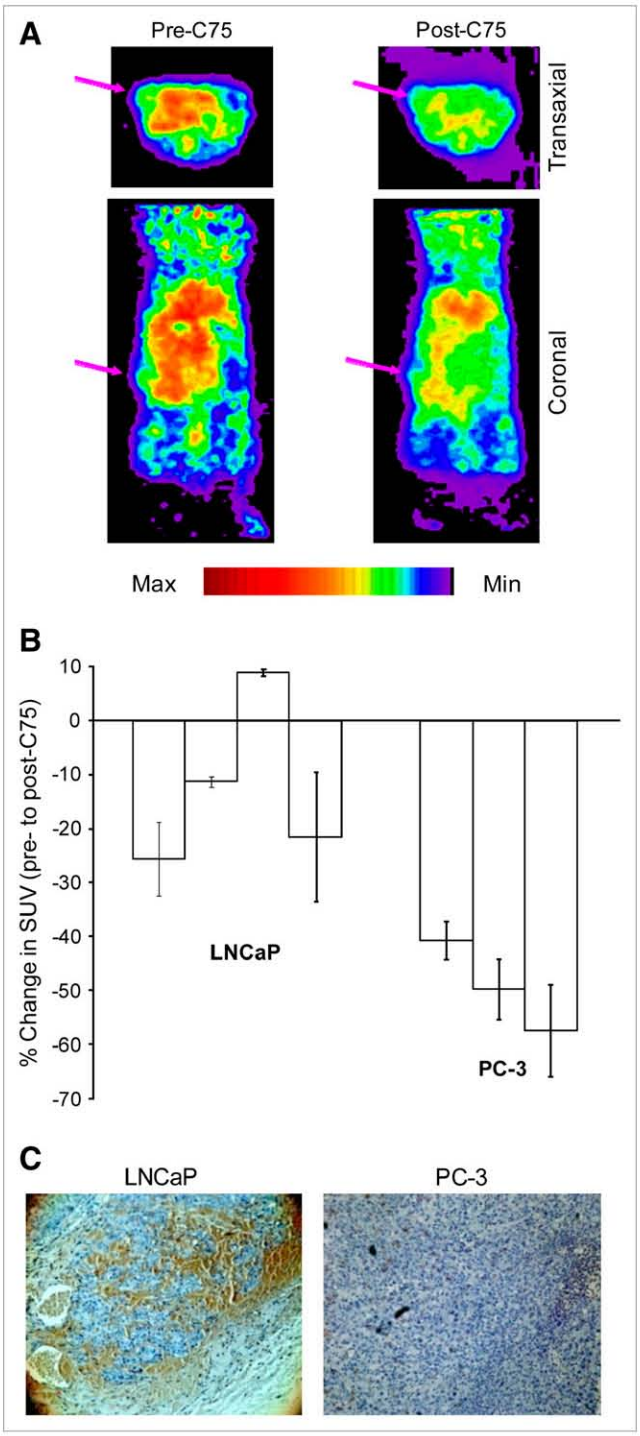

FIGURE 4. (A) Representative image slices of an LNCaP tumor-bearing mouse after intravenous injection of 3.7–7.4 MBq (100–200 μCi) 1-^{11}C-acetate. Arrows mark tumor location. (B) Overall change in SUV in solid PC-3 and LNCaP tumors in mice pre- and posttreated with C75. Data are expressed as mean ± SD. (C) Representative immunohistochemical staining of harvested prostate tumors for FAS (brown), showing a strong reactivity in LNCaP. Whereas PC-3 has almost none (10× magnification). Three slices per tumor were analyzed.

(*16*). Despite these findings, no definitive explanation for increased uptake has been made.

Acetate can be metabolized by several distinct pathways in cells. Of course, acetate can be metabolized through the TCA cycle. In tumor cells, acetate can also be used as a substrate or a substrate precursor during fatty acid synthesis. Acetate is a precursor for acetyl-CoA, which can then be converted to malonyl-CoA by ACC. Acetyl-CoA and malonyl-CoA also provide substrate for fatty acid elongation in the mitochondria and endoplasmic reticulum, respectively. In addition, acetate is a precursor for cholesterol synthesis. As a result, 1-^{11}C-acetate incorporation could be affected by multiple pathways. Considering that FAS and the fatty acid synthesis pathway are highly expressed and active in multiple cancers—prostate cancer, in particular—this pathway could be a major determinant of 1-^{11}C-acetate uptake in prostate tumors.

Researchers have postulated that increased acetate uptake in malignancies may be due to increased lipid biosynthesis. Accordingly, one study recently observed the uptake and metabolism of ^{14}C-acetate into 4 nonprostate tumor cell lines (LS174T, human colon adenocarcinoma; RPMI2650, human nasal septum tumor; A2780, human ovary carcinoma; and A375, human malignant melanoma) and 1 fibroblast model (*37*). The authors demonstrated that all malignant lines examined had significantly higher uptake over the fibroblasts and that the acetate incorporated into the lipid-soluble fractions, and primarily phosphatidylcholine (PC). Interestingly, Swinnen et al. have demonstrated that FAS-derived palmitate primarily partitions to detergent-insoluble lipid fractions in which PC is the primary constituent (*38*). Similarly, uptake of 2-^{14}C-acetate has also been measured in CWR22 and PC-3 tumors in castrated and noncastrated mice (*39*). The authors found that acetate uptake correlated with androgen receptor expression, suggesting that acetate uptake can be affected by androgen. FAS has been shown to be overexpressed in prostate cancer (*18–22*); however, specific examination of FAS levels in correlation with 1-^{11}C-acetate uptake by PET have yet to be reported. Because high levels of FAS expression have also been found to be an indicator of a poor prognosis in patients with prostate cancer, resulting in a 4.45-fold higher risk of death (*40*), we hypothesized that a noninvasive imaging method such as 1-^{11}C-acetate PET for the determination of FAS in tumors could provide clinicians with an additional tool for individualized therapy.

In this current study, pharmacologic inhibition of the FAS pathway was used to demonstrate the specificity of 1-^{11}C-acetate for imaging FAS expression by blocking the protein. C75-treated cells showed a significant decrease in cellular accumulation of 1-^{11}C-acetate compared with that of controls but still showed an appreciable amount of cellular uptake (Fig. 1A). It is likely that either all of the FAS was not blocked or other described pathways are also involved. Inhibition of fatty acid synthesis with TOFA, a pharmacologic inhibitor of ACC—the rate-limiting enzyme

involved in fatty acid biosynthesis—also had significant impact of the cellular accumulation of 1-^{11}C-acetate (Fig. 1B). The demonstration that TOFA is a more efficient inhibitor of fatty acid synthesis than C75 (Fig. 2A–2C) correlates well with differences in 1-^{11}C-acetate uptake. Furthermore, because blockade of the 2 key enzymes involved in fatty acid synthesis affected acetate uptake, our data demonstrate that a large portion of 1-^{11}C-acetate tumor uptake and retention is related to the fatty acid synthesis pathway.

Demonstrating that in vivo uptake of 1-^{11}C-acetate in 4 prostate tumor models correlated with FAS levels (Fig. 3), it is evident that FAS is at least involved in 1-^{11}C-acetate uptake in vivo—to our knowledge, the first time this relationship has been demonstrated. After showing that 1-^{11}C-acetate cellular uptake can be diminished with FAS inhibition in vitro and that uptake correlates to FAS expression levels in vivo, we performed a FAS-blocking study in vivo with C75 (Fig. 4). With each mouse serving as its own control, specific changes in overall tumor uptake were calculated and showed a small average change in the LNCaP mice (~12%) and a larger effect in the PC-3 model (~49%). LNCaP has a higher expression of FAS (Fig. 4C); therefore, the amount of C75 given is likely to show less of an effect than in PC-3 mice, where its lower expression of FAS would result in a more extreme response with the same amount of C75.

Inhibition of FAS with C75, orlistat, triclosan, and many other compounds has led to promising in vitro and in vivo results confirming FAS as a viable target for cancer therapies (*41,42*). Although FAS represents an important therapeutic target, there has been no in vivo demonstration that FAS inhibitors significantly block fatty acid synthesis in tumors. One study with ^{18}F-FDG to monitor the effects of C75 on tumor glucose metabolism in a rodent model of human A549 lung cancer was reported recently (*26*). A transient, reversible decrease in glucose metabolism and tumor metabolic volume was noted after C75 treatment, with the peak effect seen at 4 h. This, however, was an indirect measure of fatty acid synthesis, whereas the use 1-^{11}C-acetate shows a direct measurement. The data presented herein provide validation for further development of 1-^{11}C-acetate PET, as a measure of fatty acid synthesis, and incorporation of the technology into preclinical in vivo models and clinical studies. Such information could provide important validation of the efficacy of FAS inhibitors and represents a unique tool in aiding the translation of new FAS inhibitors for the treatment of cancer into the clinical setting.

As mentioned earlier, acetate may also be metabolized by other pathways. The TCA cycle is a major factor in acetate metabolism throughout the body, and its presence in the cells needs to be considered. In one experiment, 3-nitropropionic acid (a known inhibitor of the TCA cycle) was added during cell uptake and showed a 14.3% ± 3.7% reduction of 1-^{11}C-acetate uptake in the PC-3 model (data not shown). It has been shown that small interfering RNA (siRNA)-mediated knockdown of FAS in MDA-MB-435 mammary carcinoma cells can also affect expression of genes related to the TCA cycle and glycolysis and may also influence acetate metabolism indirectly (*43*). This supports, in part, the idea that TCA could be a major contributor to the retention of 1-^{11}C-acetate and is regulated by the fatty acid synthesis pathway. Given the role of cholesterol in prostate cancer (*44*), and that in some cell lines increased fatty acid synthesis has been shown to be accompanied by an increase in cholesterol synthesis (*45*), further studies on the ability of the cholesterol synthesis pathway to regulate PET of 1-^{11}C-acetate uptake in prostate cancer may also be warranted. On the other hand, the data presented herein clearly identify FAS and the fatty acid synthesis pathway as an important determinant of 1-^{11}C-acetate uptake in PET of prostate cancer.

CONCLUSION

These findings are promising in that they suggest a possible biomarker for more-effective treatments in prostate cancer patients, and possibly others, as FAS expression has shown links to poor prognosis in other cancers as well. Moreover, because FAS inhibitors are being developed as antitumor agents, this technology also provides a unique opportunity to monitor the effectiveness and the validation of new FAS inhibitors for translation into a clinical setting.

ACKNOWLEDGMENTS

The authors thank Amanda Roth, Nicole Fettig, Margaret Morris, Lori Strong, and Susan Adams for technical support; the cyclotron facility staff for radiopharmaceutical production; and Drs. Nobuyuki Oyama and Gordon Parry for their helpful discussions. We are grateful for financial support from the U.S. Department of Defense (grant PC 040435), the National Institutes of Health (grant F32 CA110422-03), and the National Cancer Institute (grant CA 114104).

REFERENCES

1. Jemal A, Siegel R, Ward E, Murray T, Xu J, Thun MJ. Cancer statistics, 2007. *CA Cancer J Clin.* 2007;57:43–66.
2. Gretzer MB, Partin AW. PSA markers in prostate cancer detection. *Urol Clin North Am.* 2003;30:677–686.
3. Akin O, Hricak H. Imaging of prostate cancer. *Radiol Clin North Am.* 2007; 45:207–222.
4. Fricke E, Machtens S, Hofmann M, et al. Positron emission tomography with ^{11}C-acetate and ^{18}F-FDG in prostate cancer patients. *Eur J Nucl Med Mol Imaging.* 2003;30:607–611.
5. Agus DB, Golde DW, Sgouros G, Ballangrud A, Cordon-Cardo C, Scher HI. Positron emission tomography of a human prostate cancer xenograft: association of changes in deoxyglucose accumulation with other measures of outcome following androgen withdrawal. *Cancer Res.* 1998;58:3009–3014.
6. Jadvar H, Xiankui L, Shahinian A, et al. Glucose metabolism of human prostate cancer mouse xenografts. *Mol Imaging.* 2005;4:91–97.
7. Morris MJ, Akhurst T, Osman I, et al. Fluorinated deoxyglucose positron emission tomography imaging in progressive metastatic prostate cancer. *Urology.* 2002;59:913–918.
8. Oyama N, Akino H, Suzuki Y, et al. Prognostic value of 2-deoxy-2-[F-18]fluoro-D-glucose positron emission tomography imaging for patients with prostate cancer. *Mol Imaging Biol.* 2002;4:99–104.

9. Oyama N, Akino H, Suzuki Y, et al. The increased accumulation of [^{18}F]fluorodoxyglucose in untreated prostate cancer. *Jpn J Clin Oncol.* 1999;29: 623–629.
10. Effert PJ, Bares R, Handt S, Wolff JM, Bull U, Jakse G. Metabolic imaging of untreated prostate cancer by positron emission tomography with ^{18}fluorine-labeled deoxyglucose. *J Urol.* 1996;155:994–998.
11. Hofer C, Laubenbacher C, Block T, Breul J, Hartung R, Schwaiger M. Fluorine-18-fluorodeoxyglucose positron emission tomography is useless for the detection of local recurrence after radical prostatectomy. *Eur Urol.* 1999;36:31–35.
12. Albrecht S, Buchegger F, Soloviev D, et al. ^{11}C-Acetate PET in the early evaluation of prostate cancer recurrence. *Eur J Nucl Med Mol Imaging.* 2007;34: 185–196.
13. Oyama N, Akino H, Kanamaru H, et al. ^{11}C-Acetate PET imaging of prostate cancer. *J Nucl Med.* 2002;43:181–186.
14. Oyama N, Miller TR, Dehdashti F, et al. ^{11}C-Acetate PET imaging of prostate cancer: detection of recurrent disease at PSA relapse. *J Nucl Med.* 2003;44: 549–555.
15. Sandblom G, Sorensen J, Lundin N, Haggman M, Malmstrom P-U. Positron emission tomography with C11-acetate for tumor detection and localization in patients with prostate-specific antigen relapse after radical prostatectomy. *Urology.* 2006;67:996–1000.
16. Wachter S, Tomek S, Kurtaran A, et al. ^{11}C-Acetate positron emission tomography imaging and image fusion with computed tomography and magnetic resonance imaging in patients with recurrent prostate cancer. *J Clin Oncol.* 2006;24: 2513–2519.
17. Wakil SJ. Fatty acid synthase, a proficient multifunctional enzyme. *Biochemistry.* 1989;28:4523–4530.
18. Dhanasekaran SM, Barrette TR, Ghosh D, et al. Delineation of prognostic biomarkers in prostate cancer. *Nature.* 2001;412:822–826.
19. Swinnen JV, Roskams T, Joniau S, et al. Overexpression of fatty acid synthase is an early and common event in the development of prostate cancer. *Int J Cancer.* 2002;98:19–22.
20. Welsh JB, Sapinosa LM, Su AI, et al. Analysis of gene expression identifies candidate markers and pharmacological targets in prostate cancer. *Cancer Res.* 2001;61:5974–5978.
21. Pizer ES, Pflug BR, Bova GS, Han WF, Udan MS, Nelson JB. Increased fatty acid synthase as a therapeutic target in androgen-independent prostate cancer progression. *Prostate.* 2001;47:102–110.
22. Rossi S, Graner E, Febbo P, et al. Fatty acid synthase expression defines distinct molecular signatures in prostate cancer. *Mol Cancer Res.* 2003;1:707–715.
23. Myers RB, Oelschlager DK, Weiss HL, Frost AR, Grizzle WE. Fatty acid synthase: an early molecular marker of progression of prostatic adenocarcinoma to androgen independence. *J Urol.* 2001;165:1027–1032.
24. Kuhajda FP, Jenner K, Wood FD, et al. Fatty acid synthesis: a potential selective target for antineoplastic therapy. *Proc Natl Acad Sci USA.* 1994;91:6379–6383.
25. Kuhajda FP, Pizer ES, Li JN, Mani NS, Frehywot GL, Townsend CA. Synthesis and antitumor activity of an inhibitor of fatty acid synthase. *Proc Natl Acad Sci USA.* 2000;97:3450–3454.
26. Lee JS, Orita H, Gabrielson K, et al. FDG-PET for pharmacodynamic assessment of the fatty acid synthase inhibitor C75 in an experimental model of lung cancer. *Pharm Res.* 2007;24:1202–1207.
27. Pflug BR, Pecher SM, Brink AW, Nelson JB, Foster BA. Increased fatty acid synthase expression and activity during progression of prostate cancer in the TRAMP model. *Prostate.* 2003;57:245–254.
28. Moerlein SM, Gaehle GG, Welch MJ. Robotic preparation of sodium acetate C-11 injection for use in clinical PET. *Nucl Med Biol.* 2002;29:613–621.
29. Loftus TM, Jaworsky DE, Frehywot GL, et al. Reduced food intake and body weight in mice treated with fatty acid synthase inhibitors. *Science.* 2000;288: 2379–2381.
30. Landree LE, Hanlon AL, Strong DW, et al. C75, a fatty acid synthase inhibitor, modulates AMP-activation protein kinase to alter neuronal energy metabolism. *J Biol Chem.* 2004;279:3817–3827.
31. Kridel SJ, Axelrod F, Rozenkrantz N, Smith JW. Orlistat is a novel inhibitor of fatty acid synthase with antitumor activity. *Cancer Res.* 2004;64:2070–2075.
32. Little JL, Wheeler FB, Fels DR, Koumenis C, Kridel SJ. Inhibition of fatty acid synthase induces endoplasmic reticulum stress in tumor cells. *Cancer Res.* 2007; 67:1262–1269.
33. Tai Y-C, Ruangma A, Rowland D, et al. Performance evaluation of the microPET Focus: a third-generation microPET scanner dedicated to animal imaging. *J Nucl Med.* 2005;46:455–463.
34. Defrise M, Kinahan PE, Townshend DW, Michel C, Sibomana M, Newport DF. Exact and approximate rebinning algorithms for 3-D PET data. *IEEE Trans Med Imaging.* 1997;16:145–158.
35. Shreve P, Chiao PC, Humes HD, Schwaiger M, Gross MD. Carbon-11 acetate PET imaging in renal disease. *J Nucl Med.* 1995;36:1595–1601.
36. Kotzerke J, Volkmer BG, Neumaier B, Gschwend JE, Hautmann RE, Reske SN. Carbon-11 acetate positron emission tomography can detect local recurrence of prostate cancer. *Eur J Nucl Med Mol Imaging.* 2002;29:1380–1384.
37. Yoshimoto M, Waki A, Yonekura Y, et al. Characterization of acetate metabolism in tumor cells in relation to cell proliferation: acetate metabolism in tumor cells. *Nucl Med Biol.* 2001;28:117–122.
38. Swinnen JV, Van Veldhoven PP, Timmermans L, et al. Fatty acid synthase drives the synthesis of phospholipids partitioning into detergent-resistant membrane microdomains. *Biochem Biophys Res Commun.* 2003;302:898–903.
39. Jadvar H, Li X, Park R, Shahinian A, Conti P. Quantitative autoradiography of radiolabeled acetate in mouse xenografts of human prostate cancer [abstract]. *J Nucl Med.* 2006;47(suppl 1):421P–422P.
40. Bandyopadhyay S, Pai SK, Watabe M, et al. FAS expression inversely correlates with PTEN level in prostate cancer and a PI 3-kinase inhibitor synergizes with FAS siRNA to induce apoptosis. *Oncogene.* 2005;24:5389–5395.
41. Lupu R, Menendez JA. Pharmacological inhibitors of fatty acid synthase (FASN)–catalyzed endogenous fatty acid biosynthesis: a new family of anticancer agents? *Curr Pharm Biotechnol.* 2006;7:483–493.
42. Kuhajda FP. Fatty acid synthase and cancer: new application of an old pathway. *Cancer Res.* 2006;66:5977–5980.
43. Knowles LM, Smith JW. Genome-wide changes accompanying knockdown of fatty acid synthase in breast cancer. *BMC Genomics* [serial online]. 2007;8:168. Available at: http://www.biomedcentral.com/1471-2164/8/168.
44. Hager MH, Soloman KR, Freeman MR. The role of cholesterol in prostate cancer. *Curr Opin Clin Nutr Metab Care.* 2006;9:379–385.
45. Porstmann T, Griffiths B, Chung Y-L, et al. PKB/Akt induces transcription of enzymes involved in cholesterol and fatty acid biosynthesis via activation of SREBP. *Oncogene.* 2005;24:6465–6481.

Chapter 7
Fatty Acid Synthase Activity in Tumor Cells

Joy L. Little and Steven J. Kridel

Abstract While normal tissues are tightly regulated by nutrition and a carefully balanced system of glycolysis and fatty acid synthesis, tumor cells are under significant evolutionary pressure to bypass many of the checks and balances afforded normally. Cancer cells have high energy expenditure from heightened proliferation and metabolism and often show increased lipogenesis. Fatty acid synthase (FASN), the enzyme responsible for catalyzing the ultimate steps of fatty acid synthesis in cells, is expressed at high levels in tumor cells and is mostly absent in corresponding normal cells. Because of the unique expression profile of FASN, there is considerable interest not only in understanding its contribution to tumor cell growth and proliferation, but also in developing inhibitors that target FASN specifically as an anti-tumor modality. Pharmacological blockade of FASN activity has identified a pleiotropic role for FASN in mediating aspects of proliferation, growth and survival. As a result, a clearer understanding of the role of FASN in tumor cells has been developed.

Keywords Cancer · fatty acid synthase · lipogenesis

Abbreviations FASN, fatty acid synthase ACC, acetyl-CoA-carboxylase ACL, ATP-citrate lyase NADPH, nicotinamide adenine dinucleotide phosphate MAT, malonyl acetyl transferases KS, ketoacyl synthase KR, β-ketoacyl reductase DH, β-hydroxyacyl dehydratase ER, enoyl reductase TE, thioesterase ACP, acyl carrier protein VLCFA, very long chain fatty acids ELOVL, elongation of very long chain fatty acids SCD1, stearoyl-CoA desaturase-1 AMPK, AMP-activated kinase ME, malic enzyme FASKOL, liver-specific deletion of FAS PPARα, Peroxisome Proliferator-Activating Receptor alpha HMG-CoA, 3-hydroxy-3-methyl-glutaryl-CoA SREBP, sterol response element binding protein S1P, site-one protease S2P, site-two

S.J. Kridel
Department of Cancer Biology and Comprehensive Cancer Center, Wake Forest University School of Medicine, Medical Center Boulevard, Winston-Salem, NC 27157, USA

P.J. Quinn, X. Wang (eds.), *Lipids in Health and Disease*,

protease RIPCre, Cre-recombinase under the control of rat insulin 2 promoter CPT1, carnitine palmityl transferase 1 MCD, malonyl-CoA desaturase SCAP, SREBP cleavage activating protein NF-Y, nuclear factor Y SP1, stimulatory protein 1 RNAi, RNA interference PI3K, phosphatidylinositol-3 kinase KGF, keratinocyte growth factor EGF, epidermal growth factor JNK, cJun N-terminal kinase RTK, receptor tyrosine kinase AR, androgen receptor PR, progesterone receptor USP2a, ubiquitin-specific protease 2a EGCG, epigallocatechin-3-gallate TOFA, 5-(tetradecyloxy)-2-furoic acid FDA, food and drug administration.

7.1 Fatty Acid Synthesis

7.1.1 The FASN Enzyme

One of the metabolic hallmarks of a tumor cell is increased lipogenesis (Kuhajda, 2006; Swinnen et al., 2006). In fact, in many instances the vast majority of fatty acids in tumors are synthesized *de novo* (Ookhtens et al., 1984). In mammalian cells, fatty acid synthase (FASN) is the central enzyme of long chain fatty acid synthesis. FASN is a multifunctional polypeptide that is comprised of seven separate functional domains (Fig. 7.1A). The individual domains of FASN work in concert to catalyze thirty-two different reactions to synthesize the sixteen carbon fatty acid palmitate, using acetyl-CoA and malonyl-CoA as substrates and nicotinamide adenine dinucleotide phosphate (NADPH) as an electron donor. The fatty acid synthesis reaction mechanism can be separated into three functional groupings: (1) to bind and condense the substrates, (2) to reduce the intermediates and (3) to release the final saturated long chain fatty acid palmitate (Fig. 7.1B). The malonyl acetyl transferase (MAT) domain binds malonyl-CoA and acetyl-CoA, while the ketoacyl synthase (KS) domain acts to condense the acyl chain (Fig. 7.1B). This β-ketoacyl moiety is then reduced in steps by the β-ketoacyl reductase (KR), β-hydroxyacyl dehydratase (DH), and enoyl reductase (ER) domains to a saturated acyl intermediate. This derivative can then be elongated by repeating the reactions catalyzed by the five previous enzyme activities for seven cycles until the thioesterase (TE) domain cleaves the final product, the sixteen carbon fatty acid palmitate. Throughout the entire synthesis of palmitate, the acyl carrier protein (ACP) acts as a coenzyme to bind intermediates by a 4'-phosphopantetheine group (Fig. 7.1B). In total, approximately 30 intermediates are involved in the process, but it is the high specificity of the TE domain for a 16 carbon fatty acid, as well as the MAT specificity for malonyl-CoA, that are responsible for preventing leakage of intermediates (Wakil, 1989). The overall FASN reaction is as follows:

$$\text{Acetyl-CoA} + 7\text{Malonyl-CoA} + 14\text{NADPH} + 14\text{H}^+ \rightarrow$$
$$\text{Palmitic-acid} + 7\text{CO}_2 + 8\text{CoA} + 14\text{NADP}^+ + 6\text{H}_2\text{O}$$

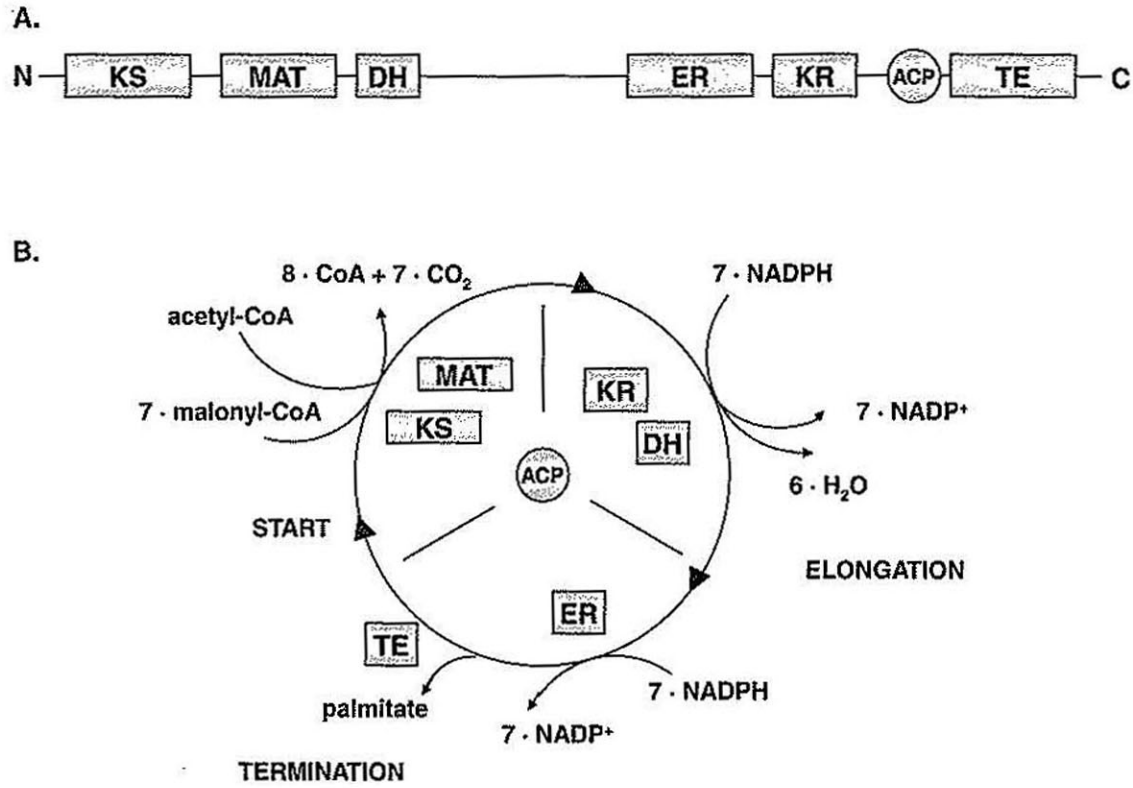

Fig. 7.1 The FASN Enzyme. **A.** The FASN polypeptide comprises seven functional domains: the ketoacyl synthase (KS), malonyl acetyl transferase (MAT), β-hydroxyacyl dehydratase (DH), enoyl reductase (ER), β-ketoacyl reductase (KR), the acyl carrier protein (ACP), and thioesterase (TE) domains. **B.** The FASN reaction mechanism. The MAT domain of the enzyme binds malonyl-CoA and acetyl-CoA, while the KS domain acts to condense the growing acyl chain. The resulting β-ketoacyl moiety is then reduced in steps by the KR, DH, and ER to a saturated acyl intermediate. This process is repeated in seven cycles, after which, the TE domain releases the sixteen carbon fatty acid palmitate

The structure of FASN has yet to be definitively characterized, as there are two distinct models (Smith, 2006). Early complementation studies suggest that FASN functions as a homodimer in head-to-tail conformation with two simultaneous reactions beginning in one subunit and finishing in the other (Wakil, 1989; Smith et al., 2003; Rangan et al., 1998; Rangan et al., 2001). However a more recent crystal structure analysis of porcine FASN challenges this historical model. The 4.5 Å structure reveals FASN as an intertwined dimer in a conformation resembling an "X" with one central core region with two arms and two legs (Maier et al., 2006). However, at this lower resolution, the definitive placement of the flexible TE domain and ACP is not possible. It is also unclear whether the body of the FASN complex can be identified as two distinct monomers. In this model, the KS domain is near the bottom of the central core of the complex and two MAT domains are in the "legs" of the X shape. The DH domains are located in the top half of the central region just under the ER domains. Adjacent to the ER domains are the KR domains that comprise the "arms" of this X complex. The study equates the reaction

pockets of this structure as having "double hot dog" folds but observes asymmetry of the two sides of the reaction chambers that may reveal hinge regions that allow different conformations of the FASN complex (Maier et al., 2006; Smith, 2006).

7.1.2 Other Players in the Fatty Acid Synthesis Pathway

While FASN is the central enzyme of fatty acid synthesis, other enzymes and pathways upstream of FASN are required to generate and supply substrates. Glucose enters the cell and is converted through glycolysis to pyruvate which is then shuttled into the mitochondria to enter the citric acid cycle. Citrate is shuttled out of the mitochondria, where ATP-citrate lyase (ACL) catalyzes the conversion of citrate to oxaloacetate and acetyl-CoA. Acetyl-CoA Carboxylase (ACC) catalyzes the conversion of acetyl-CoA to malonyl-CoA in the rate limiting and first committed step of lipogenesis. Unlike FASN, which is primarily regulated transcriptionally, ACC is negatively regulated by post-translational phosphorylation at serine 79 by AMP-activated kinase (AMPK). Energy deficiency stimulates AMPK to regulate energy consumption of cells, specifically by regulating ACC among other enzymes. Fatty acid synthesis requires NADPH, which is provided through the hexose monophosphate shunt and malic enzyme (ME) to donate electrons (Wakil et al., 1983). Recent findings also suggest that glutamine metabolism can generate sufficient NADPH in glycolytic tumor cells, as well as act as a carbon source for fatty acid synthesis (Deberardinis et al., 2007).

After fatty acid synthesis, downstream enzymes can further modify palmitate for various cellular functions. In the endoplasmic reticulum, the 16 carbon fatty acid can be modified to fatty acids with eighteen or more carbons known as very long chain fatty acids (VLCFA), such as stearate (18:0) by a family of elongase enzymes called elongation of very long chain fatty acids (ELOVL1-6) (Jakobsson et al., 2006). Palmitate and stearate can also be desaturated by stearoyl-CoA desaturase-1 (SCD1) at the cis-9 carbon to palmitoleate (16:1) and oleate (18:1), respectively (Sampath and Ntambi, 2005).

7.2 FASN Expression

7.2.1 FASN Expression in Normal Cells

In normal tissue, FASN is expressed and active in cells that have a high lipid metabolism, such as liver and adipose tissues, to generate triglycerides in response to excess caloric intake (Jayakumar et al., 1995; Volpe and Marasa,

1975; Wakil et al., 1983). FASN is also expressed in a niche-specific manner in specialized tissues such as lactating mammary glands (Kusakabe et al., 2000; Thompson and Smith, 1985) cycling endometrium (Pizer et al., 1997; Kusakabe et al., 2000), and various other cell types including type II alveolar cells to produce lung surfactant (Buechler and Rhoades, 1980; Kusakabe et al., 2000), brain cells (Kusakabe et al., 2000; Jayakumar et al., 1995), and seminal vesicles to produce seminal fluid (Kusakabe et al., 2000). FASN is only weakly detectable, if at all, in other rapidly dividing normal tissues such as the intestinal epithelium, stomach epithelium, and hematopoietic cells in adults and is not detectable in most other adult tissues (Kusakabe et al., 2000).

Despite the low expression profile in most adult tissues, FASN is critical for developing embryos and is highly expressed in proliferative fetal cells (Kusakabe et al., 2000). The importance of FASN in development is underscored by the fact that mice with homozygous deletions of the *FASN* gene display an embryonic lethal phenotype (Chirala et al., 2003). *FASN* $^{-/-}$ mice die before implantation around embryonic day 3.5, most likely because developing embryos are unable to acquire enough fatty acids from the mother for adequate membrane biogenesis. The importance of FASN during development is further highlighted by the fact that the majority of heterozygotes are also resorbed after implantation. Those that survive do not live long beyond birth, indicating that one *FASN* allele is usually insufficient for embryogenesis, implantation, and developing tissues (Chirala et al., 2003). The importance of the fatty acid synthesis pathway in development is further supported by the demonstration that deletion of *ACC1* in mice also results in an embryonic lethal phenotype (Abu-Elheiga et al., 2005).

Mice harboring tissue-specific deletions of *FASN* have been generated to facilitate understanding of the role of FASN in normal tissue. To date *FASN* has been deleted in liver, β-cells, and hypothalamus (Chakravarthy et al., 2005, 2007). To knock out *FASN* in the liver, mice with a "floxed" *FASN* allele were crossed with mice harboring an allele of Cre driven by a rat albumin promoter. Although this liver-specific deletion of *FASN* (FASKOL) leaves animals viable without severe physiological effects, it is not without consequence. When FASKOL mice are fed a diet containing zero fat or are fasted for prolonged periods, they develop symptoms similar to those seen in mice engineered to lack Peroxisome Proliferator-Activating Receptor alpha (PPARα) (Kersten et al., 1999). Both *PPARα* knockout and FASKOL mice become hypoglycemic, develop steatosis (fatty liver) that correlates with reduced serum and liver cholesterol, reduced expression of 3-hydroxy-3-methyl-glutaryl-CoA (HMG-CoA) reductase, decreased cholesterol biosynthesis activity, and elevated sterol response element binding protein 2 (SREBP-2) expression. While the hypoglycemia and fatty liver may be reversed with dietary fat, all effects including cholesterol biosynthesis, HMG-CoA reductase and SREBP2 levels, as well as cholesterol levels in the serum and liver are rescued by administration of a PPARα agonist. This reveals distinct levels of metabolic regulation between *de novo* and dietary fat and indicates that products downstream of FASN activity regulate

cholesterol, glucose, and fatty-acid homeostasis in the liver through activation of PPARα (Chakravarthy et al., 2005). Interestingly, mice with a liver-specific knockout of *ACC1* are still able to undergo fatty acid synthesis, but this discrepancy can be attributed to compensatory production of malonyl-CoA by the ACC2 isoform (Harada et al., 2007).

To determine whether FASN plays a role in pancreatic β-cell function, a knockout of *FASN* was generated. Crossing floxed *FASN* mice with mice harboring Cre under the control of rat insulin 2 promoter (RIPCre) causes specific deletion of *FASN* in pancreatic β-islet cells, as well as the hypothalamus, a region of the brain known for controlling motivational states, such as feeding. The resulting *FASN* knockout (FASKO) mice exhibit reduced feeding behavior and are highly active, even while maintained on a high fat diet (Chakravarthy et al., 2007). This correlates with studies showing the small molecule FASN inhibitor C75 acts in the hypothalamus to stimulate fatty acid oxidation via carnitine palmityl transferase 1 (CPT1) and induces a reversible anorexic phenotype (see Section 7.4.2). Interestingly, the β-cells lacking FASN are unaffected as loss of FASN does not alter insulin or glucose levels during glucose tolerance testing or stimulation either *in vivo* or *in vitro*. Therefore, the fasting phenotype of FASKO mice appears to be solely attributable to the effects on the hypothalamus. As a matter of fact, this observation is in agreement with a recent study showing FASN is not required for normal insulin secretion of β-cells *in vitro* (Joseph et al., 2007). Intracerebroventricular injection of FASKO mice with a small molecule drug Wy14,643 to activate PPARα restores feeding and weight gain, indicating that FASN controls PPARα activation in the hypothalamus. Pharmacological activation of PPARα in these mice also restores expression of CPT-1 and malonyl-CoA desaturase (MCD) that control cellular levels of malonyl-CoA by controlling the rate of transfer of fatty acids into the mitochondria for β-oxidation and malonyl-CoA stability, respectively (Chakravarthy et al., 2007). These studies elucidate the importance of FASN in energy homeostasis and provide a mechanism through which FASN can regulate its effects.

7.2.2 FASN Expression in Tumor Cells

As discussed above, FASN has historically been studied in relation to normal physiology and as a central mediator of energy balance. In the last few decades, however, it has become clear that FASN is associated with tumor development. Accordingly, high FASN expression has been identified in many tumor types (Kuhajda, 2000, 2006). Haptoglobin-related protein (Hpr) was demonstrated to correlate with breast cancer stage, prognosis, as well as recurrence and patient survival (Kuhajda, et al., 1989a,b). Shortly after this observation, Hpr, or oncogenic antigen (OA-519) protein was identified as FASN (Kuhajda et al.,

1994). Since these discoveries, FASN upregulation has been demonstrated in every type of solid tumor. An initial retrospective study showed FASN expression correlated with staining of the proliferation marker MIB-1 to predict survival of breast cancer patients (Jensen et al., 1995). Subsequent studies confirmed the association of FASN with breast cancer recurrence, as well as shorter overall and disease-free survival in early breast cancer patients (Alo et al., 1996, 1999b). Breast cancer is not the only tumor type with elevated FASN levels. FASN expression is associated with prostate cancer prognosis, progression, and stage (Shurbaji, et al., 1992, 1996; Epstein et al., 1995). As a matter of fact, FASN is upregulated in androgen-independent prostate tumors and expression correlates with disease stage, as the highest levels of FASN expression are in androgen independent metastases (Pizer et al., 2001; Rossi et al., 2003). FASN expression correlates with poor prognosis, advanced progression, and/or decreased survival in a number of other cancers of different origins including: ovarian (Gansler et al., 1997; Alo et al., 2000), melanoma (Innocenzi et al., 2003; Kapur et al., 2005), nephroblastoma (Wilms tumor) (Camassei et al., 2003b), retinoblastoma (Camassei et al., 2003a), bladder (Visca et al., 2003), pancreas (Alo et al., 2007), soft tissue sarcoma (Takahiro et al., 2003), non-small cell lung cancer (Visca et al., 2004), endometrium (Sebastiani et al., 2004), and Paget's disease of the vulva (Alo et al., 2005). While FASN expression correlates with decreased survival and/or poor prognosis in a large number of tumor types, there are tumor types that show elevated FASN expression but no correlation with patient survival or disease stage (Rashid et al., 1997; Nemoto et al., 2001; Silva et al., 2008). In addition, there are several tumor types that show increased FASN expression, but correlation with disease progression or patient survival has not been investigated or published at this time. These tumors include hyperplastic parathyroid (Alo et al., 1999a), stomach carcinoma (Kusakabe et al., 2002), mesothelioma (Gabrielson et al., 2001), glioma (Zhao et al., 2006), and hepatocellular carcinoma (Yahagi et al., 2005).

Increased FASN expression in tumors is an early, common event (Swinnen et al., 2002; Myers et al., 2001) and its correlation with reduced survival and increased recurrence rationalizes the potential for anti-FASN tumor therapeutics (Kuhajda, 2000, 2006; Kridel et al., 2007). As evidence that lipogenesis as a whole is important in cancer, many of the enzymes upstream of FASN show altered expression patterns in human tumor cells, as well. For instance, ACL is overexpressed in cancer cells of breast and bladder (Szutowicz et al., 1979; Turyn et al., 2003). ACC is overexpressed in breast and prostate cancer cells (Milgraum et al., 1997; Swinnen et al., 2000b, 2006; Heemers et al., 2003). Interestingly, the tumor suppressor breast cancer susceptibility gene 1 (BRCA1) can bind the phosphorylated inactive ACC to prevent re-activation (Moreau et al., 2006). In addition, squamous cell carcinomas of the lung show lower immunohistochemical staining of phosphorylated inactive ACC than adenocarcinoma with poor prognosis (Conde et al., 2007). The strong

functional correlation between upstream mediators of fatty acid synthesis and cancer underscores the importance of this pathway in tumor biology.

7.3 FASN Regulation

7.3.1 FASN Regulation in Normal Cells

In nonmalignant tissues, FASN expression is primarily regulated at the transcriptional level (Fig. 7.2A) (Hillgartner et al., 1995). There is a single *FASN* gene and the signals in normal cells that stimulate *FASN* transcription are numerous but strictly defined (Amy et al., 1990). Transcription of *FASN* is stimulated by dietary carbohydrate, glucose, insulin, amino acids, sterols and cyclic-AMP through specific response elements (Paulauskis and Sul, 1988; Rufo et al., 2001; Foufelle et al., 1992; Moustaid et al., 1994; Wang and Sul, 1998; Wakil et al., 1983; Rangan et al., 1996; Wakil, 1989). Hormones such as the thyroid hormone triiodothyronine (T3) (Moustaid and Sul, 1991), progesterone (Lacasa et al., 2001), androgen (Heemers et al., 2003) and adrenal glucocorticoids (Volpe and Marasa, 1975) can also upregulate FASN in liver and adipose tissues. *FASN* transcription is mediated by multiple transcription factors.

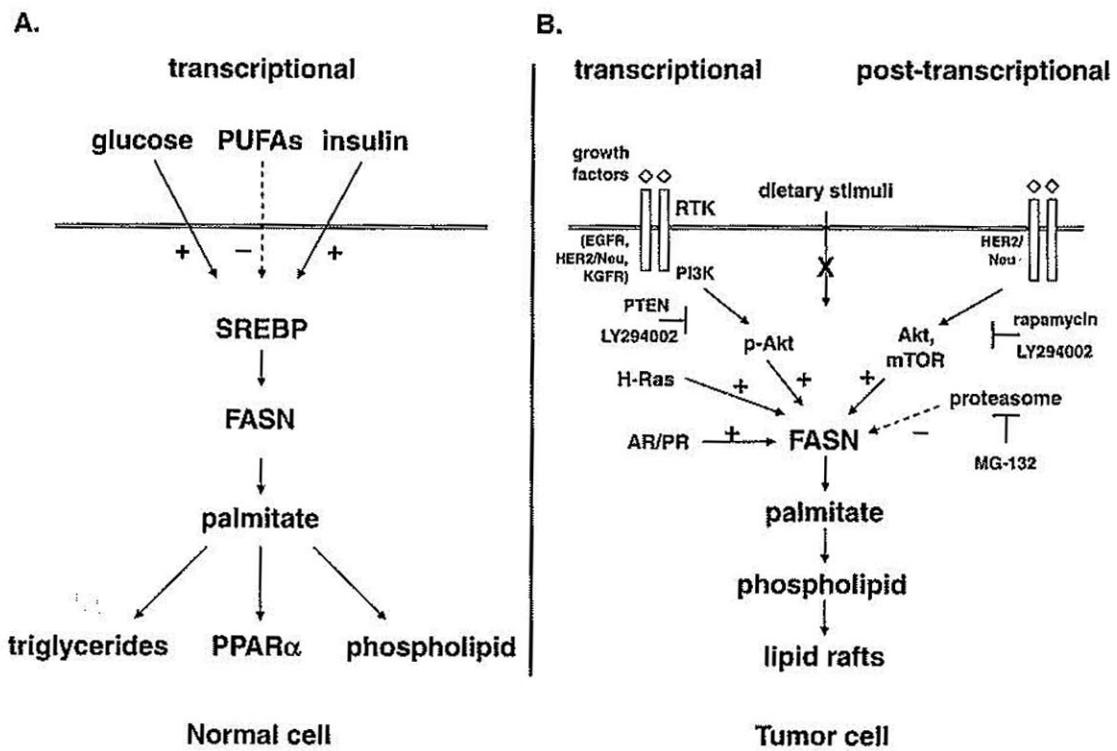

Fig. 7.2 Regulation of FASN Expression in Normal and Tumor Cells. **A.** In normal cells (hepatocytes and adipocytes) FASN expression is primarily regulated through transcriptional mechanisms. **B.** In tumor cells, FASN expression is regulated by transcriptional and non-transcriptional mechanisms via multiple pathways

Upstream stimulatory factors (USFs) are required for insulin mediation of FASN expression, but other factors such as nuclear factor Y (NF-Y) and stimulatory protein 1 (SP1) can also play a role in *FASN* transcription (Teran-Garcia et al., 2007; Bennett et al., 1995). However, the vast majority of FASN-regulatory signals act through a family of transcription factors known as sterol response element binding proteins (SREBPs) that control lipid homeostasis and bind to various elements in the *FASN* promoter. There are three SREBP family members: SREBP-1a, SREBP-1c, and SREBP-2. SREBP-1a and SREBP-1c have been most widely linked to regulation of lipogenic gene transcription, while SREBP-2 is most linked to cholesterol metabolism. The SREBPs exist as endoplasmic reticulum membrane bound precursors that are activated after proteolytic processing by site-one and site-two proteases (S1P, S2P). When sterol levels are low, S1P cleaves the SREBP molecule to release the N terminal portion from the endoplasmic reticulum (Sakai et al., 1998). SREBP then binds to the SREBP cleavage activating protein (SCAP) and is translocated to the Golgi where S2P further processes the molecule so that the transcription factor is activated. The processed SREBP then translocates to the nucleus to bind specific E box motifs and sterol response elements (SREs) (Magana and Osborne, 1996). There is evidence that dietary factors stimulate the expression of FASN in a manner mediated through signaling pathways such as the phosphoinositide-3 kinase (PI3K) pathway. For instance, nonmalignant 3T3-L1 adipocytes regulate insulin-mediated FASN expression through Akt in a manner independent of both mitogen activated protein kinase (MAPK) and P70 S6 kinase, but dependent on SREBPs (Wang and Sul, 1998; Porstmann et al., 2005).

Expression of FASN is tightly controlled so that transcription does not continue unabated under typical circumstances. Polyunsaturated fatty acids (PUFAs) (Xu et al., 1999; Moon et al., 2002; Jump et al., 1994), sterols (Adams et al., 2004; Bennett et al., 1995), and leptin (Fukuda et al., 1999) all act to repress FASN transcription and do so by specifically down-regulating SREBP-1 in hepatocytes (Worgall et al., 1998; Teran-Garcia et al., 2007). This highly complex organization of checks and balances for FASN expression is necessary to supply the cell with essential *de novo* fatty acids for cellular function and growth (Fig. 7.2A). Just as importantly, controls keep the cell from continuing unnecessary lipogenesis.

7.3.2 FASN Regulation in Tumor Cells

While FASN expression is tightly controlled through dietary and hormonal stimuli in nonmalignant cells, tumor cells ignore these restrictions and increase FASN beyond typical levels (Fig. 7.2B). In fact, an early study of orthotopic hepatomas revealed that while low-fat, high-fat, and high-cholesterol diets all affected rates of fatty acid synthesis in the normal liver, the rates of hepatoma

fatty acid synthesis were unchanged (Sabine et al., 1967). It has since been discovered that deregulation of upstream signals drive FASN expression in a manner that is largely transcriptional in tumors (Fig. 7.2B) (Swinnen et al., 2006).

Overexpression of FASN in tumor cells is induced at the transcriptional level by receptor tyrosine kinase (RTK)-stimulation of Ras and Akt (Fig. 7.2B). Keratinocyte growth factor (KGF) can induce the Akt- and cJun N-terminal kinase (JNK)-dependent expression of FASN in pulmonary cancer cells (Chang et al., 2005). Epidermal growth factor (EGF) has also been shown to increase FASN in prostate cancer cells (Swinnen et al., 2000a).

In addition to growth factor signaling, activation of the RTK HER2/Neu is linked with *FASN* expression in tumor cells. HER2/Neu upregulates PI3K-dependent *FASN* transcription in breast cancer cells (Kumar-Sinha et al., 2003; Yoon et al., 2007). Interestingly, blocking HER2/Neu with Herceptin decreases FASN expression (Kumar-Sinha et al., 2003). In fact, there appears to be a crosstalk between these pathways, as inhibition of FASN activity leads to the downregulation of HER2/NEU (Menendez et al., 2004). While HER2/Neu is primarily associated with breast cancer progression, HER2/Neu and FASN expression correlate in squamous cell carcinomas of the tongue, as well (Silva et al., 2008). Surprisingly, HER2/Neu can also regulate FASN expression in prostate cancer cells (Yeh et al., 1999). These data suggest there is a coordinate regulation of activated HER2/Neu and FASN upregulation in tumor cells.

Downstream of RTK signaling, the PI3K/Akt pathway has been shown to upregulate FASN. Loss of PTEN is a frequent transformation event in cancer, that leads to a gain of function in Akt signaling (Mulholland et al., 2006; Blanco-Aparicio et al., 2007). In prostate cancer cells, this signaling cascade drives androgen receptor (AR)-mediated oncogenic transcription and progression to metastatic disease (Wang et al., 2003; Mulholland et al., 2006). The PTEN-null LNCaP tumor cell line has high levels of FASN. Reintroducing PTEN or using the PI3K inhibitor LY294002 can decrease FASN expression, whereas introducing constitutively active Akt can restore FASN expression (Van de Sande et al., 2002). The connection between FASN expression and PI3K activity is further observed in prostate carcinoma samples with high Gleason scores, where high FASN expression correlates with phosphorylated Akt that is localized to the nucleus (Van de Sande et al., 2005). Moreover, a crosstalk between these pathways has been identified. In ovarian cancer cell lines, phosphorylated Akt correlates with and drives FASN expression. Conversely, inhibiting FASN results in decreased Akt phosphorylation (Wang et al., 2005). These data suggest that PI3K signaling through Akt is an important mediator of *FASN* transcription in tumor cells.

In addition to RTK-driven stimulation of Akt, there is evidence that the small GTP-ase protein Ras can influence FASN expression in tumors. Constitutively active H-ras induces increased PI3K and MAPK-dependent FASN expression in MCF-10A cells (Yang et al., 2002). Consistent with this notion, the expression of activated K-ras correlates with FASN expression in human

colorectal cancer samples (Ogino, et al., 2006, 2007). Altogether, these data suggest that RTK signaling, Ras, and PI3K-Akt pathways can drive transcriptional up-regulation of FASN expression in tumor cells (Fig. 7.2B).

Not surprisingly, hormones are another common factor driving FAS expression in tumor cells (Fig. 7.2B). Progestins stimulate FASN expression in breast cancer cells (Chalbos et al., 1987; Lacasa et al., 2001; Menendez et al., 2005a). Consistent with this finding, increased FASN expression in endometrial carcinoma correlates with expression of both estrogen and progesterone receptors (PR) (Pizer et al., 1998b). In prostate cancer, FASN expression can be regulated by androgens in prostate cancer through upregulation of transcription factors such as S14 and SREBPs (Swinnen et al., 1997a,b; Heemers et al., 2000, 2001). In addition, HER2/Neu can drive activation of AR in prostate cancer cells to increase MAPK-dependent induction of FASN in the absence of androgen (Yeh et al., 1999).

While the main mechanism of FASN overexpression in tumors is through transcriptional upregulation, there is also evidence that FASN is regulated by post-transcriptional mechanisms (Fig. 7.2B). For instance, HER2/Neu driven expression of both FASN and ACC can be regulated at the translational level through Akt, PI3K, and mTOR-dependent mechanisms (Yoon et al., 2007). FASN stabilization is tightly linked with the de-ubiquitinating enzyme ubiquitin-specific protease 2a (USP2A) in prostate cancer cells. USP2A is androgen regulated and is not only upregulated similarly to FASN, but actually interacts with FASN to enhance FASN stability (Graner et al., 2004). Treating prostate tumor cells with the proteasome inhibitor MG-132, also increases FASN expression, further supporting evidence that FASN is regulated by the proteasome (Graner et al., 2004). Interestingly, yeast studies provided early evidence of FASN regulation by proteasomal degradation (Egner et al., 1993). It is also worth mentioning that FASN can also be upregulated in cancer cells by *FASN* gene amplification (Shah et al., 2006). The fact that numerous mechanisms act to increase FASN expression in tumor cells highlights the importance of FASN in tumor progression.

7.3.3 Palmitate Utilization in Normal and Tumor Cells

Upregulation of FASN activity causes the increased production of fatty acids, particularly palmitate. While the mechanisms that drive FASN expression are different in tumors as compared to normal cells, the utilization of its products differs, as well. Fatty acids are used for a variety of cellular functions. In nonmalignant adipose and hepatic tissue, palmitate is incorporated into triglycerides for secretion and storage to be ultimately used as an energy source through β-oxidation (Thupari et al., 2002). Fatty acids such as palmitate can also comprise a regulatory pool that activates energy mediators such as PPARα in the liver and hypothalamus (Chakravarthy, et al., 2005, 2007). In addition,

key signaling molecules, such as Ras and Hedgehog, can be palmitoylated to target these proteins to cellular membranes (Resh, 2006). So far, a link between protein palmitoylation and FASN activity has not been established though. In development, fatty acids can segregate into phospholipids to create cellular membranes (Chirala et al., 2003). Similarly, tumor FASN-derived palmitate segregates into phospholipid microdomains known as lipid rafts (Fig. 7.2B) (Swinnen et al., 2003). Lipid rafts are involved in a number of key biological functions including signal transduction, polarization, trafficking, and migration (Freeman et al., 2005, 2007). Considering that palmitate can ultimately be used for a number of cellular processes, including being elongated and desaturated for subsequent events, it is apparent that FASN occupies an important niche in tumor cells.

7.4 Inhibiting FASN Activity

7.4.1 Small Molecule Inhibitors of FASN

Because of the unique expression of FASN in tumors, much emphasis has been put toward the development of pharmacological agents that inhibit FASN activity and, therefore, inhibit tumor growth and progression. Historically, a *Cephalosporium caerulens* mycotoxin metabolite known as cerulenin [(2S, 3R)-2,3-epoxy-4-oxo-7,10-dodecadienoylamide] has been the primary FASN inhibitor used in biological studies. Cerulenin covalently binds the β-ketoacyl synthase domain in FASN that is responsible for binding and condensing the substrates (Funabashi et al., 1989). More recently, C75 was formulated as a synthetic analog of cerulenin due to instability and poor systemic availability of cerulenin (Kuhajda et al., 2000). C93 is the newest generation of C75 analogues (Zhou et al., 2007). Both C75 and C93 target the β-ketoacyl synthase activity of FASN (Kuhajda et al., 2000; Zhou et al., 2007). Recently, orlistat (Xenical©), a FDA-approved drug for obesity that targets gastrointestinal lipases, was described as a novel inhibitor of FASN thioesterase activity (Kridel et al., 2004). There also exists a growing body of literature showing that various natural products such as the green tea polyphenolic component epigallocatechin-3-gallate (EGCG) can inhibit FASN activity (Tian, 2006).

7.4.2 Effects In Vivo

To date, all small molecule inhibitors of FASN have demonstrated ability to block tumor growth *in vivo*. Cerulenin greatly increases survival and delays progression of ovarian cancer xenografts without significantly affecting fatty acid synthesis in the liver (Pizer et al., 1996b). C75 reduces growth of several tumor xenograft models, including prostate, breast, ovarian and mesothelioma

(Pizer et al., 2000, 2001; Wang et al., 2005; Gabrielson et al., 2001). C93 and C75 both reduce ovarian and lung cancer xenograft growth (Zhou et al., 2007; Orita et al., 2007). The novel FASN inhibitor orlistat has also been shown to inhibit prostate tumor xenograft growth (Kridel et al., 2004). FASN inhibitors also work in genetic models of tumorigenesis, including the *Neu-N* murine mammary transgenic model (Hennigar et al., 1998; Pflug et al., 2003; Alli et al., 2005). While FASN inhibitors are not typically given orally due to poor bioavailability, recent work shows that C93 can work *in vivo* after oral administration (Orita et al., 2007). Surprisingly, cerulenin, C75 and related compounds induce a reversible anorexic phenotype that is associated with β-oxidation in the hypothalamus. This phenotype is mimicked in mice with *FASN* deleted in the hypothalamus (see Section 7.2.1) (Loftus et al., 2000; Thupari et al., 2004; Tu et al., 2005; Orita et al., 2007; Chakravarthy et al., 2007). Interestingly, the anorexic effect of FASN inhibitors has been overcome with newer generation drugs like C93 that can reduce tumor growth with no anorexic effect (Orita et al., 2007). The discrepancy between the knockout studies and pharmacological findings has yet to be explained.

7.4.3 *Cell Cycle Effects* In Vitro

To determine the cellular consequences of FASN inhibition, numerous studies have focused on the *in vitro* anti-tumor effects of these inhibitors. Many studies have linked FASN inhibitors with cell cycle and growth arrest (Fig. 7.3). Cerulenin acts *in vitro* to inhibit fatty acid synthesis-mediated growth of breast carcinoma cells that can be rescued with palmitate (Kuhajda et al., 1994). Cerulenin induces a block at the G2/M cell cycle checkpoint in an androgen-independent

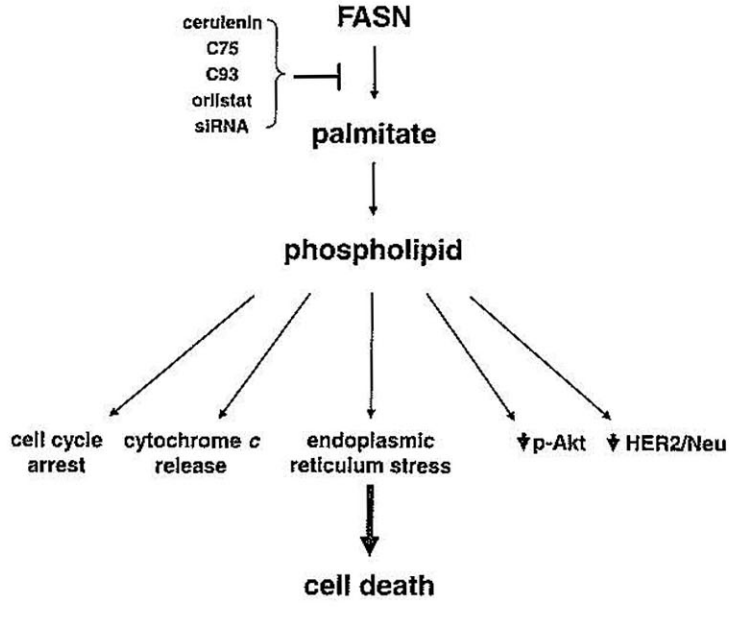

Fig. 7.3 Inhibiting FASN in Tumor Cells. Several small molecule drugs can inhibit FASN activity. Blockade of FASN activity leads to a reduction in lipogenesis and phospholipid content in tumor cells. Inhibiting FASN also induces cycle arrest, cytochrome *c* release, and endoplasmic reticulum stress. In addition, FASN inhibitors can reduce the activation and expression of Akt and HER2/Neu

prostate cancer cell line that correlates with an induction of cyclin-dependent kinase inhibitors p21 and p27 (Furuya et al., 1997). However, glioma cells accumulate in S phase after cerulenin treatment (Zhao et al., 2006). Different hepatocellular carcinoma cell lines treated with C75 undergo either G1 or G2 cell cycle arrest independent of p53 status (Gao et al., 2006). In melanoma A-375 cells, cerulenin induces accumulation of cells in S phase, while C75 induces accumulation of G2/M phase cells (Ho et al., 2007). RKO colorectal cancer cells treated with either cerulenin or C75 show a transient accumulation of cells in S and G2/M phases, but accumulation in G1 and G2/M phases later (Li et al., 2001). Both cerulenin and C75 induce S phase arrest and inhibit DNA replication in breast, colorectal, and promyelocytic leukemia cancer cells (Pizer et al., 1998a). Orlistat induces cell cycle arrest by downregulating Skp2, a deubiquinating enzyme, leading to decreased turnover of p27/kip1, therefore blocking prostate tumor cells from entering S phase (Knowles et al., 2004). Orlistat has also been shown to induce an accumulation of breast cancer cells in S phase (Menendez et al., 2005b). Use of RNA interference (RNAi) to mediate knockdown of both the FASN and ACCα genes induces a decrease in S phase cells, further supporting the role of fatty acid synthesis in progression to or in S phase (Brusselmans et al., 2005). The data show there is little consensus on the phase that tumor cells arrest growth after inhibition of FASN in various tumor cells, which may be attributed to different tumor cell types. It is likely that a lack of *de novo* fatty acid synthesis in tumor cells impacts phospholipid synthesis required for proper DNA synthesis and cell cycle progression (Jackowski, 1994).

7.4.4 Cell Signaling Effects

The effects of FASN inhibitors are also mediated through key tumor signaling pathways. For example, it has been demonstrated that pharmacological inhibition of FASN activity results in reduced Akt activation in multiple tumor cell lines (Fig. 7.3) (Wang et al., 2005; Liu et al., 2006). As mentioned previously, it has been demonstrated that PI3K and Akt can drive FASN expression in tumor cells (Fig. 7.2B) (Van de Sande et al., 2002; Wang et al., 2005). The demonstration that reduced FASN activity negatively affects Akt activation identifies a feedback between the two pathways. Not surprisingly, inhibiting the PI3K pathway synergizes with cell death induced by genetic and pharmacological inhibition of *FASN* (Bandyopadhyay et al., 2005; Wang et al., 2005; Liu et al., 2006).

In addition to the PI3K pathway, HER2/Neu has also been linked with FASN expression in breast and prostate cancer cells (Kumar-Sinha et al., 2003; Yoon et al., 2007; Yeh et al., 1999). Inhibiting FASN with cerulenin and C75 reduces expression of Her2/neu expression in breast cancer cell lines (Fig. 7.3) (Menendez et al., 2004; Kumar-Sinha et al., 2003). Additionally, inhibiting Her2/Neu with Herceptin synergizes with FASN inhibitors to induce

cell death (Menendez et al., 2004). Altogether, these data indicate that the very pathways that drive FASN expression in malignant cells are also affected when FASN activity is blocked. Moreover, tumor cell killing can be potentiated when FASN inhibitors are combined with inhibitors of these signaling pathways. The reason for this crosstalk has not been clearly defined, but it is tempting to speculate that inhibition of FASN activity directly impacts on lipid raft function, which results in reduced kinase signaling.

7.4.5 In Vitro *Tumor Cell Death*

In addition to cell cycle arrest, all FASN inhibitors induce cell death in tumor cells (Pizer et al., 1996a, 1998a; Kridel et al., 2004; Zhou et al., 2007). Cerulenin induces breast and prostate cancer cell death that correlates with DNA fragmentation and morphology characteristic of apoptosis (Pizer, et al., 1996a, 2000; Furuya, et al., 1997). The mitochondria have also been linked to facilitation of cell death induced by cerulenin. For instance, the pro-apoptotic mitochondrial factor Bax is induced in cells treated with cerulenin. (Heiligtag et al., 2002). This correlation between cerulenin and the mitochondrial pathway of apoptosis is further supported by the induction of cytochrome *c* release (Fig. 7.3) (Heiligtag et al., 2002). FASN inhibition has been linked to p53 status of tumor cells, but whether p53 plays any role in FASN-expressing cells is unclear, as FASN is expressed in tumors independent of p53 status. FASN is strongly and significantly associated with p53 expression in hyperplastic parathyroids (Alo et al., 1999a). In various cancer cells, blocking p 53 activity with a dominant negative construct potentiates FASN inhibitor-induced cell death (Li et al., 2001). Conversely, others have reported that FASN inhibitors work equally well in tumors independent of p53 status (Heiligtag et al., 2002).

Cell death induced by FASN inhibitors could be a result of the cell lacking fatty acid for membrane biogenesis. Inhibiting FASN and ACC reduces incorporation of fatty acid into membrane phospholipids, which occurs in the endoplasmic reticulum (Zhou et al., 2003). Inhibiting FASN incorporation into phospholipids corresponds to a decrease in cell volume and other morphological changes ultimately leading to apoptosis (De Schrijver et al., 2003). Inhibiting FASN with small molecules (cerulenin, C75, orlistat), or with siRNAs induces endoplasmic reticulum stress and activation of the unfolded protein response (UPR) (Little et al., 2007). The UPR is able to induce cell death if homeostasis is not restored and, therefore, FASN inhibitors may be inducing cel death that is mediated by the UPR (Fig. 7.3) (Little et al., 2007).

When FASN is inhibited malonyl-CoA accumulates (Pizer et al., 2000). One hypothesis for the mechanism of FASN inhibitor-induced cell death is attributed to this accumulation of malonyl-CoA and, potentially, its interaction with CPT-1, the enzyme responsible for transferring fatty acids into the

mitochondria for oxidation. Malonyl-CoA acts as a natural inhibitor of CPT-1 activity to prevent fatty acids being simultaneously synthesized and then oxidized (McGarry et al., 1983). Driving this hypothesis is a study showing that co-treating breast or ovarian cancer cells with the ACC inhibitor 5-(tetradecyloxy)-2-furoic acid (TOFA) partially rescues cell death induced by FASN inhibitors C75 and cerulenin (Pizer et al., 2000; Zhou et al., 2003). However, C75 alone can increase CPT-1 activity and directly compete with malonyl-CoA (Thupari et al., 2002; Yang et al., 2005). Therefore, it is important to note that MCF-7 cells co-treated with C75 and the CPT-1 inhibitor etomoxir show no effect on C75-induced cell death (Zhou et al., 2003). Hence, malonyl-CoA accumulation, not CPT-1 activation, is mediating death induced by FASN inhibitors (Fig. 7.3). In addition, siRNA-mediated knockdown of FASN induces accumulation of ceramide and malonyl-CoA that leads to inhibition of CPT-1 and induction of apoptotic genes *BNIP3*, *TRAIL*, and *DAPK2* (Bandyopadhyay et al., 2006).

Upstream lipogenesis mediators ACL and ACC are also important in maintaining tumor cell survival. RNAi-mediated knockdown or chemical inhibition of ACL in human tumor cells decreases proliferation and induces cell death *in vitro* and limits tumor growth by stimulating differentiation of tumor cells *in vivo* (Hatzivassiliou et al., 2005). ACL inhibition can also can impair Akt-mediated tumorigenesis and induce tumor cell death (Bauer et al., 2005). In addition, silencing ACC using RNAi induces apoptosis in breast and prostate cancer cells (Brusselmans et al., 2005; Chajes et al., 2006). Chemical inhibition of ACC can also induce tumor cell death (Beckers et al., 2007). While the effects of FASN inhibitors on tumor cells are clearly pleiotropic, and in some cases maybe even specific to the tumor type, it is evident that many of the effects can ultimately be tied to decreases in de novo synthesized fatty acids which can be extended to phospholipid synthesis. Whatever the mechanisms may be, the data clearly suggest that FASN occupies an important regulatory position in tumor cells to facilitate the processes that lead to tumor cell proliferation and survival.

7.5 Concluding Remarks

In summary, FASN is upregulated in multiple tumor types and correlates with poor patient prognosis and reduced survival. Correspondingly, a body of literature has demonstrated a requirement of FASN activity for tumor cell viability. Phospholipids synthesized from FASN-derived palmitate are important for cell cycle progression, lipid raft signaling, and endoplasmic reticulum homeostasis, all of which contribute to tumor cell survival, thereby, underscoring the importance of FASN. These findings signify a central role for fatty acid synthesis in critical cellular processes. In addition, tumor cells have developed feedback mechanisms to mediate crosstalk between FASN and signaling

pathways like PI3-kinase and Her2/Neu. The discovery and development of pharmacological agents that block FASN activity suggest that FASN can be targeted for anti-tumor therapy. So far, anti-FASN drugs have successfully inhibited tumor growth in several tumor models with minimal side effects. Therefore, FASN represents a highly tractable anti-tumor target with significant clinical potential.

Acknowledgments The authors would like to apologize to those whose work we were unable to cite. We would also like to thank Isabelle Berquin and members of the Kridel laboratory for critical reading of the manuscript. Work in the Kridel laboratory is supported by the NIH/NCI (CA114104) and Department of Defense Prostate Cancer Research Program (W81XWH-07-1-0024).

References

Abu-Elheiga, L., Matzuk, M. M., Kordari, P., Oh, W., Shaikenov, T., Gu, Z. and Wakil, S. J., Mutant mice lacking acetyl-CoA carboxylase 1 are embryonically lethal, *Proc Natl Acad Sci USA* 102 (2005) 12011–12016.

Adams, C. M., Reitz, J., De Brabander, J. K., Feramisco, J. D., Li, L., Brown, M. S. and Goldstein, J. L., Cholesterol and 25-Hydroxycholesterol Inhibit Activation of SREBPs by Different Mechanisms, Both Involving SCAP and Insigs, *J Biol Chem* 279 (2004) 52772–52780.

Alli, P. M., Pinn, M. L., Jaffee, E. M., McFadden, J. M. and Kuhajda, F. P., Fatty acid synthase inhibitors are chemopreventive for mammary cancer in neu-N transgenic mice, *Oncogene* 24 (2005) 39–46.

Alo, P. L., Amini, M., Piro, F., Pizzuti, L., Sebastiani, V., Botti, C., Murari, R., Zotti, G. and Di Tondo, U., Immunohistochemical expression and prognostic significance of fatty acid synthase in pancreatic carcinoma, *Anticancer Res* 27 (2007) 2523–2527.

Alo, P. L., Galati, G. M., Sebastiani, V., Ricci, F., Visca, P., Mariani, L., Romagnoli, F., Lombardi, G. and Tondo, U. D., Fatty acid synthase expression in Paget's disease of the vulva, *Int J Gynecol Pathol* 24 (2005) 404–408.

Alo, P. L., Visca, P., Framarino, M. L., Botti, C., Monaco, S., Sebastiani, V., Serpieri, D. E. and Di Tondo, U., Immunohistochemical study of fatty acid synthase in ovarian neoplasms, *Oncol Rep* 7 (2000) 1383–1388.

Alo, P. L., Visca, P., Marci, A., Mangoni, A., Botti, C. and Di Tondo, U., Expression of fatty acid synthase (FAS) as a predictor of recurrence in stage I breast carcinoma patients, *Cancer* 77 (1996) 474–482.

Alo, P. L., Visca, P., Mazzaferro, S., Serpieri, D. E., Mangoni, A., Botti, C., Monaco, S., Carboni, M., Zaraca, F., Trombetta, G. and Di Tondo, U., Immunohistochemical study of fatty acid synthase, Ki67, proliferating cell nuclear antigen, and p53 expression in hyperplastic parathyroids, *Ann Diagn Pathol* 3 (1999a) 287–293.

Alo, P. L., Visca, P., Trombetta, G., Mangoni, A., Lenti, L., Monaco, S., Botti, C., Serpieri, D. E. and Di Tondo, U., Fatty acid synthase (FAS) predictive strength in poorly differentiated early breast carcinomas, *Tumori* 85 (1999b) 35–40.

Amy, C. M., Williams-Ahlf, B., Naggert, J. and Smith, S., Molecular cloning of the mammalian fatty acid synthase gene and identification of the promoter region, *Biochem J* 271 (1990) 675–679.

Bandyopadhyay, S., Pai, S. K., Watabe, M., Gross, S. C., Hirota, S., Hosobe, S., Tsukada, T., Miura, K., Saito, K., Markwell, S. J., Wang, Y., Huggenvik, J., Pauza, M. E., Iiizumi, M. and Watabe, K., FAS expression inversely correlates with PTEN level in prostate cancer

and a PI 3-kinase inhibitor synergizes with FAS siRNA to induce apoptosis, *Oncogene* 24 (2005) 5389–5395.

Bandyopadhyay, S., Zhan, R., Wang, Y., Pai, S. K., Hirota, S., Hosobe, S., Takano, Y., Saito, K., Furuta, E., Iiizumi, M., Mohinta, S., Watabe, M., Chalfant, C. and Watabe, K., Mechanism of Apoptosis Induced by the Inhibition of Fatty Acid Synthase in Breast Cancer Cells, *Cancer Res* 66 (2006) 5934–5940.

Bauer, D. E., Hatzivassiliou, G., Zhao, F., Andreadis, C. and Thompson, C. B., ATP citrate lyase is an important component of cell growth and transformation, *Oncogene* 24 (2005) 6314–6322.

Beckers, A., Organe, S., Timmermans, L., Scheys, K., Peeters, A., Brusselmans, K., Verhoeven, G. and Swinnen, J. V., Chemical inhibition of acetyl-CoA carboxylase induces growth arrest and cytotoxicity selectively in cancer cells, *Cancer Res* 67 (2007) 8180–8187.

Bennett, M. K., Lopez, J. M., Sanchez, H. B. and Osborne, T. F., Sterol regulation of fatty acid synthase promoter. Coordinate feedback regulation of two major lipid pathways, *J Biol Chem* 270 (1995) 25578–25583.

Blanco-Aparicio, C., Renner, O., Leal, J. F. M. and Carnero, A., PTEN, more than the AKT pathway, *Carcinogenesis* 28 (2007) 1379–1386.

Brusselmans, K., De Schrijver, E., Verhoeven, G. and Swinnen, J. V., RNA Interference-Mediated Silencing of the Acetyl-CoA-Carboxylase-{alpha} Gene Induces Growth Inhibition and Apoptosis of Prostate Cancer Cells, *Cancer Res* 65 (2005) 6719–6725.

Buechler, K. F. and Rhoades, R. A., Fatty acid synthesis in the perfused rat lung, *Biochim Biophys Acta* 619 (1980) 186–195.

Camassei, F. D., Cozza, R., Acquaviva, A., Jenkner, A., Rava, L., Gareri, R., Donfrancesco, A., Bosman, C., Vadala, P., Hadjistilianou, T. and Boldrini, R., Expression of the lipogenic enzyme fatty acid synthase (FAS) in retinoblastoma and its correlation with tumor aggressiveness, *Invest Ophthalmol Vis Sci* 44 (2003a) 2399–2403.

Camassei, F. D., Jenkner, A., Rava, L., Bosman, C., Francalanci, P., Donfrancesco, A., Alo, P. L. and Boldrini, R., Expression of the lipogenic enzyme fatty acid synthase (FAS) as a predictor of poor outcome in nephroblastoma: an interinstitutional study, *Med Pediatr Oncol* 40 (2003b) 302–308.

Chajes, V., Cambot, M., Moreau, K., Lenoir, G. M. and Joulin, V., Acetyl-CoA Carboxylase {alpha} Is Essential to Breast Cancer Cell Survival, *Cancer Res* 66 (2006) 5287–5294.

Chakravarthy, M. V., Pan, Z., Zhu, Y., Tordjman, K., Schneider, J. G., Coleman, T., Turk, J. and Semenkovich, C. F., "New" hepatic fat activates PPARalpha to maintain glucose, lipid, and cholesterol homeostasis, *Cell Metab* 1 (2005) 309–322.

Chakravarthy, M. V., Zhu, Y., Lopez, M., Yin, L., Wozniak, D. F., Coleman, T., Hu, Z., Wolfgang, M., Vidal-Puig, A., Lane, M. D. and Semenkovich, C. F., Brain fatty acid synthase activates PPARalpha to maintain energy homeostasis, *J Clin Invest* 117 (2007) 2539–2552.

Chalbos, D., Chambon, M., Ailhaud, G. and Rochefort, H., Fatty acid synthetase and its mRNA are induced by progestins in breast cancer cells, *J Biol Chem* 262 (1987) 9923–9926.

Chang, Y., Wang, J., Lu, X., Thewke, D. P. and Mason, R. J., KGF induces lipogenic genes through a PI3K and JNK/SREBP-1 pathway in H292 cells, *J Lipid Res* 46 (2005) 2624–2635.

Chirala, S. S., Chang, H., Matzuk, M., Abu-Elheiga, L., Mao, J., Mahon, K., Finegold, M. and Wakil, S. J., Fatty acid synthesis is essential in embryonic development: fatty acid synthase null mutants and most of the heterozygotes die in utero, *Proc Natl Acad Sci USA* 100 (2003) 6358–6363.

Conde, E., Suarez-Gauthier, A., Garcia-Garcia, E., Lopez-Rios, F., Lopez-Encuentra, A., Garcia-Lujan, R., Morente, M., Sanchez-Verde, L. and Sanchez-Cespedes, M., Specific pattern of LKB1 and phospho-acetyl-CoA carboxylase protein immunostaining in human normal tissues and lung carcinomas, *Hum Pathol* 38 (2007) 1351–1360.

De Schrijver, E., Brusselmans, K., Heyns, W., Verhoeven, G. and Swinnen, J. V., RNA interference-mediated silencing of the fatty acid synthase gene attenuates growth and induces morphological changes and apoptosis of LNCaP prostate cancer cells, *Cancer Res* 63 (2003) 3799–3804.

Deberardinis, R. J., Mancuso, A., Daikhin, E., Nissim, I., Yudkoff, M., Wehrli, S. and Thompson, C. B., Beyond aerobic glycolysis: Transformed cells can engage in glutamine metabolism that exceeds the requirement for protein and nucleotide synthesis, *Proc Natl Acad Sci USA* 104 (2007) 19345–19350.

Egner, R., Thumm, M., Straub, M., Simeon, A., Schuller, H. J. and Wolf, D. H., Tracing intracellular proteolytic pathways. Proteolysis of fatty acid synthase and other cytoplasmic proteins in the yeast Saccharomyces cerevisiae, *J Biol Chem* 268 (1993) 27269–27276.

Epstein, J. I., Carmichael, M. and Partin, A. W., OA-519 (fatty acid synthase) as an independent predictor of pathologic state in adenocarcinoma of the prostate, *Urology* 45 (1995) 81–86.

Foufelle, F., Gouhot, B., Pegorier, J. P., Perdereau, D., Girard, J. and Ferre, P., Glucose stimulation of lipogenic enzyme gene expression in cultured white adipose tissue. A role for glucose 6-phosphate, *J Biol Chem* 267 (1992) 20543–20546.

Freeman, M. R., Cinar, B., Kim, J., Mukhopadhyay, N. K., Di Vizio, D., Adam, R. M. and Solomon, K. R., Transit of hormonal and EGF receptor-dependent signals through cholesterol-rich membranes, *Steroids* 72 (2007) 210–217.

Freeman, M. R., Cinar, B. and Lu, M. L., Membrane rafts as potential sites of nongenomic hormonal signaling in prostate cancer, *Trends Endocrinol Metabol* 16 (2005) 273–279.

Fukuda, H., Iritani, N., Sugimoto, T. and Ikeda, H., Transcriptional regulation of fatty acid synthase gene by insulin/glucose, polyunsaturated fatty acid and leptin in hepatocytes and adipocytes in normal and genetically obese rats, *Eur J Biochem* 260 (1999) 505–511.

Funabashi, H., Kawaguchi, A., Tomoda, H., Omura, S., Okuda, S. and Iwasaki, S., Binding site of cerulenin in fatty acid synthetase, *J Biochem (Tokyo)* 105 (1989) 751–755.

Furuya, Y., Akimoto, S., Yasuda, K. and Ito, H., Apoptosis of androgen-independent prostate cell line induced by inhibition of fatty acid synthesis, *Anticancer Res* 17 (1997) 4589–4593.

Gabrielson, E. W., Pinn, M. L., Testa, J. R. and Kuhajda, F. P., Increased fatty acid synthase is a therapeutic target in mesothelioma, *Clin Cancer Res* 7 (2001) 153–157.

Gansler, T. S., Hardman, W., 3rd, Hunt, D. A., Schaffel, S. and Hennigar, R. A., Increased expression of fatty acid synthase (OA-519) in ovarian neoplasms predicts shorter survival, *Hum Pathol* 28 (1997) 686–692.

Gao, Y., Lin, L. P., Zhu, C. H., Chen, Y., Hou, Y. T. and Ding, J., Growth arrest induced by C75, A fatty acid synthase inhibitor, was partially modulated by p38 MAPK but not by p53 in human hepatocellular carcinoma, *Cancer Biol Ther* 5 (2006) 978–985.

Graner, E., Tang, D., Rossi, S., Baron, A., Migita, T., Weinstein, L. J., Lechpammer, M., Huesken, D., Zimmermann, J., Signoretti, S. and Loda, M., The isopeptidase USP2a regulates the stability of fatty acid synthase in prostate cancer, *Cancer Cell* 5 (2004) 253–261.

Harada, N., Oda, Z., Hara, Y., Fujinami, K., Okawa, M., Ohbuchi, K., Yonemoto, M., Ikeda, Y., Ohwaki, K., Aragane, K., Tamai, Y. and Kusunoki, J., Hepatic de novo lipogenesis is present in liver-specific ACC1-deficient mice, *Mol Cell Biol* 27 (2007) 1881–1888.

Hatzivassiliou, G., Zhao, F., Bauer, D. E., Andreadis, C., Shaw, A. N., Dhanak, D., Hingorani, S. R., Tuveson, D. A. and Thompson, C. B., ATP citrate lyase inhibition can suppress tumor cell growth, *Cancer Cell* 8 (2005) 311–321.

Heemers, H., Maes, B., Foufelle, F., Heyns, W., Verhoeven, G. and Swinnen, J. V., Androgens stimulate lipogenic gene expression in prostate cancer cells by activation of the sterol regulatory element-binding protein cleavage activating protein/sterol regulatory element-binding protein pathway, *Mol Endocrinol* 15 (2001) 1817–1828.

Heemers, H., Vanderhoydonc, F., Heyns, W., Verhoeven, G. and Swinnen, J. V., Progestins and androgens increase expression of Spot 14 in T47-D breast tumor cells, *Biochem Biophys Res Commun* 269 (2000) 209–212.

Heemers, H., Vanderhoydonc, F., Roskams, T., Shechter, I., Heyns, W., Verhoeven, G. and Swinnen, J. V., Androgens stimulate coordinated lipogenic gene expression in normal target tissues in vivo, *Mol Cell Endocrinol* 205 (2003) 21–31.

Heiligtag, S. J., Bredehorst, R. and David, K. A., Key role of mitochondria in cerulenin-mediated apoptosis, *Cell Death Differ* 9 (2002) 1017–1025.

Hennigar, R. A., Pochet, M., Hunt, D. A., Lukacher, A. E., Venema, V. J., Seal, E. and Marrero, M. B., Characterization of fatty acid synthase in cell lines derived from experimental mammary tumors, *Biochim Biophys Acta* 1392 (1998) 85–100.

Hillgartner, F. B., Salati, L. M. and Goodridge, A. G., Physiological and molecular mechanisms involved in nutritional regulation of fatty acid synthesis, *Physiol Rev* 75 (1995) 47–76.

Ho, T. S., Ho, Y. P., Wong, W. Y., Chi-Ming Chiu, L., Wong, Y. S. and Eng-Choon Ooi, V., Fatty acid synthase inhibitors cerulenin and C75 retard growth and induce caspase-dependent apoptosis in human melanoma A-375 cells, *Biomed Pharmacother* 61 (2007) 578–587.

Innocenzi, D., Alo, P. L., Balzani, A., Sebastiani, V., Silipo, V., La Torre, G., Ricciardi, G., Bosman, C. and Calvieri, S., Fatty acid synthase expression in melanoma, *J Cutan Pathol* 30 (2003) 23–28.

Jackowski, S., Coordination of membrane phospholipid synthesis with the cell cycle, *J Biol Chem* 269 (1994) 3858–3867.

Jakobsson, A., Westerberg, R. and Jacobsson, A., Fatty acid elongases in mammals: their regulation and roles in metabolism, *Prog Lipid Res* 45 (2006) 237–249.

Jayakumar, A., Tai, M. H., Huang, W. Y., al-Feel, W., Hsu, M., Abu-Elheiga, L., Chirala, S. S. and Wakil, S. J., Human fatty acid synthase: properties and molecular cloning, *Proc Natl Acad Sci USA* 92 (1995) 8695–8699.

Jensen, V., Ladekarl, M., Holm-Nielsen, P., Melsen, F. and Soerensen, F. B., The prognostic value of oncogenic antigen 519 (OA-519) expression and proliferative activity detected by antibody MIB-1 in node-negative breast cancer, *J Pathol* 176 (1995) 343–352.

Joseph, J. W., Odegaard, M. L., Ronnebaum, S. M., Burgess, S. C., Muehlbauer, J., Sherry, A. D. and Newgard, C. B., Normal flux through ATP-citrate lyase or fatty acid synthase is not required for glucose-stimulated insulin secretion, *J Biol Chem* 282 (2007) 31592–31600.

Jump, D. B., Clarke, S. D., Thelen, A. and Liimatta, M., Coordinate regulation of glycolytic and lipogenic gene expression by polyunsaturated fatty acids, *J Lipid Res* 35 (1994) 1076–1084.

Kapur, P., Rakheja, D., Roy, L. C. and Hoang, M. P., Fatty acid synthase expression in cutaneous melanocytic neoplasms, *Mod Pathol* 18 (2005) 1107–1112.

Kersten, S., Seydoux, J., Peters, J. M., Gonzalez, F. J., Desvergne, B. and Wahli, W., Peroxisome proliferator-activated receptor alpha mediates the adaptive response to fasting, *J Clin Invest* 103 (1999) 1489–1498.

Knowles, L. M., Axelrod, F., Browne, C. D. and Smith, J. W., A fatty acid synthase blockade induces tumor cell-cycle arrest by down-regulating Skp2, *J Biol Chem* 279 (2004) 30540–30545.

Kridel, S. J., Axelrod, F., Rozenkrantz, N. and Smith, J. W., Orlistat is a novel inhibitor of fatty acid synthase with antitumor activity, *Cancer Res* 64 (2004) 2070–2075.

Kridel, S. J., Lowther, W. T. and Pemble, C. W., Fatty acid synthase inhibitors: new directions for oncology, *Expert Opin Investig Drugs* 16 (2007) 1817–1829.

Kuhajda, F. P., Fatty-acid synthase and human cancer: new perspectives on its role in tumor biology, *Nutrition* 16 (2000) 202–208.

Kuhajda, F. P., Fatty acid synthase and cancer: new application of an old pathway, *Cancer Res* 66 (2006) 5977–5980.

Kuhajda, F. P., Jenner, K., Wood, F. D., Hennigar, R. A., Jacobs, L. B., Dick, J. D. and Pasternack, G. R., Fatty acid synthesis: a potential selective target for antineoplastic therapy, *Proc Natl Acad Sci USA* 91 (1994) 6379–6383.

Kuhajda, F. P., Katumuluwa, A. I. and Pasternack, G. R., Expression of haptoglobin-related protein and its potential role as a tumor antigen, *Proc Natl Acad Sci USA* 86 (1989a) 1188–1192.

Kuhajda, F. P., Piantadosi, S. and Pasternack, G. R., Haptoglobin-related protein (Hpr) epitopes in breast cancer as a predictor of recurrence of the disease, *N Engl J Med* 321 (1989b) 636–641.

Kuhajda, F. P., Pizer, E. S., Li, J. N., Mani, N. S., Frehywot, G. L. and Townsend, C. A., Synthesis and antitumor activity of an inhibitor of fatty acid synthase, *Proc Natl Acad Sci USA* 97 (2000) 3450–3454.

Kumar-Sinha, C., Ignatoski, K. W., Lippman, M. E., Ethier, S. P. and Chinnaiyan, A. M., Transcriptome analysis of HER2 reveals a molecular connection to fatty acid synthesis, *Cancer Res* 63 (2003) 132–139.

Kusakabe, T., Maeda, M., Hoshi, N., Sugino, T., Watanabe, K., Fukuda, T. and Suzuki, T., Fatty acid synthase is expressed mainly in adult hormone-sensitive cells or cells with high lipid metabolism and in proliferating fetal cells, *J Histochem Cytochem* 48 (2000) 613–622.

Kusakabe, T., Nashimoto, A., Honma, K. and Suzuki, T., Fatty acid synthase is highly expressed in carcinoma, adenoma and in regenerative epithelium and intestinal metaplasia of the stomach, *Histopathology* 40 (2002) 71–79.

Lacasa, D., Le Liepvre, X., Ferre, P. and Dugail, I., Progesterone stimulates adipocyte determination and differentiation 1/sterol regulatory element-binding protein 1c gene expression. potential mechanism for the lipogenic effect of progesterone in adipose tissue, *J Biol Chem* 276 (2001) 11512–11516.

Li, J. N., Gorospe, M., Chrest, F. J., Kumaravel, T. S., Evans, M. K., Han, W. F. and Pizer, E. S., Pharmacological inhibition of fatty acid synthase activity produces both cytostatic and cytotoxic effects modulated by p53, *Cancer Res* 61 (2001) 1493–1499.

Little, J. L., Wheeler, F. B., Fels, D. R., Koumenis, C. and Kridel, S. J., Inhibition of fatty acid synthase induces endoplasmic reticulum stress in tumor cells, *Cancer Res* 67 (2007) 1262–1269.

Liu, X., Shi, Y., Giranda, V. L. and Luo, Y., Inhibition of the phosphatidylinositol 3-kinase/Akt pathway sensitizes MDA-MB468 human breast cancer cells to cerulenin-induced apoptosis, *Mol Cancer Ther* 5 (2006) 494–501.

Loftus, T. M., Jaworsky, D. E., Frehywot, G. L., Townsend, C. A., Ronnett, G. V., Lane, M. D. and Kuhajda, F. P., Reduced Food Intake and Body Weight in Mice Treated with Fatty Acid Synthase Inhibitors, *Science* 288 (2000) 2379–2381.

Magana, M. M. and Osborne, T. F., Two tandem binding sites for sterol regulatory element binding proteins are required for sterol regulation of fatty-acid synthase promoter, *J Biol Chem* 271 (1996) 32689–32694.

Maier, T., Jenni, S. and Ban, N., Architecture of mammalian fatty acid synthase at 4.5 A resolution, *Science* 311 (2006) 1258–1262.

McGarry, J. D., Mills, S. E., Long, C. S. and Foster, D. W., Observations on the affinity for carnitine, and malonyl-CoA sensitivity, of carnitine palmitoyltransferase I in animal and human tissues. Demonstration of the presence of malonyl-CoA in non-hepatic tissues of the rat, *Biochem J* 214 (1983) 21–28.

Menendez, J. A., Oza, B. P., Colomer, R. and Lupu, R., The estrogenic activity of synthetic progestins used in oral contraceptives enhances fatty acid synthase-dependent breast cancer cell proliferation and survival, *Int J Oncol* 26 (2005a) 1507–1515.

Menendez, J. A., Vellon, L. and Lupu, R., Antitumoral actions of the anti-obesity drug orlistat (XenicalTM) in breast cancer cells: blockade of cell cycle progression, promotion of apoptotic cell death and PEA3-mediated transcriptional repression of Her2/neu (erbB-2) oncogene, *Ann Oncol* 16 (2005b) 1253–1267.

Menendez, J. A., Vellon, L., Mehmi, I., Oza, B. P., Ropero, S., Colomer, R. and Lupu, R., Inhibition of fatty acid synthase (FAS) suppresses HER2/neu (erbB-2) oncogene overexpression in cancer cells, *Proc Natl Acad Sci USA* 101 (2004) 10715–10720.

Milgraum, L. Z., Witters, L. A., Pasternack, G. R. and Kuhajda, F. P., Enzymes of the fatty acid synthesis pathway are highly expressed in in situ breast carcinoma, *Clin Cancer Res* 3 (1997) 2115–2120.

Moon, Y. S., Latasa, M. J., Griffin, M. J. and Sul, H. S., Suppression of fatty acid synthase promoter by polyunsaturated fatty acids, *J Lipid Res* 43 (2002) 691–698.

Moreau, K., Dizin, E., Ray, H., Luquain, C., Lefai, E., Foufelle, F., Billaud, M., Lenoir, G. M. and Venezia, N. D., BRCA1 Affects Lipid Synthesis through Its Interaction with Acetyl-CoA Carboxylase, *J Biol Chem* 281 (2006) 3172–3181.

Moustaid, N., Beyer, R. S. and Sul, H. S., Identification of an insulin response element in the fatty acid synthase promoter, *J Biol Chem* 269 (1994) 5629–5634.

Moustaid, N. and Sul, H. S., Regulation of expression of the fatty acid synthase gene in 3T3-L1 cells by differentiation and triiodothyronine, *J Biol Chem* 266 (1991) 18550–18554.

Mulholland, D. J., Dedhar, S., Wu, H. and Nelson, C. C., PTEN and GSK3beta: key regulators of progression to androgen-independent prostate cancer, *Oncogene* 25 (2006) 329–337.

Myers, R. B., Oelschlager, D. K., Weiss, H. L., Frost, A. R. and Grizzle, W. E., Fatty acid synthase: an early molecular marker of progression of prostatic adenocarcinoma to androgen independence, *J Urol* 165 (2001) 1027–1032.

Nemoto, T., Terashima, S., Kogure, M., Hoshino, Y., Kusakabe, T., Suzuki, T. and Gotoh, M., Overexpression of fatty acid synthase in oesophageal squamous cell dysplasia and carcinoma, *Pathobiology* 69 (2001) 297–303.

Ogino, S., Brahmandam, M., Cantor, M., Namgyal, C., Kawasaki, T., Kirkner, G., Meyerhardt, J. A., Loda, M. and Fuchs, C. S., Distinct molecular features of colorectal carcinoma with signet ring cell component and colorectal carcinoma with mucinous component, *Mod Pathol* 19 (2006) 59–68.

Ogino, S., Kawasaki, T., Ogawa, A., Kirkner, G. J., Loda, M. and Fuchs, C. S., Fatty acid synthase overexpression in colorectal cancer is associated with microsatellite instability, independent of CpG island methylator phenotype, *Hum Pathol* 38 (2007) 842–849.

Ookhtens, M., Kannan, R., Lyon, I. and Baker, N., Liver and adipose tissue contributions to newly formed fatty acids in an ascites tumor, *Am J Physiol Regul Integr Comp Physiol* 247 (1984) R146–R153.

Orita, H., Coulter, J., Lemmon, C., Tully, E., Vadlamudi, A., Medghalchi, S. M., Kuhajda, F. P. and Gabrielson, E., Selective inhibition of fatty acid synthase for lung cancer treatment, *Clin Cancer Res* 13 (2007) 7139–7145.

Paulauskis, J. D. and Sul, H. S., Cloning and expression of mouse fatty acid synthase and other specific mRNAs. Developmental and hormonal regulation in 3T3-L1 cells, *J Biol Chem* 263 (1988) 7049–7054.

Pflug, B. R., Pecher, S. M., Brink, A. W., Nelson, J. B. and Foster, B. A., Increased fatty acid synthase expression and activity during progression of prostate cancer in the TRAMP model, *Prostate* 57 (2003) 245–254.

Pizer, E. S., Chrest, F. J., DiGiuseppe, J. A. and Han, W. F., Pharmacological inhibitors of mammalian fatty acid synthase suppress DNA replication and induce apoptosis in tumor cell lines, *Cancer Res* 58 (1998a) 4611–4615.

Pizer, E. S., Jackisch, C., Wood, F. D., Pasternack, G. R., Davidson, N. E. and Kuhajda, F. P., Inhibition of fatty acid synthesis induces programmed cell death in human breast cancer cells, *Cancer Res* 56 (1996a) 2745–2747.

Pizer, E. S., Kurman, R. J., Pasternack, G. R. and Kuhajda, F. P., Expression of fatty acid synthase is closely linked to proliferation and stromal decidualization in cycling endometrium, *Int J Gynecol Pathol* 16 (1997) 45–51.

Pizer, E. S., Lax, S. F., Kuhajda, F. P., Pasternack, G. R. and Kurman, R. J., Fatty acid synthase expression in endometrial carcinoma: correlation with cell proliferation and hormone receptors, *Cancer* 83 (1998b) 528–537.

Pizer, E. S., Pflug, B. R., Bova, G. S., Han, W. F., Udan, M. S. and Nelson, J. B., Increased fatty acid synthase as a therapeutic target in androgen-independent prostate cancer progression, *Prostate* 47 (2001) 102–110.

Pizer, E. S., Thupari, J., Han, W. F., Pinn, M. L., Chrest, F. J., Frehywot, G. L., Townsend, C. A. and Kuhajda, F. P., Malonyl-coenzyme-A is a potential mediator of cytotoxicity induced by fatty-acid synthase inhibition in human breast cancer cells and xenografts, *Cancer Res* 60 (2000) 213–218.

Pizer, E. S., Wood, F. D., Heine, H. S., Romantsev, F. E., Pasternack, G. R. and Kuhajda, F. P., Inhibition of fatty acid synthesis delays disease progression in a xenograft model of ovarian cancer, *Cancer Res* 56 (1996b) 1189–1193.

Porstmann, T., Griffiths, B., Chung, Y. L., Delpuech, O., Griffiths, J. R., Downward, J. and Schulze, A., PKB/Akt induces transcription of enzymes involved in cholesterol and fatty acid biosynthesis via activation of SREBP, *Oncogene* 24 (2005) 6465–6481.

Rangan, V. S., Joshi, A. K. and Smith, S., Fatty acid synthase dimers containing catalytically active beta-ketoacyl synthase or malonyl/acetyltransferase domains in only one subunit can support fatty acid synthesis at the acyl carrier protein domains of both subunits, *J Biol Chem* 273 (1998) 34949–34953.

Rangan, V. S., Joshi, A. K. and Smith, S., Mapping the functional topology of the animal fatty acid synthase by mutant complementation in vitro, *Biochemistry* 40 (2001) 10792–10799.

Rangan, V. S., Oskouian, B. and Smith, S., Identification of an inverted CCAAT box motif in the fatty-acid synthase gene as an essential element for modification of transcriptional regulation by cAMP, *J Biol Chem* 271 (1996) 2307–2312.

Rashid, A., Pizer, E. S., Moga, M., Milgraum, L. Z., Zahurak, M., Pasternack, G. R., Kuhajda, F. P. and Hamilton, S. R., Elevated expression of fatty acid synthase and fatty acid synthetic activity in colorectal neoplasia, *Am J Pathol* 150 (1997) 201–208.

Resh, M. D., Trafficking and signaling by fatty-acylated and prenylated proteins, *Nat Chem Biol* 2 (2006) 584–590.

Rossi, S., Graner, E., Febbo, P., Weinstein, L., Bhattacharya, N., Onody, T., Bubley, G., Balk, S. and Loda, M., Fatty acid synthase expression defines distinct molecular signatures in prostate cancer, *Mol Cancer Res* 1 (2003) 707–715.

Rufo, C., Teran-Garcia, M., Nakamura, M. T., Koo, S. H., Towle, H. C. and Clarke, S. D., Involvement of a unique carbohydrate-responsive factor in the glucose regulation of rat liver fatty-acid synthase gene transcription, *J Biol Chem* 276 (2001) 21969–21975.

Sabine, J. R., Abraham, S. and Chaikoff, I. L., Control of lipid metabolism in hepatomas: insensitivity of rate of fatty acid and cholesterol synthesis by mouse hepatoma BW7756 to fasting and to feedback control, *Cancer Res* 27 (1967) 793–799.

Sakai, J., Nohturfft, A., Goldstein, J. L. and Brown, M. S., Cleavage of Sterol Regulatory Element-binding Proteins (SREBPs) at Site-1 Requires Interaction with SREBP Cleavage-activating Protein. Evidence from in vivo competition studies, *J Biol Chem* 273 (1998) 5785–5793.

Sampath, H. and Ntambi, J. M., The fate and intermediary metabolism of stearic acid, *Lipids* 40 (2005) 1187–1191.

Sebastiani, V., Visca, P., Botti, C., Santeusanio, G., Galati, G. M., Piccini, V., Capezzone de Joannon, B., Di Tondo, U. and Alo, P. L., Fatty acid synthase is a marker of increased risk of recurrence in endometrial carcinoma, *Gynecol Oncol* 92 (2004) 101–105.

Shah, U. S., Dhir, R., Gollin, S. M., Chandran, U. R., Lewis, D., Acquafondata, M. and Pflug, B. R., Fatty acid synthase gene overexpression and copy number gain in prostate adenocarcinoma, *Hum Pathol* 37 (2006) 401–409.

Shurbaji, M. S., Kalbfleisch, J. H. and Thurmond, T. S., Immunohistochemical detection of a fatty acid synthase (OA-519) as a predictor of progression of prostate cancer, *Hum Pathol* 27 (1996) 917–921.

Shurbaji, M. S., Kuhajda, F. P., Pasternack, G. R. and Thurmond, T. S., Expression of oncogenic antigen 519 (OA-519) in prostate cancer is a potential prognostic indicator, *Am J Clin Pathol* 97 (1992) 686–691.

Silva, S. D., Perez, D. E., Alves, F. A., Nishimoto, I. N., Pinto, C. A. L., Kowalski, L. P. and Graner, E., ErbB2 and fatty acid synthase (FAS) expression in 102 squamous cell carcinomas of the tongue: Correlation with clinical outcomes, *Oral Oncol* 44(5) (2008) 484–490.

Smith, S., Architectural options for a fatty acid synthase, *Science* 311 (2006) 1251–1252.

Smith, S., Witkowski, A. and Joshi, A. K., Structural and functional organization of the animal fatty acid synthase, *Prog Lipid Res* 42 (2003) 289–317.

Swinnen, J. V., Brusselmans, K. and Verhoeven, G., Increased lipogenesis in cancer cells: new players, novel targets, *Curr Opin Clin Nutr Metab Care* 9 (2006) 358–365.

Swinnen, J. V., Esquenet, M., Goossens, K., Heyns, W. and Verhoeven, G., Androgens stimulate fatty acid synthase in the human prostate cancer cell line LNCaP, *Cancer Res* 57 (1997a) 1086–1090.

Swinnen, J. V., Heemers, H., Deboel, L., Foufelle, F., Heyns, W. and Verhoeven, G., Stimulation of tumor-associated fatty acid synthase expression by growth factor activation of the sterol regulatory element-binding protein pathway, *Oncogene* 19 (2000a) 5173–5181.

Swinnen, J. V., Roskams, T., Joniau, S., Van Poppel, H., Oyen, R., Baert, L., Heyns, W. and Verhoeven, G., Overexpression of fatty acid synthase is an early and common event in the development of prostate cancer, *Int J Cancer* 98 (2002) 19–22.

Swinnen, J. V., Ulrix, W., Heyns, W. and Verhoeven, G., Coordinate regulation of lipogenic gene expression by androgens: evidence for a cascade mechanism involving sterol regulatory element binding proteins, *Proc Natl Acad Sci USA* 94 (1997b) 12975–12980.

Swinnen, J. V., Van Veldhoven, P. P., Timmermans, L., De Schrijver, E., Brusselmans, K., Vanderhoydonc, F., Van de Sande, T., Heemers, H., Heyns, W. and Verhoeven, G., Fatty acid synthase drives the synthesis of phospholipids partitioning into detergent-resistant membrane microdomains, *Biochem Biophys Res Commun* 302 (2003) 898–903.

Swinnen, J. V., Vanderhoydonc, F., Elgamal, A. A., Eelen, M., Vercaeren, I., Joniau, S., Van Poppel, H., Baert, L., Goossens, K., Heyns, W. and Verhoeven, G., Selective activation of the fatty acid synthesis pathway in human prostate cancer, *Int J Cancer* 88 (2000b) 176–179.

Szutowicz, A., Kwiatkowski, J. and Angielski, S., Lipogenetic and glycolytic enzyme activities in carcinoma and nonmalignant diseases of the human breast, *Br J Cancer* 39 (1979) 681–687.

Takahiro, T., Shinichi, K. and Toshimitsu, S., Expression of fatty acid synthase as a prognostic indicator in soft tissue sarcomas, *Clin Cancer Res* 9 (2003) 2204–2212.

Teran-Garcia, M., Adamson, A. W., Yu, G., Rufo, C., Suchankova, G., Dreesen, T. D., Tekle, M., Clarke, S. D. and Gettys, T. W., Polyunsaturated fatty acid suppression of fatty acid synthase (FASN): evidence for dietary modulation of NF-Y binding to the Fasn promoter by SREBP-1c, *Biochem J* 402 (2007) 591–600.

Thompson, B. J. and Smith, S., Biosynthesis of fatty acids by lactating human breast epithelial cells: an evaluation of the contribution to the overall composition of human milk fat, *Pediatr Res* 19 (1985) 139–143.

Thupari, J. N., Kim, E. K., Moran, T. H., Ronnett, G. V. and Kuhajda, F. P., Chronic C75 treatment of diet-induced obese mice increases fat oxidation and reduces food intake to reduce adipose mass, *Am J Physiol Endocrinol Metab* 287 (2004) E97–E104.

Thupari, J. N., Landree, L. E., Ronnett, G. V. and Kuhajda, F. P., C75 increases peripheral energy utilization and fatty acid oxidation in diet-induced obesity, *Proc Natl Acad Sci USA* 99 (2002) 9498–9502.

Tian, W. X., Inhibition of fatty acid synthase by polyphenols, *Curr Med Chem* 13 (2006) 967–977.

Tu, Y., Thupari, J. N., Kim, E. K., Pinn, M. L., Moran, T. H., Ronnett, G. V. and Kuhajda, F. P., C75 alters central and peripheral gene expression to reduce food intake and increase energy expenditure, *Endocrinology* 146 (2005) 486–493.

Turyn, J., Schlichtholz, B., Dettlaff-Pokora, A., Presler, M., Goyke, E., Matuszewski, M., Kmiec, Z., Krajka, K. and Swierczynski, J., Increased activity of glycerol 3-phosphate dehydrogenase and other lipogenic enzymes in human bladder cancer, *Horm Metab Res* 35 (2003) 565–569.

Van de Sande, T., De Schrijver, E., Heyns, W., Verhoeven, G. and Swinnen, J. V., Role of the phosphatidylinositol 3′-kinase/PTEN/Akt kinase pathway in the overexpression of fatty acid synthase in LNCaP prostate cancer cells, *Cancer Res* 62 (2002) 642–646.

Van de Sande, T., Roskams, T., Lerut, E., Joniau, S., Van Poppel, H., Verhoeven, G. and Swinnen, J. V., High-level expression of fatty acid synthase in human prostate cancer tissues is linked to activation and nuclear localization of Akt/PKB, *J Pathol* 206 (2005) 214–219.

Visca, P., Sebastiani, V., Botti, C., Diodoro, M. G., Lasagni, R. P., Romagnoli, F., Brenna, A., De Joannon, B. C., Donnorso, R. P., Lombardi, G. and Alo, P. L., Fatty acid synthase (FAS) is a marker of increased risk of recurrence in lung carcinoma, *Anticancer Res* 24 (2004) 4169–4173.

Visca, P., Sebastiani, V., Pizer, E. S., Botti, C., De Carli, P., Filippi, S., Monaco, S. and Alo, P. L., Immunohistochemical expression and prognostic significance of FAS and GLUT1 in bladder carcinoma, *Anticancer Res* 23 (2003) 335–339.

Volpe, J. J. and Marasa, J. C., Hormonal regulation of fatty acid synthetase, acetyl-CoA carboxylase and fatty acid synthesis in mammalian adipose tissue and liver, *Biochim Biophys Acta* 380 (1975) 454–472.

Wakil, S. J., Fatty acid synthase, a proficient multifunctional enzyme, *Biochemistry* 28 (1989) 4523–4530.

Wakil, S. J., Stoops, J. K. and Joshi, V. C., Fatty acid synthesis and its regulation, *Annu Rev Biochem* 52 (1983) 537–579.

Wang, D. and Sul, H. S., Insulin stimulation of the fatty acid synthase promoter is mediated by the phosphatidylinositol 3-kinase pathway. Involvement of protein kinase B/Akt, *J Biol Chem* 273 (1998) 25420–25426.

Wang, H. Q., Altomare, D. A., Skele, K. L., Poulikakos, P. I., Kuhajda, F. P., Di Cristofano, A. and Testa, J. R., Positive feedback regulation between AKT activation and fatty acid synthase expression in ovarian carcinoma cells, *Oncogene* 24 (2005) 3574–3582.

Wang, S., Gao, J., Lei, Q., Rozengurt, N., Pritchard, C., Jiao, J., Thomas, G. V., Li, G., Roy-Burman, P., Nelson, P. S., Liu, X. and Wu, H., Prostate-specific deletion of the murine Pten tumor suppressor gene leads to metastatic prostate cancer, *Cancer Cell* 4 (2003) 209–221.

Worgall, T. S., Sturley, S. L., Seo, T., Osborne, T. F. and Deckelbaum, R. J., Polyunsaturated Fatty Acids Decrease Expression of Promoters with Sterol Regulatory Elements by Decreasing Levels of Mature Sterol Regulatory Element-binding Protein, *J Biol Chem* 273 (1998) 25537–25540.

Xu, J., Nakamura, M. T., Cho, H. P. and Clarke, S. D., Sterol regulatory element binding protein-1 expression is suppressed by dietary polyunsaturated fatty acids. A mechanism for the coordinate suppression of lipogenic genes by polyunsaturated fats, *J Biol Chem* 274 (1999) 23577–23583.

Yahagi, N., Shimano, H., Hasegawa, K., Ohashi, K., Matsuzaka, T., Najima, Y., Sekiya, M., Tomita, S., Okazaki, H., Tamura, Y., Iizuka, Y., Ohashi, K., Nagai, R., Ishibashi, S., Kadowaki, T., Makuuchi, M., Ohnishi, S., Osuga, J.-i. and Yamada, N., Co-ordinate activation of lipogenic enzymes in hepatocellular carcinoma, *Eur J Cancer* 41 (2005) 1316–1322.

Yang, N., Kays, J. S., Skillman, T. R., Burris, L., Seng, T. W. and Hammond, C., C75 [4-Methylene-2-octyl-5-oxo-tetrahydro-furan-3-carboxylic Acid] Activates Carnitine Palmitoyltransferase-1 in Isolated Mitochondria and Intact Cells without Displacement of Bound Malonyl CoA, *J Pharmacol Exp Ther* 312 (2005) 127–133.

Yang, Y. A., Han, W. F., Morin, P. J., Chrest, F. J. and Pizer, E. S., Activation of fatty acid synthesis during neoplastic transformation: role of mitogen-activated protein kinase and phosphatidylinositol 3-kinase, *Exp Cell Res* 279 (2002) 80–90.

Yeh, S., Lin, H.-K., Kang, H.-Y., Thin, T. H., Lin, M.-F. and Chang, C., From HER2/Neu signal cascade to androgen receptor and its coactivators: A novel pathway by induction of androgen target genes through MAP kinase in prostate cancer cells, *Proc Natl Acad Sci USA* 96 (1999) 5458–5463.

Yoon, S., Lee, M. Y., Park, S. W., Moon, J. S., Koh, Y. K., Ahn, Y. H., Park, B. W. and Kim, K. S., Up-regulation of acetyl-CoA carboxylase alpha and fatty acid synthase by human epidermal growth factor receptor 2 at the translational level in breast cancer cells, *J Biol Chem* 282 (2007) 26122–26131.

Zhao, W., Kridel, S., Thorburn, A., Kooshki, M., Little, J., Hebbar, S. and Robbins, M., Fatty acid synthase: a novel target for antiglioma therapy, *Br J Cancer* 95 (2006) 869–878.

Zhou, W., Han, W. F., Landree, L. E., Thupari, J. N., Pinn, M. L., Bililign, T., Kim, E. K., Vadlamudi, A., Medghalchi, S. M., El Meskini, R., Ronnett, G. V., Townsend, C. A. and Kuhajda, F. P., Fatty acid synthase inhibition activates AMP-activated protein kinase in SKOV3 human ovarian cancer cells, *Cancer Res* 67 (2007) 2964–2971.

Zhou, W., Simpson, P. J., McFadden, J. M., Townsend, C. A., Medghalchi, S. M., Vadlamudi, A., Pinn, M. L., Ronnett, G. V. and Kuhajda, F. P., Fatty Acid Synthase Inhibition Triggers Apoptosis during S Phase in Human Cancer Cells, *Cancer Res* 63 (2003) 7330–7337.

Preferential Cytotoxicity of Bortezomib toward Hypoxic Tumor Cells via Overactivation of Endoplasmic Reticulum Stress Pathways

Diane R. Fels,[1,2] Jiangbin Ye,[1] Andrew T. Segan,[1] Steven J. Kridel,[2] Michael Spiotto,[3] Michael Olson,[3] Albert C. Koong,[3] and Constantinos Koumenis[1]

[1]Department of Radiation Oncology, University of Pennsylvania School of Medicine, Philadelphia, Pennsylvania; [2]Department of Cancer Biology, Wake Forest University School of Medicine, Winston-Salem, North Carolina; and [3]Department of Radiation Oncology, Stanford University School of Medicine, Stanford, California

Abstract

Hypoxia is a dynamic feature of the tumor microenvironment that contributes to drug resistance and cancer progression. We previously showed that components of the unfolded protein response (UPR), elicited by endoplasmic reticulum (ER) stress, are also activated by hypoxia *in vitro* and *in vivo* animal and human patient tumors. Here, we report that ER stressors, such as thapsigargin or the clinically used proteasome inhibitor bortezomib, exhibit significantly higher cytotoxicity toward hypoxic compared with normoxic tumor cells, which is accompanied by enhanced activation of UPR effectors *in vitro* and UPR reporter activity *in vivo*. Treatment of cells with the translation inhibitor cycloheximide, which relieves ER load, ameliorated this enhanced cytotoxicity, indicating that the increased cytotoxicity is ER stress–dependent. The mode of cell death was cell type–dependent, because DLD1 colorectal carcinoma cells exhibited enhanced apoptosis, whereas HeLa cervical carcinoma cells activated autophagy, blocked apoptosis, and eventually led to necrosis. Pharmacologic or genetic ablation of autophagy increased the levels of apoptosis. These results show that hypoxic tumor cells, which are generally more resistant to genotoxic agents, are hypersensitive to proteasome inhibitors and suggest that combining bortezomib with therapies that target the normoxic fraction of human tumors can lead to more effective tumor control. [Cancer Res 2008;68(22):9323–30]

Introduction

Tumor hypoxia, or fluctuating regions of low oxygen tension, is an important feature of the tumor microenvironment that is known to promote cancer progression, decrease response to therapy, and predict poor overall patient survival (1). Hypoxic tumor cells activate hypoxia-inducible factor (HIF)–dependent and HIF-independent survival mechanisms that promote adaptation to low oxygen availability (2, 3). Previous work from our laboratory and others showed that cells respond to hypoxic stress by phosphorylating the translation initiation factor eIF2α, thereby reducing global translation rates (4–7). The eIF2α phosphorylation at Ser^{51} under hypoxia is dependent upon the endoplasmic reticulum (ER) kinase PERK (4, 7) and was found to occur independently of HIF-1α status, as HIF-1α $^{-/-}$ mouse embryonic fibroblasts (MEF) exhibited similar levels of eIF2α phosphorylation as HIF-$1\alpha^{+/+}$ MEFs (4).

This rapid and reversible inhibition of protein synthesis under hypoxia not only leads to energy conservation, by reducing the quantity of proteins being made that require folding within the ER (8), but also up-regulates gene products involved in the recovery from ER stress, such as protein chaperones and others, promoting amino acid sufficiency and redox homeostasis (6, 9). Some of the effects of PERK activation are mediated by activating transcription factor 4 (ATF4), a transcription factor translationally up-regulated by ER stress in an eIF2α phosphorylation–dependent manner (8). This PERK-eIF2α-ATF4 pathway is one arm of a larger, coordinated ER stress program, known as the unfolded protein response (UPR). In addition to PERK, UPR signaling is mediated by two other ER transmembrane proteins: IRE1 and ATF6. Upon ER stress, active IRE1 processes XBP-1 mRNA, removing a 26-nucleotide intron to generate a spliced XBP-1 mRNA encoding the functional XBP-1 transcription factor (10, 11). Together, these pathways coordinately up-regulate transcription of UPR target genes, such as the ER chaperone BiP/GFP78, and proteins involved in ER-associated degradation (ERAD), which aid in restoring ER homeostasis. However, IRE1 and another UPR target, CHOP, are also involved in ER stress–induced apoptosis (12). Thus, the UPR, while activated as a prosurvival response under moderate or intermittent ER stress, can also lead to cell death under conditions of severe or chronic stress (8).

The ERAD system shuttles misfolded proteins from the ER lumen to the cytosol, where they become ubiquitinated and degraded by the 26S proteasome (13). Bortezomib (PS-341; Velcade), a highly selective and reversible inhibitor of the 26S proteasome approved for clinical use against multiple myeloma, is in clinical trials as a single agent or in combination with chemotherapeutics against other solid tumor malignancies (14). The mechanisms involved in its anticancer activity are still being elucidated, but evidence suggests that it is in part due to the altered degradation of key regulatory proteins, such as IκB (15). More recently, bortezomib was shown to induce ER stress–dependent and ER-dependent apoptosis by blocking the ERAD system, thereby promoting the accumulation of misfolded proteins in the ER that induce proteotoxicity and cell death (13, 16–19).

Several studies have established that the UPR is activated in human tumors and that disruption of the UPR inhibits tumor growth. GRP78/BiP, a major ER chaperone protein that negatively regulates UPR activation, is up-regulated in many human tumors, confers drug resistance, promotes angiogenesis, and correlates with malignancy (20–22). Results from our laboratory showed that cells with a compromised PERK-eIF2α pathway are more sensitive to

Note: Supplementary data for this article are available at Cancer Research Online (http://cancerres.aacrjournals.org/).

Requests for reprints: Constantinos Koumenis, Department of Radiation Oncology, University of Pennsylvania School of Medicine, Philadelphia, PA 19104-6072. Phone: 215-898-0076; Fax: 215-898-0090; E-mail: koumenis@xrt.upenn.edu.

doi:10.1158/0008-5472.CAN-08-2873

hypoxic stress *in vitro* and grow smaller tumors *in vivo*, suggesting that this pathway is important for hypoxia tolerance in growing tumors (9). Moreover, ATF4 levels are increased by hypoxia in a HIF-independent manner and up-regulated near necrotic areas in human tumors (9, 23, 24). Romero-Ramirez and colleagues showed that the IRE1–XBP-1 pathway is also critical for surviving hypoxic stress *in vitro* and, more importantly, for optimal tumor growth *in vivo* (25). Whereas one attractive approach to target the UPR in tumors is to develop inhibitors against its critical effectors (e.g., against PERK or IRE1), we postulated that another approach could take advantage of its prodeath activity under extreme or prolonged stress.

Materials and Methods

Cell lines and reagents. DLD1 human colorectal adenocarcinoma cells, HeLa human cervical adenocarcinoma cells (American Type Culture Collection, ATCC), HT1080 human fibrosarcoma cells, and PERK MEFs were maintained in DMEM. HT29 colorectal adenocarcinoma cells (ATCC) were cultured in McCoy's 5A medium. All media were supplemented with penicillin, streptomycin, 10% fetal bovine serum, and L-glutamine (2 mmol/L). Bortezomib (Velcade; PS-341; Millennium Pharmaceuticals), thapsigargin, staurosporine, MG132, cycloheximide, chloroquine, and etoposide (Sigma) were dissolved in DMSO and stored at −20°C.

Hypoxia treatments. Cells were placed in an In vivo 400 Hypoxia Workstation (Biotrace, Inc.) for the times indicated. Cells were sustained as indicated at severe hypoxia (<0.2% O_2, 5% CO_2, 10% H_2) or moderate hypoxia (1% O_2, 5% CO_2). Oxygen concentrations were verified using the OxyLite pO_2 E-series probe (Oxford Optronix).

Immunoblotting. Immunoblotting was performed as previously described (4). Primary antibodies used are detailed in the supplementary material.

Nuclear-cytoplasmic fractionation. Isolating nuclear protein was performed as described in the supporting information. Nuclear protein (40–70 μg) was analyzed by immunoblotting for ATF4, CHOP, and XBP-1.

Detecting XBP-1 splicing by reverse transcription–PCR. Total RNA was isolated using TRIzol according to the manufacturer's protocol. cDNA was generated from 2 μg RNA using AMV-reverse transcriptase (Promega). XBP-1 was amplified by PCR, as described in the supplementary material.

Bioluminescence experiments. HT1080 cells or PERK MEFs stably expressing the ATF4-luciferase construct were treated as indicated, washed with 1 × PBS, and lysed (30 min, 24°C) in 400 μL 1 × reporter lysis buffer (Promega). Lysates (100 μL) were mixed with an equal volume of luciferase substrate (Promega) and assayed using a luminometer. CB17-SCID mice were injected SQ with 0.5 to 2 × 106 HT1080-CMV-luc cells on the left flank and HT1080-ATF4-luc cells on the right flank and allowed to grow for 2 to 3 wk. Mice were then injected i.p. with vehicle or bortezomib (1 mg/kg), and 8 h later, optical bioluminescence imaging was performed using the IVIS-100 system (Xenogen). Mice were imaged for 1 to 4 min per acquisition scan. Signal intensities were analyzed using Living Image software (Xenogen). Quantification based on five untreated mice and four treated mice in two experiments. Average tumor volume was 1,808 ± 321 mm3 (HT1080-CMV-luc) and 1,311 ± 293 mm3 (HT1080-ATF4-luc).

Small interfering RNA transfections. Beclin1 or nontargeting negative control small interfering RNAs (siRNA; 50 nmol/L, Dharmacon) were transfected into HeLa cells (1 × 106 per plate) using siPORT NeoFX (Ambion). At 30 h posttransfection, the cells were treated as indicated, harvested for immunoblots, or plated for clonogenic survival assays.

Clonogenic survival assays. Cells were plated in 6-cm diameter dishes at three different densities (100, 300, and 1,000 per plate) and exposed to normoxic or hypoxic conditions (0–1% O_2) before treatment with vehicle (DMSO) or different concentrations of thapsigargin, etoposide, MG132, or bortezomib for the indicated times. For the cycloheximide experiments, cycloheximide (1 μg/mL) was added at the same time as the various doses of bortezomib. Then, the drug/medium was removed, and the cells were

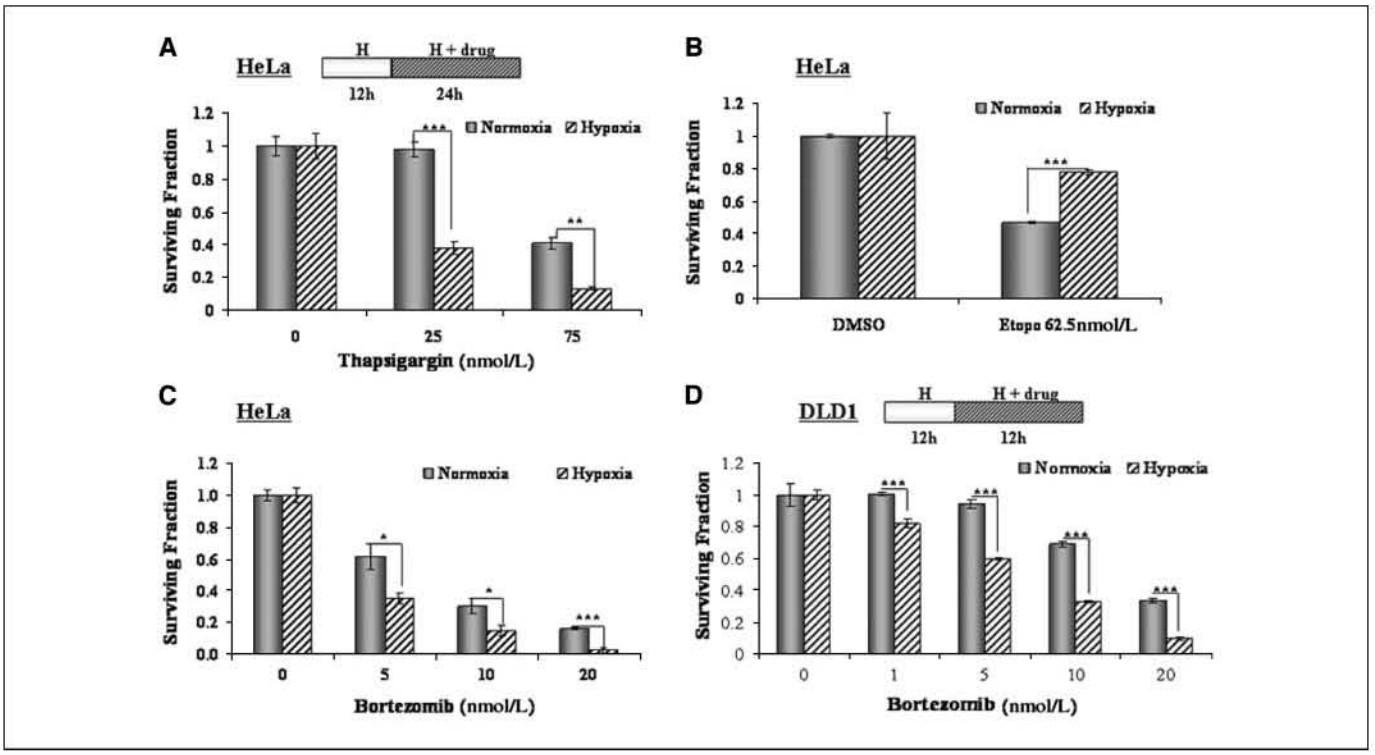

Figure 1. Hypoxic tumor cells are sensitive to ER stressors. Tumor cells were exposed to normoxic or hypoxic conditions for 12 h before treatment with the indicated agents for 12 h (DLD1) or 24 h (HeLa). *Bars*, SE. *A*, clonogenic survival of HeLa cells treated with thapsigargin. **, $P = 0.001$; ***, $P = 0.0002$. *B*, hypoxic HeLa cells are more resistant to etoposide. ***, $P < 0.001$. *C*, clonogenic survival of HeLa cells treated with bortezomib. *, $P \leq 0.03$; ***, $P < 0.001$. *D*, hypoxic DLD1 cells are also more sensitive to bortezomib than normoxic cells. ***, $P < 0.001$.

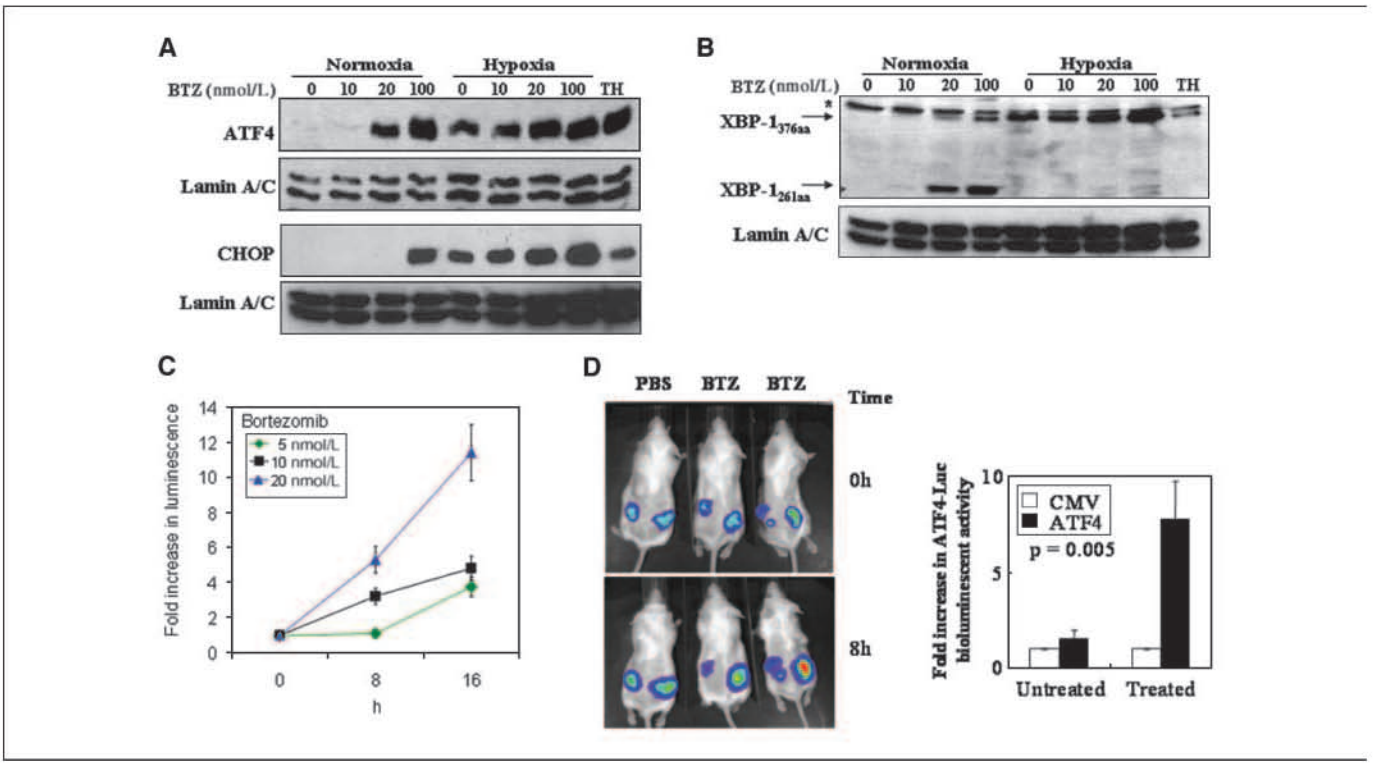

Figure 2. Bortezomib enhances UPR signaling under normoxia and hypoxia. *A*, ATF4 levels in HeLa cells exposed to normoxic or hypoxic conditions for 2 h before treatment with DMSO or bortezomib for 6 h. Thapsigargin (*TH*; 1 μmol/L, 4 h) was used as a positive control. CHOP levels in HeLa cells exposed to hypoxia 6 h before treatment with DMSO or bortezomib for 12 h. Thapsigargin (*TH*; 500 nmol/L, 12 h) was used as a positive control. Nuclear protein was isolated and immunoblotted for ATF4 and CHOP; lamin A/C (loading control). *B*, active XBP-1 protein ($XBP\text{-}1_{376aa}$) was induced in HeLa cells exposed to normoxia or hypoxia for 6 h before treatment with DMSO or bortezomib for 18 h. Thapsigargin (1 μmol/L, 12 h) was used as a control. Nuclear protein was isolated and immunoblotted for XBP-1; lamin A/C (loading control). *C*, HT1080-ATF4-Luc cells were treated with DMSO or bortezomib, and luminescence was measured 8 h later. *D*, *left*, mice with HT1080-CMV-Luc tumors on the left flank and HT1080-ATF4-Luc tumors on the right flank were given i.p. injections of the vehicle or bortezomib (1 mg/kg) and imaged for optical bioluminescence 8 h later. *Right*, quantitation of *in vivo* bioluminescence of mice (*left*). Results are normalized to CMV-luc activity in untreated (vehicle-injected) animals.

rinsed with 1 × PBS and allowed to incubate in fresh medium under normal conditions for 7 to 14 d. Platings were performed in triplicate. After incubation, cells were fixed with 10% methanol–10% acetic acid and stained with a 0.4% solution of crystal violet. Colonies with >50 cells were counted. Plating efficiencies were determined for each treatment and normalized to controls. Error bars represent SE.

Analysis of autophagy and necrosis. Acridine orange staining and electron microscopy for analysis of autophagy and lactate dehydrogenase (LDH) detection assay and HMGB1 isolation for analysis of necrosis were performed, as described in the supplementary material.

GFP-LC3 transfections. HeLa cells were transfected with 0.4 μg pcDNA3.1/GFP-LC3 plasmid using Lipofectamine LTX and PLUS reagent (Invitrogen), and at 24 h posttransfection, cells were treated for 4 h with DMSO, bortezomib, or chloroquine under normoxic or hypoxic conditions. The cells were stained with Hoechst 33342 (1:1,000, 5 min, room temperature), rinsed with 1 × PBS, fixed using 4% paraformaldehyde (15 min, room temperature), and mounted on glass slides with hardening gel. Images were obtained using a Nikon epifluorescence microscope at 60× magnification.

Results

Hypoxia sensitizes human tumor cells to the ER stressor thapsigargin. Tumor hypoxia increases cellular resistance to various chemotherapeutic agents (1).We hypothesized that hypoxic cells would be hypersensitive to agents that induce ER stress. To test this, we compared the cytotoxic effects of thapsigargin, a pharmacologic inhibitor of the SERCA pump, on normoxic and hypoxic tumor cells. As shown in Fig. 1*A*, HeLa cells preexposed to hypoxia (<0.2% O_2) were significantly more sensitive to low doses of thapsigargin compared with normoxic cells. In contrast, etoposide, a genotoxic chemotherapeutic agent, was less effective in killing tumor cells under hypoxia (Fig. 1*B*). The preferential sensitivity to thapsigargin was also evident under more moderate hypoxic conditions (1% O_2; Supplementary Fig. S1*A*). This response was not cell type–specific, as hypoxic HT29 colorectal cells were also more sensitive to thapsigargin compared with their normoxic counterparts (data not shown). These results suggested that hypoxic tumor cells are preferentially sensitive to pharmacologic ER stressors.

Hypoxic tumor cells are preferentially sensitive to the proteasome inhibitor bortezomib. Although a potent UPR activator, thapsigargin has a narrow therapeutic window because it is also highly toxic toward normal, untransformed cells (26). Therefore, its clinical potential is limited. Conversely, the dipeptide boronic acid proteasome inhibitor bortezomib (PS-341; Velcade), which was shown to induce ER stress in human tumor cells, is in clinical use (14, 16–19). Whereas Veschini and colleagues reported that endothelial cells (human umbilical vascular endothelial cells) are sensitive to bortezomib (27), its toxicity toward hypoxic tumor cells has not been examined. Low nanomolar concentrations of bortezomib induced the accumulation of ubiquitinated proteins under both normoxia and hypoxia, indicating that bortezomib inhibited 26S proteasome activity to the same extent (Supplementary Fig. S1*C*). Similar to the results obtained with thapsigargin,

hypoxic HeLa cells were significantly more sensitive to bortezomib compared with normoxic cells (Fig. 1*C* and Supplementary Fig. S1*B*). A similar response was seen in DLD1 colorectal carcinoma cells treated with bortezomib (Fig. 1*D* and Supplementary Fig. S1*B*). Moreover, hypoxic DLD1 cells were also hypersensitive to another proteasome inhibitor, MG132, compared with normoxic cells (Supplementary Fig. S1*D*), indicating that this increased sensitivity was not due to nonspecific effects of bortezomib. These results show that hypoxic tumor cells are more sensitive to proteasome inhibition and suggest that the enhanced cytotoxicity may be due to the overactivation of ER stress–dependent pathways.

UPR signaling is enhanced in hypoxic tumor cells treated with bortezomib. Although it has been reported that bortezomib can induce the UPR in solid tumor cell lines (17–19), other studies have shown that it compromised UPR activation in myeloma cells (16). To assess the effect of hypoxia and bortezomib on the UPR, we analyzed the induction of UPR targets ATF4, CHOP, and XBP-1. Under normoxic conditions, bortezomib induced eIF2α phosphorylation in a dose-dependent manner (Supplementary Fig. S2*A*). Hypoxia alone induced eIF2α phosphorylation, and although this phosphorylation was not enhanced with bortezomib, the levels of the downstream targets ATF4 and CHOP, which accumulate in an eIF2α phosphorylation–dependent manner, were enhanced with the combined treatment (Fig. 2*A*). Thapsigargin treatment also induced a robust accumulation of ATF4 and CHOP. A higher concentration of thapsigargin was used compared with treatment in the clonogenic assay experiments (Fig. 1), because the duration of the treatments here was substantially shorter and we wanted to avoid any toxicity by this agent. Whereas the reason for the maximal induction of eIF2α phosphorylation by the combined stress is unclear, it is likely due to the activation of the GADD34-PP1 negative feedback loop responsible for dephosphorylating eIF2α, which may limit further phosphorylation of eIF2α (28, 29).

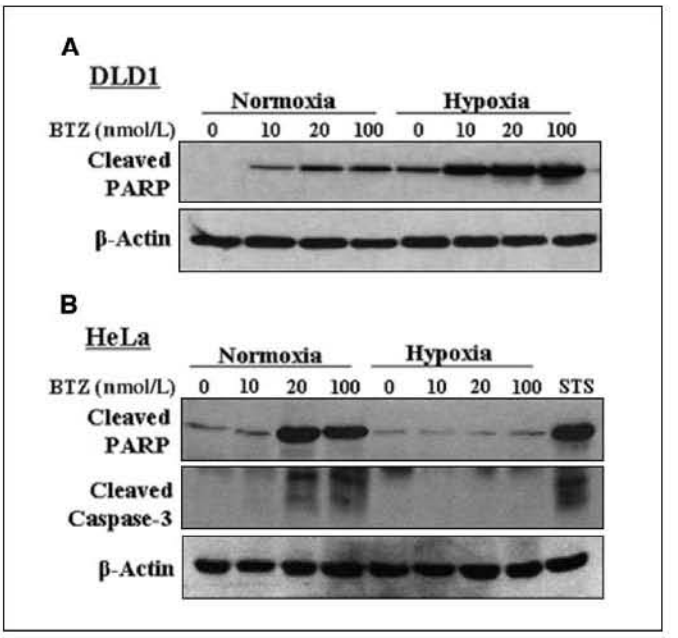

Figure 4. Bortezomib induces apoptotic cell death in hypoxic DLD1 but not in HeLa cells. *A*, DLD1 cells were exposed to normoxic or hypoxic conditions for 12 h before treatment with DMSO or bortezomib for 24 h. Immunoblotting was performed using antibodies specific for cleaved PARP and β-actin (loading control). *B*, HeLa cells were exposed to normoxic or hypoxic conditions for 12 h before treatment with DMSO or bortezomib for 24 h. Staurosporine (*STS*; 1 μmol/L, 4 h) was used as a control. Immunoblotting was performed using antibodies specific for cleaved caspase-3, cleaved PARP, and β-actin (loading control).

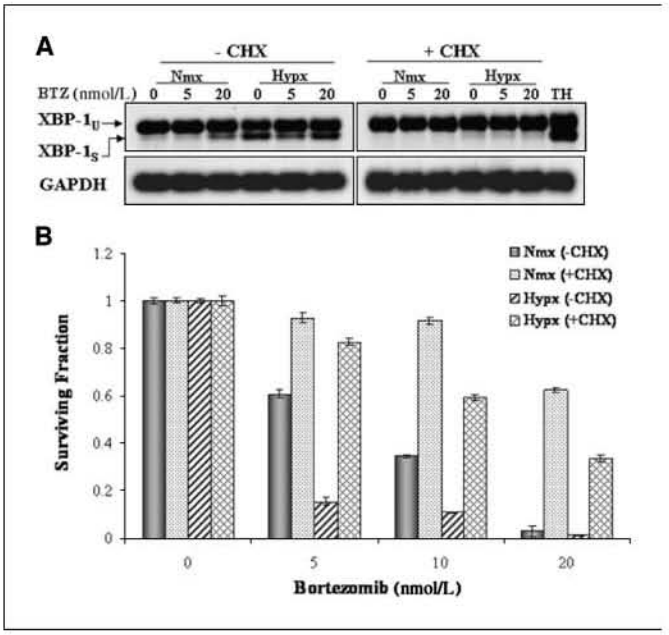

Figure 3. Ameliorating ER stress with cycloheximide (*CHX*) reverses the enhanced cytotoxic activity of bortezomib toward hypoxic tumor cells. *A*, unspliced XBP-1_U (473 bp) and spliced XBP-1_S (447 bp) mRNA detected by RT-PCR on RNA from HeLa cells exposed to normoxia or hypoxia for 6 h before treatment with DMSO, bortezomib, and cycloheximide (1 μg/mL) for 18 h. Thapsigargin (250 nmol/L, 8 h) was used as a control; glyceraldehyde-3-phosphate dehydrogenase (*GAPDH*) was used as a loading control. *B*, clonogenic survival of HeLa cells exposed to normoxic or hypoxic conditions for 12 h before treatment with DMSO, bortezomib, and cycloheximide (1 μg/mL) for 24 h. Experiments were performed in triplicate; *bars*, SE.

To assess the activity of the IRE1-dependent UPR pathway under these conditions, we examined XBP-1 mRNA splicing and the accumulation of the active XBP-1 protein. Bortezomib alone led to an accumulation of the spliced XBP-1 mRNA in a dose-dependent manner, as detected by reverse transcription–PCR (RT-PCR; Supplementary Fig. S2*B-C*). XBP-1 mRNA splicing was induced by hypoxia alone; however, the amount of spliced XBP-1 mRNA was not further enhanced by the addition of bortezomib, indicating a binary "on-off" rather than a graded response to hypoxia.

The spliced mRNA encodes for the larger functional XBP-1 (XBP-1_{376aa}) transcription factor, which can be distinguished from the nonfunctional protein (XBP-1_{261aa}) encoded by the unprocessed XBP-1 mRNA by their difference in electrophoretic mobilities (10). In HeLa cells treated with bortezomib under normoxic conditions, only at the higher doses were both forms of XBP-1 protein detected (Fig. 2*B*). The accumulation of the XBP-1_{261aa} protein in the presence of bortezomib suggests that this form was stabilized in the absence of a functional proteasome. Hypoxia alone induced the expression of XBP-1_{376aa}, which was further enhanced by bortezomib, suggesting that all available spliced XBP-1 mRNAs being processed are translated into active transcription factor. Altogether, these results show that bortezomib hyperactivates both the PERK and IRE1 arms of the UPR in hypoxic tumor cells.

Bortezomib treatment increases UPR reporter gene activity *in vitro* and *in vivo*. We further examined the effects of

bortezomib using an ATF4-luciferase reporter *in vitro* and *in vivo*. HT1080 fibrosarcoma cells were stably transfected with a luciferase reporter gene fused to the 5'-untranslated region of ATF4, which confers translational up-regulation to any 5'-fused heterologous reporter gene under conditions of ER stress in a PERK-dependent manner (Supplementary Fig. S3). Bortezomib induced a dose-dependent and time-dependent increase in ATF4-luciferase reporter activity (Fig. 2*C*). We also tested whether bortezomib could activate the reporter in an *in vivo* tumor model by using the ATF4-luciferase expressing HT1080 cells to grow tumor xenografts in nude mice. All tumors exhibited a basal level of ATF4-luciferase reporter activity, likely reflecting activation by ER stress produced by the tumor microenvironment. However, the tumors treated with bortezomib showed an increase in bioluminescence after 8 hours compared with the vehicle-treated tumors (Fig. 2*D*), demonstrating that bortezomib enhanced the ATF4-luciferase reporter activity *in vivo*. These results suggest that bortezomib can further increase the levels of ER stress produced by the tumor microenvironment.

Ameliorating ER stress protects hypoxic tumor cells from bortezomib. The results, thus far, suggested that the enhanced cytotoxicity produced by the combination of hypoxia and bortezomib induced levels of ER stress incompatible with tumor cell survival. Therefore, we hypothesized that amelioration of ER protein load should reduce the cytotoxicity of the combined treatment. We examined the effects of cycloheximide, previously shown to decrease ER stress by reducing the overall levels of client proteins in the ER (30), on XBP-1 mRNA splicing under the combined treatment. Cycloheximide blocked IRE1-dependent XBP-1 splicing in HeLa cells by both individual treatments, as well as their combination (Fig. 3*A*). More importantly, cycloheximide significantly reduced the cytotoxic effect of bortezomib in HeLa cells (Fig. 3*B*). This effect was more pronounced under hypoxic conditions, indicating the overall amount of ER stress produced by the combination of limited oxygen availability and proteasome inhibition led to increased lethality to tumor cells.

To further examine the role of increased ER stress in the enhanced sensitivity of tumor cells to the combined effects of hypoxia and bortezomib, we exposed cells lacking a functional UPR to the combination treatment. PERK $^{/}$ MEFs are more sensitive to ER stressors, including thapsigargin and hypoxia, compared with PERK$^{+/+}$ MEFs (4, 30, 31). PERK $^{/}$ MEFs were more sensitive to the combination of hypoxia and bortezomib compared with MEFs with wild-type PERK function (Supplementary Fig. S4), indicating that the cytotoxicity of bortezomib to hypoxic cells resulted from the high levels of ER stress generated, being incompatible with cell survival.

Hypoxic tumor cells treated with bortezomib undergo apoptosis and autophagy. To further investigate the mechanism of cell death under hypoxia and bortezomib, we analyzed the expression of apoptotic markers in DLD1 and HeLa cells. In DLD1 cells, bortezomib induced cleavage of poly(ADP-ribose) polymerase (PARP; Fig. 4*A*) and processing of caspase-4 (Supplementary Fig. S5*A*), which has been implicated in ER stress–induced apoptosis (32). This activity was enhanced under hypoxia. In HeLa cells, bortezomib induced similar processing of PARP, caspase-3, and caspase-4. Surprisingly, the processing of PARP and caspase-3 in HeLa cells was completely abolished under severe or moderate hypoxia (Fig. 4*B* and Supplementary Fig. S5*B*), suggesting that preexposure to hypoxia blocked apoptosis induced by bortezomib downstream of caspase-4 but upstream of caspase-3 and PARP cleavage. This lack of terminal apoptosis was also supported by the fact that bortezomib did not significantly enhance the sub-G_1

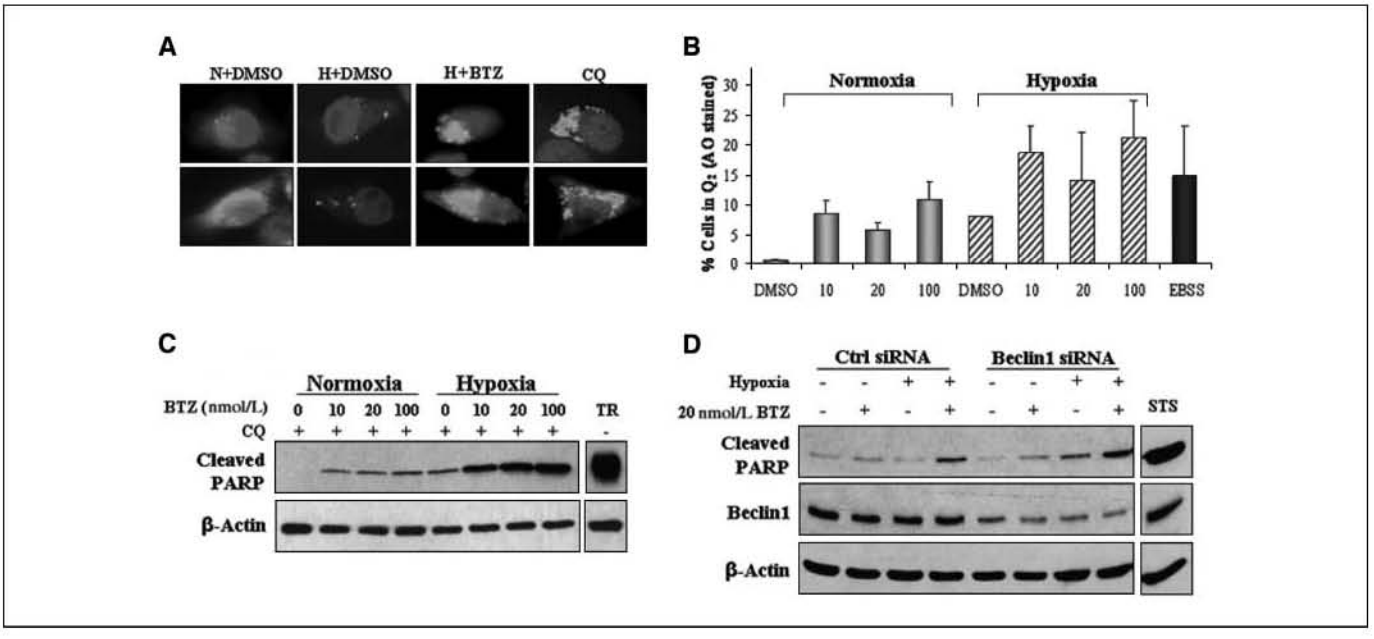

Figure 5. Bortezomib induces increased autophagy in hypoxic HeLa cells. *A,* HeLa cells treated 24-h posttransfection with GFP-LC3 were exposed to normoxic or hypoxic conditions with bortezomib for 4 h. Chloroquine (*CQ*; 10 μmol/L, 4 h) was used as a control. Two different cells are shown for each treatment. *B,* HeLa cells were exposed to normoxic or hypoxic conditions for 6 h before treatment with DMSO or bortezomib for 18 h. EBSS was used as a control. Cells were stained with acridine orange, and red fluorescence was detected by flow analysis. *C,* HeLa cells were exposed to normoxic or hypoxic conditions for 12 h before treatment with DMSO or bortezomib for 24 h. Chloroquine (10 μmol/L) was present during the last 4 h of treatment. TRAIL (*TR*; 50 ng/mL, 4 h) was used as a control. Immunoblotting was performed using antibodies specific for cleaved PARP and β-actin (loading control). *D,* HeLa cells, transfected with siRNA against Beclin1 or a nontargeting control siRNA, were treated 30-h posttransfection as in *B*. Staurosporine (*STS*; 1 μmol/L, 4 h) was used as a control. Immunoblotting was performed using antibodies specific for Beclin1, cleaved PARP, and β-actin (loading control).

population (Supplementary Fig. S5*C*) in hypoxic HeLa cells. These results suggested that, although the combined effects of hypoxia and bortezomib led to increased cell death in several tumor cell types, the mode of cell death induced by the combined treatment was cell type–dependent.

Previous work in yeast (33, 34) and mammalian cells (35, 36) established that ER stress can activate autophagy, a highly conserved lysosome-dependent mechanism for degrading intracellular constituents. It has been proposed that autophagy, as a prosurvival mechanism under short-term nutrient deprivation, can counteract apoptotic mechanisms and that the inhibition of autophagy makes cells more susceptible to stress-induced apoptosis (37). Interestingly, hypoxic HeLa cells treated with bortezomib had more and larger cytoplasmic vacuoles compared with similarly treated normoxic HeLa cells, suggesting that autophagy was occurring under these conditions (Supplementary Fig. S6*A*). The LC3-II protein, processed from the phosphatidylethanolamine conjugation of LC3-I, translocates to the autophagosome membrane and is used as a marker of autophagy (38). GFP-LC3 remained mostly cytoplasmic in HeLa cells treated with DMSO or bortezomib alone, whereas it seemed more punctate in hypoxic HeLa cells (Fig. 5*A*). HeLa cells treated under hypoxia with chloroquine, an agent known to increase the lysosomal pH and allow for LC3-II accumulation, exhibited a strong punctate pattern, indicating that most of the GFP-LC3 was incorporated into autophagosome membranes. A similar pattern of GFP-LC3 was seen in the hypoxic HeLa cells treated with bortezomib. Electron microscopy (Supplementary Fig. S6*B*) confirmed that the vesicles formed in hypoxic HeLa cells treated with 20 nmol/L bortezomib exhibited the classical double-membrane morphology characteristic of autophagosomes. To quantitate the level of autophagy under these conditions, we analyzed the intensity of acridine orange staining in normoxic and hypoxic HeLa cells treated with bortezomib. Whereas bortezomib alone increased the intensity of acridine orange staining, the levels under hypoxia were further enhanced with bortezomib (Fig. 5*B*).

To test if HeLa cells activate autophagy as a survival response under low oxygen and proteasome inhibition, we blocked autophagy with pharmacologic and genetic ablation. HeLa cells treated during the last 4 hours of bortezomib treatment with chloroquine, which inhibits the progression of autophagy (39), led to increased levels of cleaved PARP in hypoxic cells (Fig. 5*C*), indicating that blocking autophagy under the combined treatment led to enhanced apoptosis. Knockdown of Beclin1, an important regulator of autophagy (40), by siRNA in hypoxic HeLa cells treated with bortezomib, resulted in increased PARP cleavage (Fig. 5*D*). However, overall clonogenic survival was not substantially altered (Supplementary Fig. S6*C*), suggesting that hypoxic HeLa cells activated autophagy as an adaptive response that initially blocked bortezomib-induced apoptosis but did not ultimately prevent cell death.

Hypoxic HeLa cells treated with bortezomib undergo necrosis. Previous works suggested that necrosis, yet another form of cell death, may be triggered by metabolic stress under conditions of defective apoptosis or prolonged autophagy (37). Therefore, we analyzed the extracellular activity of LDH and levels of HMGB1, two markers of necrosis. LDH, a cytoplasmic enzyme, and HMGB1, a chromatin-binding protein, are released into the extracellular space under conditions that compromise the integrity of the plasma membrane (41). Although there was very low LDH activity detected in the media of HeLa cells treated with bortezomib under normoxic conditions, it was increased in bortezomib-treated hypoxic cells (Fig. 6*A*). Furthermore, bortezomib enhanced the levels of HMGB1 in the extracellular media of hypoxic HeLa cells compared with normoxic cells (Fig. 6*B*), suggesting that the increase in HeLa cell lethality induced by the combination of bortezomib and hypoxia correlated with enhanced necrosis.

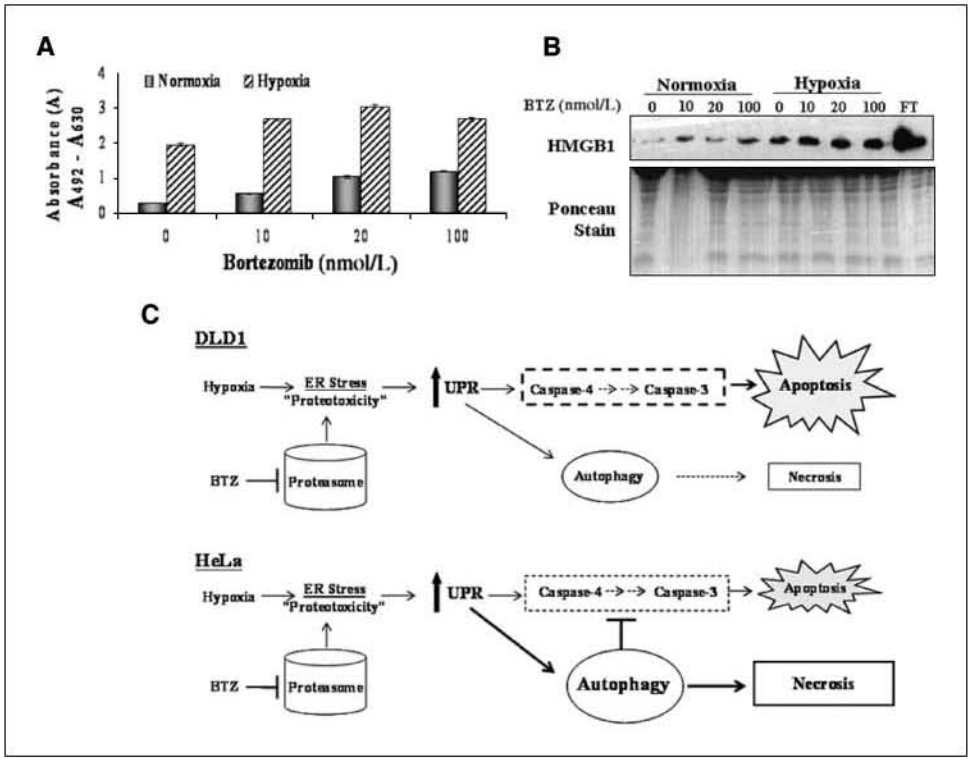

Figure 6. Hypoxic HeLa cells treated with bortezomib undergo necrotic death. *A*, HeLa cells were exposed to normoxic or hypoxic conditions for 12 h before treatment with DMSO or bortezomib for 24 h. LDH activity was assayed in media off each sample at the indicated doses. *Bars*, SE. *B*, protein was isolated from the media off HeLa cells treated as in *A*. Freeze/thawed HeLa cells (*FT*) were used as a control. Immunoblotting was performed using an antibody specific for HMGB1; the Ponceau-stained membrane is shown as a loading control. *C*, model describing the lethal effects of the combination of hypoxia and the proteasome inhibitor bortezomib in DLD1 cells (*top*) or HeLa cells (*bottom*). See Discussion for more details.

Discussion

We have investigated the effects of combining ER stressors with the physiologic stress of hypoxia on tumor cells. Although we found that hypoxia and bortezomib individually induce ER stress by allowing unfolded proteins to accumulate in the ER, combining these stresses together enhances UPR activity and cytototoxicity against solid tumor cells. Importantly, reducing the protein burden on the ER with cycloheximide alleviates not only UPR signaling but also the cytotoxicity of either stress alone and in combination, suggesting that the severe toxicity of hypoxia and bortezomib combined is induced by the increased amount of ER stress generated. Interestingly, the mechanism of clonogenic cell death is different in the two tumor cell types tested. In DLD1 cells, the ER stress generated by hypoxia and bortezomib induced significant ER-dependent apoptosis (Fig. 6*C, top*). However, HeLa cells responded to the combined treatment by robust activation of autophagy, which blocked apoptosis and eventually led to necrotic cell death (Fig. 6*C, bottom*). It is possible that some tumor cells, like DLD1, either have a lower apoptotic threshold or have more rapid kinetics of apoptosis, compared with cells like HeLa, in which the combined treatment leads to autophagy.

Whereas several studies have now established that proteasome inhibitors activate UPR, there are reports suggesting that they may compromise UPR signaling. Lee and colleagues reported the sensitivity of myeloma cells to proteasome inhibition was in part due to disrupted IRE1-mediated signaling (16). Similarly, MG132 did not appreciably activate IRE1 or ATF6 in MEFs but led to GCN2-dependent eIF2α phosphorylation and reduced rates of translation (42). Our results show that solid tumor cells, treated with bortezomib under normoxic and hypoxic conditions, up-regulated the PERK and IRE-dependent arms of the UPR (Fig. 2). These apparent differences likely reflect variations in the UPR pathways in the cell types used (e.g., multiple myeloma versus cervical or colorectal carcinoma) or the treatment durations and doses of the proteasome inhibitors. In our study, we examined the effects of bortezomib at low physiologic doses, which have been reported to exist in the plasma of bortezomib-treated patients. Interestingly, in agreement with the report by Lee and colleagues, we also observed up-regulation of unspliced XBP-1 protein by bortezomib treatment, which could inhibit spliced XBP-1 (16). However, under hypoxic conditions, XBP-1 splicing was complete and no accumulation of the smaller XBP-1 protein was evident, suggesting that the combination of bortezomib and hypoxia led to UPR overactivation.

Autophagy can provide a survival advantage for tumor cells in regions of metabolic stress, such as in the hypoxic tumor microenvironment (37, 43). Because autophagy is generally viewed as a prosurvival mechanism and an impediment to chemotherapy, our findings suggest that it may be possible to overcome this prosurvival pathway induced by hypoxia and "push" hypoxic tumor cells into necrosis by overactivating ER stress–dependent mechanisms. It will be interesting to test the combined effects of bortezomib and autophagy inhibitors like chloroquine *in vivo*, which we predict will show even greater cytotoxicity toward hypoxic tumor cells.

The precise mechanism of hypoxia-induced, ER-dependent cell death is still unknown. One potential player may be the proapoptotic protein CHOP. In agreement with other reports (18, 19), CHOP was induced by bortezomib, hypoxia, and the combined treatment. However, markers of terminal apoptosis were not detected in HeLa cells under the combination treatment, even in the presence of CHOP, suggesting that autophagy may also be able to block the prodeath functions of CHOP. Caspase-4 is also activated by the IRE1-TRAF2-ASK1 complex, which is induced upon ER stress (44). Indeed, others have reported that bortezomib can induce phosphorylation of c-Jun-NH_2-kinase (18), which is also involved in proteasome inhibition–induced autophagy and important for tumor cell survival after ER stress (36, 45). Although our results point to enhanced ER stress–induced events in tumor cells under the combined stresses of hypoxia and proteasome inhibition, we cannot exclude the possibility that other non–ER-dependent pathways may also be involved. For example, some of cytotoxic effects of bortezomib toward hypoxic tumor cells could be due to the inhibition of nuclear factor-κB via IκB stabilization (15). However, our findings that thapsigargin, an ER stressor with a different mode of action from proteasome inhibitors, exhibits similarly preferential cytotoxicity toward hypoxic tumor cells supports the notion that the combined cytotoxicity occurs through an ER stress–dependent mechanism.

A recent report by Shin and colleagues indicates that bortezomib, despite increasing HIF-1α levels, actually inhibited HIF-1α transcriptional activity by enhancing the interaction with the factor-inhibiting HIF (46). These findings suggest that the inhibitory effects of bortezomib on angiogenesis and increased cell death may involve the inhibition of HIF-1α activity. Although we cannot rule out a role for HIF-1α inhibition in increasing bortezomib-induced lethality toward hypoxic tumor cells, it is unlikely that this mechanism plays a significant role in this response for the following reasons. First, as mentioned earlier, UPR activation under hypoxia was found to occur independently of HIF-1α status, as HIF-1α $^{-/-}$ MEFs exhibited similar levels of eIF2α phosphorylation as HIF-$1\alpha^{+/+}$ MEFs (4). Second, thapsigargin, an ER stressor that does not inhibit HIF-1α levels or activity, shows a similar synergy with hypoxia as bortezomib. Third, it has been shown that HIF-1α plays little, if any, role in promoting epithelial cell survival under stringent hypoxic conditions. The fact that thapsigargin causes ER stress by a different mechanism than bortezomib and also preferentially kills hypoxic tumor cells argues against a HIF-mediated role in this response, at least in the epithelial cell lines tested.

Currently, tumor hypoxia represents a significant clinical problem. However, the reliance of hypoxic tumor cells on a functional UPR may provide a unique therapeutic opportunity. Indeed, the concept of hypoxia-selective cytotoxicity has received significant attention, and one such hypoxia-selective agent, tirapazamine, is in late-phase clinical trials (1). One approach to target the UPR in tumors is to develop inhibitors that would compromise UPR signaling via PERK, IRE1, or molecular chaperones like GRP78/BiP (47, 48), and screening of small molecule libraries is under way by several groups.[4] Our findings suggest a second approach for targeting the UPR in hypoxic tumor cells, which relies on a clinically used agent to hyperactivate the UPR in hypoxic cells. As only a fraction of a patient's tumor is hypoxic at any given time, administering low doses of an ER stressor, such as bortezomib, is unlikely to eradicate the bulk of the tumor and provide efficient tumor control. However, we propose that the significance of our findings lie in the opportunity to incorporate bortezomib with other modalities like radiotherapy and chemotherapy, which preferentially target normoxic tumor cells with the expectation that killing the hypoxic cells will allow for more effective tumor control and longer overall patient survival.

[4] A.C. Koong et al., unpublished results.

Disclosure of Potential Conflicts of Interest

No potential conflicts of interest were disclosed.

Acknowledgments

Received 7/28/2008; revised 9/2/2008; accepted 9/2/2008.

Grant support: NIH grants CA94214 (D.R. Fels, J. Ye, A.T. Segan, S.S. Kridel, and C. Koumenis) and CA112108 (M. Spiotto, M. Olson, and A.C. Koong).

The costs of publication of this article were defrayed in part by the payment of page charges. This article must therefore be hereby marked *advertisement* in accordance with 18 U.S.C. Section 1734 solely to indicate this fact.

We thank Drs. Julian Lum and Craig Thompson (University of Pennsylvania) for the GFP-LC3 plasmid, the anti-LC3 antibody, and the helpful discussions; Dr. Andrew Thorburn (University of Colorado) for the pcDNA3.1/GFP-LC3 plasmid; and Dr. Serge Fuchs (University of Pennsylvania) for critically reading our manuscript.

References

1. Brown JM. Tumor hypoxia in cancer therapy. Methods Enzymol 2007;435:297–321.
2. Semenza GL. Targeting HIF-1 for cancer therapy. Nat Rev Cancer 2003;3:721–32.
3. Le QT, Denko NC, Giaccia AJ. Hypoxic gene expression and metastasis. Cancer Metastasis Rev 2004;23:293–310.
4. Koumenis C, Naczki C, Koritzinsky M, et al. Regulation of protein synthesis by hypoxia via activation of the endoplasmic reticulum kinase PERK and phosphorylation of the translation initiation factor eIF2α. Mol Cell Biol 2002;22:7405–16.
5. Blais JD, Filipenko V, Bi M, et al. Activating Transcription Factor 4 Is Translationally Regulated by Hypoxic Stress. Mol Cell Biol 2004;24:7469–82.
6. Koritzinsky M, Magagnin MG, van den Beucken T, et al. Gene expression during acute and prolonged hypoxia is regulated by distinct mechanisms of translational control. EMBO J 2006;25:1114–25.
7. Liu L, Cash TP, Jones RG, Keith B, Thompson CB, Simon MC. Hypoxia-induced energy stress regulates mRNA translation and cell growth. Mol Cell 2006;21:521–31.
8. Ron D, Walter P. Signal integration in the endoplasmic reticulum unfolded protein response. Nat Rev Mol Cell Biol 2007;8:519–29.
9. Bi M, Naczki C, Koritzinsky M, et al. ER stress-regulated translation increases tolerance to extreme hypoxia and promotes tumor growth. EMBO J 2005;24:3470–81.
10. Yoshida H, Matsui T, Yamamoto A, Okada T, Mori K. XBP1 mRNA is induced by ATF6 and spliced by IRE1 in response to ER stress to produce a highly active transcription factor. Cell 2001;107:881–91.
11. Calfon M, Zeng H, Urano F, et al. IRE1 couples endoplasmic reticulum load to secretory capacity by processing the XBP-1 mRNA. Nature 2002;415:92–6.
12. Zinszner H, Kuroda M, Wang X, et al. CHOP is implicated in programmed cell death in response to impaired function of the endoplasmic reticulum. Genes Dev 1998;12:982–95.
13. Travers KJ, Patil CK, Wodicka L, Lockhart DJ, Weissman JS, Walter P. Functional and genomic analyses reveal an essential coordination between the unfolded protein response and ER-associated degradation. Cell 2000;101:249–58.
14. Richardson PG, Mitsiades C, Hideshima T, Anderson KC. BORTEZOMIB: proteasome inhibition as an effective anticancer therapy. Annu Rev Med 2006;57:33–47.
15. Hideshima T, Richardson P, Chauhan D, et al. The proteasome inhibitor PS-341 inhibits growth, induces apoptosis, and overcomes drug resistance in human multiple myeloma cells. Cancer Res 2001;61:3071–6.
16. Lee A-H, Iwakoshi NN, Anderson KC, Glimcher LH. Proteasome inhibitors disrupt the unfolded protein response in myeloma cells. Proc Natl Acad Sci U S A 2003;100:9946–51.
17. Fribley A, Zeng Q, Wang C-Y. Proteasome inhibitor PS-341 induces apoptosis through induction of endoplasmic reticulum stress-reactive oxygen species in head and neck squamous cell carcinoma cells. Mol Cell Biol 2004;24:9695–704.
18. Nawrocki ST, Carew JS, Dunner K, Jr., et al. Bortezomib inhibits PKR-like endoplasmic reticulum (ER) kinase and induces apoptosis via ER stress in human pancreatic cancer cells. Cancer Res 2005;65:11510–9.
19. Obeng E, Carlson L, Gutman D, Harrington JW, Lee K, LH. B. Proteasome inhibitors induce a terminal unfolded protein response in multiple myeloma cells. Blood 2006;107:4907–16.
20. Reddy RK, Mao C, Baumeister P, Austin RC, Kaufman RJ, Lee AS. Endoplasmic reticulum chaperone protein GRP78 protects cells from apoptosis induced by topoisomerase inhibitors: role of ATP binding site in suppression of caspase-7 activation. J Biol Chem 2003;278:20915–24. Epub 2003 Mar 28.
21. Dong D, Ni M, Li J, et al. Critical role of the stress chaperone GRP78/BiP in tumor proliferation, survival, and tumor angiogenesis in transgene-induced mammary tumor development. Cancer Res 2008;68:498–505.
22. Pyrko P, Schonthal AH, Hofman FM, Chen TC, Lee AS. The unfolded protein response regulator GRP78/BiP as a novel target for increasing chemosensitivity in malignant gliomas. Cancer Res 2007;67:9809–16.
23. Ameri K, Lewis CE, Raida M, Sowter H, Hai T, Harris AL. Anoxic induction of ATF-4 through HIF-1-independent pathways of protein stabilization in human cancer cells. Blood 2004;103:1876–82.
24. Koditz J, Nesper J, Wottawa M, et al. Oxygen-dependent ATF-4 stability is mediated by the PHD3 oxygen sensor. Blood 2007;110:3610–7.
25. Romero-Ramirez L, Cao H, Nelson D, et al. XBP1 is essential for survival under hypoxic conditions and is required for tumor growth. Cancer Res 2004;64:5943–7.
26. Denmeade SR, Jakobsen CM, Janssen S, et al. Prostate-specific antigen-activated thapsigargin prodrug as targeted therapy for prostate cancer. J Natl Cancer Inst 2003;95:990–1000.
27. Veschini L, Belloni D, Foglieni C, et al. Hypoxia-inducible transcription factor-1 α determines sensitivity of endothelial cells to the proteosome inhibitor bortezomib. Blood 2007;109:2565–70.
28. Novoa I ZY, Zeng H, Jungreis R, Harding HP, Ron D. Stress-induced gene expression requires programmed recovery from translational repression. EMBO J 2003;22:1180–7.
29. Ma Y, Hendershot LM. Delineation of a negative feedback regulatory loop that controls protein translation during endoplasmic reticulum stress. J Biol Chem 2003;278:34864–73.
30. Harding HP, Zhang Y, Bertolotti A, Zeng H, Ron D. Perk is essential for translational regulation and cell survival during the unfolded protein response. Mol Cell 2000;5:897–904.
31. Scheuner D, Song B, McEwen E, et al. Translational control is required for the unfolded protein response and *in vivo* glucose homeostasis. Mol Cell 2001;7:1165–76.
32. Hitomi J, Katayama T, Eguchi Y, et al. Involvement of caspase-4 in endoplasmic reticulum stress-induced apoptosis and A{β}-induced cell death. J Cell Biol 2004;165:347–56.
33. Bernales S MK, Walter P. Autophagy counterbalances endoplasmic reticulum expansion during the unfolded protein response. PLoS Biol 2006;4:e423.
34. Yorimitsu T, Nair U, Yang Z, Klionsky DJ. Endoplasmic reticulum stress triggers autophagy. J Biol Chem 2006;281:30299–304.
35. Kouroku Y, Fujita E, Tanida I, et al. ER stress (PERK/eIF2α phosphorylation) mediates the polyglutamine-induced LC3 conversion, an essential step for autophagy formation. Cell Death Differ 2007;14:230–9. Epub 2006 Jun 23.
36. Ogata M, Hino S-I, Saito A, et al. Autophagy is activated for cell survival after endoplasmic reticulum stress. Mol Cell Biol 2006;26:9220–31.
37. Degenhardt K, Mathew R, Beaudoin B, et al. Autophagy promotes tumor cell survival and restricts necrosis, inflammation, and tumorigenesis. Cancer Cell 2006;10:51–64.
38. Kabeya Y, Mizushima N, Ueno T, et al. LC3, a mammalian homologue of yeast Apg8p, is localized in autophagosome membranes after processing. EMBO J 2000;19:5720–8.
39. Amaravadi RK, Thompson CB. The roles of therapy-induced autophagy and necrosis in cancer treatment. Clin Cancer Res 2007;13:7271–9.
40. Liang XH, Jackson S, Seaman M, et al. Induction of autophagy and inhibition of tumorigenesis by beclin 1. Nature 1999;402:672–6.
41. Scaffidi P, Misteli T, Bianchi ME. Release of chromatin protein HMGB1 by necrotic cells triggers inflammation. Nature 2002;418:191–5.
42. Jiang H-Y, Wek RC. Phosphorylation of the {α}-subunit of the eukaryotic initiation factor-2 (eIF2{α}) reduces protein synthesis and enhances apoptosis in response to proteasome inhibition. J Biol Chem 2005;280:14189–202.
43. Karantza-Wadsworth V, Patel S, Kravchuk O, et al. Autophagy mitigates metabolic stress and genome damage in mammary tumorigenesis. Genes Dev 2007;21:1621–35.
44. Urano F, Wang X, Bertolotti A, et al. Coupling of stress in the ER to activation of JNK protein kinases by transmembrane protein kinase IRE1. Science 2000;287:664–6.
45. Ding W-X, Ni H-M, Gao W, et al. Linking of autophagy to ubiquitin-proteasome system is important for the regulation of endoplasmic reticulum stress and cell viability. Am J Pathol 2007;171:513–24.
46. Shin DH, Chun YS, Lee DS, Huang LE, Park JW. Bortezomib inhibits tumor adaptation to hypoxia by stimulating the FIH-mediated repression of hypoxia-inducible factor-1. Blood 2008;111:3131–6. Epub 2008 Jan 3.
47. Fu Y, Lee AS. Glucose regulated proteins in cancer progression, drug resistance and immunotherapy. Cancer Biol Ther 2006;5:741–4. Epub 2006 Jul 1.
48. Ma Y, Hendershot LM. The role of the unfolded protein response in tumour development: friend or foe? Nat Rev Cancer 2004;4:966–77.

Disruption of crosstalk between the fatty acid synthesis and proteasome pathways enhances unfolded protein response signaling and cell death

Joy L. Little,[1] Frances B. Wheeler,[1] Constantinos Koumenis,[2] and Steven J. Kridel[1]

[1]Department of Cancer Biology, Comprehensive Cancer Center, Wake Forest University School of Medicine, Winston-Salem, North Carolina and [2]Department of Radiation Oncology, University of Pennsylvania School of Medicine, Philadelphia, Pennsylvania

Abstract

Fatty acid synthase (FASN) is the terminal enzyme responsible for fatty acid synthesis and is up-regulated in tumors of various origins to facilitate their growth and progression. Because of several reports linking the FASN and proteasome pathways, we asked whether FASN inhibitors could combine with bortezomib, the Food and Drug Administration-approved proteasome inhibitor, to amplify cell death. Indeed, bortezomib treatment augmented suboptimal FASN inhibitor concentrations to reduce clonogenic survival, which was paralleled by an increase in apoptotic markers. Interestingly, FASN inhibitors induced accumulation of ubiquinated proteins and enhanced the effects of bortezomib treatment. In turn, bortezomib increased fatty acid synthesis, suggesting crosstalk between the pathways. We hypothesized that cell death resulting from crosstalk perturbation was mediated by increased unfolded protein response (UPR) signaling. Indeed, disruption of crosstalk activated and saturated the adaptation arm of UPR signaling, including eIF2α phosphorylation, activating transcription factor 4 expression, and X-box-binding protein 1 splicing. Furthermore, although single agents did not activate the alarm phase of the UPR, crosstalk interruption resulted in activated c-Jun NH_2-terminal kinase and C/EBP homologous protein-dependent cell death. Combined, the data support the concept that the UPR balance between adaptive to stress signaling can be exploited to mediate increased cell death and suggests novel applications of FASN inhibitors for clinical use. [Mol Cancer Ther 2008;7(12):3816–24]

Introduction

Fatty acid synthase (FASN) is the central enzyme responsible for catalyzing the ultimate steps of fatty acid synthesis in mammalian cells (1, 2). Interestingly, high levels of FASN expression have been noted in many types of tumors. Accordingly, FASN expression levels correlate with advanced tumor stage and grade, poor patient prognosis, and reduced overall and disease-free survival (3–5). A functional correlation between FASN expression levels and tumor cell survival has been firmly established with the development of small-molecule inhibitors of FASN that induce cell death specifically in tumor cells and reduce tumor growth in spontaneous and xenograft tumor models (6–10).

FASN inhibitors induce several antitumor effects including cell cycle arrest and cell death (3–5). Some of the effects of FASN inhibitors are mediated through key tumor signaling pathways. For instance, it has been shown that pharmacologic inhibition of FASN activity results in reduced Akt phosphorylation in multiple tumor cell lines (11, 12). Conversely, phosphoinositide 3-kinase and Akt can drive FASN expression in tumor cells (12, 13). The demonstration that reduced FASN activity negatively affects Akt activation identifies feedback between the two pathways. As a result, blocking both pathways results in amplified cell death (11, 12, 14). Synergy between FASN inhibitors and other chemotherapeutics has been noted in multiple cell lines (15–19). It has also be shown that FASN overexpression protects breast cancer cells from chemotherapy-induced cell death (20). The demonstrated links between FASN, oncogenic pathways, and ultimate response to chemotherapy underscore the potential of FASN inhibitors for clinical use and suggest novel strategies for targeting tumor cells to improve cell-killing efficiency.

In prostate cancer, FASN expression is stabilized by the ubiquitin-specific protease 2a, a deubiquitinating enzyme (21). Treating prostate tumor cells with the proteasome inhibitor MG-132 also increases FASN expression, supporting evidence of FASN regulation by the proteasome (21). Inhibition of the proteasome can also stabilize nuclear SREBP-1 and increase FASN expression (22). Conversely, inhibiting FASN affects the proteasome pathway. Specifically, inhibition of FASN reduces expression of the E3 ubiquitin ligase Skp2 that is responsible for mediating the stability of key cellular proteins such as p27 (23). FASN

Received 6/13/08; revised 9/16/08; accepted 9/27/08.

Grant support: National Cancer Institute grant 5R01CA114104-02 and Department of Defense grant W81XWH-07-1-0024 (S.J. Kridel).

The costs of publication of this article were defrayed in part by the payment of page charges. This article must therefore be hereby marked *advertisement* in accordance with 18 U.S.C. Section 1734 solely to indicate this fact.

Requests for reprints: Steven J. Kridel, Department of Cancer Biology, Comprehensive Cancer Center, Wake Forest University School of Medicine, Medical Center Boulevard, Winston-Salem, NC, 27157. Phone: 336-716-7299; Fax: 336-716-0255. E-mail: skridel@wfubmc.edu

doi:10.1158/1535-7163.MCT-08-0558

inhibition also affects the expression profiles of several E2 ubiquitin conjugation enzymes and several E3 ubiquitin ligases (24). Combined, these data suggest a level of crosstalk between the FASN and proteasome pathways.

Previous work from our laboratory showed that inhibition of FASN activity induces endoplasmic reticulum (ER) stress and activation of the unfolded protein response (UPR; ref. 25). Interestingly, bortezomib (Velcade, PS-341), a Food and Drug Administration-approved inhibitor of the 26S proteasome, also activates the UPR in tumor cells (26–30). Given the connections between the proteasome and FASN, especially in prostate cancer, and that inhibitors of each induce ER stress, we hypothesized that FASN inhibitors and bortezomib could enhance prostate tumor cell death through UPR-driven mechanisms. The data presented herein show that functional crosstalk between the FASN and a proteasome pathway in prostate tumor cell lines is the basis for UPR-mediated death by two clinically relevant ER stressing agents.

Materials and Methods

Materials

The PC-3, DU145, and FS-4 cells were obtained from the American Type Culture Collection. Cell culture medium and supplements were from Invitrogen. Antibodies against eukaryotic translation initiation factor 2α (eIF2α), phospho-eIF2α, phospho-c-Jun NH_2-terminal kinase (JNK), total JNK (Thr^{183}/Tyr^{185}), phospho-c-Jun (Ser^{63}), lamin A/C, α-tubulin, cleaved caspase-3 (Asp^{175}), and cleaved PARP (Asp^{214}) were from Cell Signaling Technologies. Antibody against FASN was from BD Transduction Labs. Antibody against β-actin was from Sigma. Antibodies against C/EBP homologous protein (CHOP; R-20), activating transcription factor 4 (ATF4; CREB2 C-20), ubiquitin (FL-76), and X-box-binding protein 1 (XBP-1; M-186) were from Santa Cruz Biotechnology. TRIzol was from Invitrogen. Avian myeloblastosis virus reverse transcriptase and Taq polymerase were from Promega. [^{14}C]acetate was purchased from GE Healthcare. Oligonucleotides were synthesized by Integrated DNA Technologies, except for those designed for siRNA, which were synthesized by Dharmacon. Orlistat was purchased from Roche, bortezomib was purchased from Millennium Pharmaceuticals, and JNK inhibitor II, SP600125, and JNK inhibitor V, AS601245, were from Calbiochem. All other reagents were purchased from Sigma, Calbiochem, or Bio-Rad.

Cell Culture and Drug Treatments

Prostate tumor cell lines were maintained in RPMI 1640 and FS-4 human foreskin fibroblasts were maintained in DMEM-high glucose, both supplemented with 10% fetal bovine serum at 37°C and 5% CO_2. Cells were treated for the times and with drug concentrations as indicated. Orlistat was extracted from capsules in ethanol as described previously and stored at −80°C (8). Further dilutions were made in DMSO. Bortezomib was dissolved in DMSO and stored as individual 20 μmol/L aliquots at −20°C.

Immunoblot Analysis

Cells were harvested after the indicated treatments, washed with ice-cold PBS, and lysed in buffer containing 1% Triton X-100 to prepare for immunoblots. Lysis buffer was supplemented with protease, kinase, and phosphatase inhibitors 200 μmol/L phenylmethylsulfonyl fluoride, 5 μg/mL aprotinin, 5 μg/mL pepstatin A, 5 μg/mL leupeptin, 1 μmol/L sodium fluoride, 1 μmol/L sodium orthovanadate, and 50 μmol/L okadaic acid just before use. For nuclear proteins, such as ATF4, CHOP, and XBP-1, nuclear extracts were obtained by harvesting cells, washing with ice-cold PBS, and then lysing cells using a harvest buffer containing 10 mmol/L HEPES (pH 7.9), 50 mmol/L NaCl, 500 mmol/L sucrose, 100 μmol/L EDTA, 0.5% Triton X-100 with 1 mmol/L DTT, 10 mmol/L tetrasodium pyrophosphate, 100 mmol/L sodium fluoride, 17.5 mmol/L β-glycerophosphate, 1 μmol/L sodium orthovanadate, 1 mmol/L phenylmethylsulfonyl fluoride, 4 μg/mL aprotinin, and 2 μg/mL pepstatin A added just before use to separate the cytoplasmic and nuclei. The nuclei were pelleted in a swinging bucket rotor and then washed with buffer containing 10 mmol/L HEPES (pH 7.9), 10 mmol/L KCl, 100 μmol/L EDTA, and 100 μmol/L EGTA with 1 mmol/L DTT, 1 mmol/L phenylmethylsulfonyl fluoride, 1 μmol/L sodium orthovanadate, 4 μg/mL aprotinin, and 2 μg/mL pepstatin added just before use. The nuclei were then lysed in a buffer containing 10 mmol/L HEPES (pH 7.9), 500 mmol/L NaCl, 100 μmol/L EDTA, 100 μmol/L EGTA, and 0.1% NP-40 with 1 mmol/L DTT, 1 mmol/L phenylmethylsulfonyl fluoride, 1 μmol/L sodium orthovanadate, 4 μg/mL aprotinin, and 2 μg/mL pepstatin added just before use. Protein samples were electrophoresed through 10%, 12%, or 13.5% SDS-polyacrylamide gels and transferred to nitrocellulose, except for blots to detect phospho-eIF2α and eIF2α, which were transferred to Immobilon-P membrane (polyvinylidene difluoride). Immunoreactive bands were detected by enhanced chemiluminescence (Perkin-Elmer). Lamin A/C and β-actin were used as loading controls for immunoblots.

Quantification of Ubiquitin-Modified Proteins

Autoradiographs were scanned using a HP ScanJet4890. The digital files were then quantified using UN-SCAN-IT. The average intensity of ubiquitin detection was calculated relative to vehicle-treated samples for each blot. Then, the values for three independent experiments were averaged and graphed on a logarithmic scale.

Fatty Acid Synthesis Assays

To measure fatty acid synthesis, 1×10^5 cells per well were seeded in 24-well plates. Cells were treated with FASN inhibitors or bortezomib as indicated for 2 h. [^{14}C]acetate (1 μCi) was added to each well for an additional 2 h. Cells were collected and washed and lipids were extracted and quantified by scintillation counting as described previously (8).

Clonogenic Survival Assays

PC-3 and DU145 cells were plated in 6-well plates at a density of 2,000 per well 48 h before each experiment. Fresh medium containing the indicated drugs was added at the

indicated concentrations for 16 h. The medium was then removed, the wells were washed, and fresh medium was added. Plates were incubated until macroscopic colonies were formed. Visualization of colonies was done as described previously (25). Colonies were quantified by counting.

Combination Index and Statistical Calculations

PC-3 cells were treated with a dose response of orlistat, bortezomib, or the combination and analyzed for clonogenic survival. Calculations were done based on the Chou-Talalay method that calculates a combination index based on the equation: combination index = (D1) / (Dx1) + (D2) / (Dx2) + (D1)(D2) / (Dx1)(Dx2), where (D1) and (D2) are the doses of the individual drugs that have "x" effect when used in combination and (Dx1) and (Dx2) are the doses of the drugs having "x" effect when used separately (31). A combination index < 1 indicates synergism.

For clonogenic survival assays, survival of treated cells was normalized relative to vehicle-treated cells and *P* values between combined and single-agent treated cells were determined by two-tailed Student's *t* tests. For fatty acid synthesis assays, bortezomib-treated cells were compared with vehicle-treated cells and *P* values were determined by two-tailed Student's *t* test. For the ubiquitin modification blots, the quantification of three separate blots was averaged for each treatment and then significance measured relative to untreated controls by two-tailed Student's *t* test.

Detection of XBP-1 Splicing and GADD34 Expression and Suppression of CHOP Expression with siRNA

Cells were exposed to the various drug treatments or transfected with siRNA for the indicated times. Reverse transcription-PCR was done for XBP-1 splicing and GADD34 expression as described previously (25). To knockdown CHOP levels, a siGENOME SMARTpool siRNA oligonucleotide cocktail against *CHOP* (1, AAAUGAAGAGGAAGAAUCA; 2, GAAUCUGCACCAAGCAUGA; 3, CCAGCAGAGGUCACAAGCA; and 4, GAGCUCUGAUUGACCGAAU) and one control siRNA against luciferase as a negative control (Luc sense, CUUACGUGAUACUUCGAUU) were designed and synthesized by Dharmacon. The individual siRNAs (83 nmol/L) were transfected into cells at plating with siPORT *NeoFX* transfection reagent (Ambion) according to manufacturer's instructions. After 48 h, transfection medium was removed and fresh medium containing indicated drug was added to cells. After indicated treatment times, cells were collected and nuclear protein was harvested for immunoblot analysis of CHOP and lamin A/C or tubulin.

Results

We hypothesized that the identified connections between the fatty acid synthesis and proteasome pathways would provide a novel strategy to target UPR activation and increase cell death in prostate tumor cells. To test this hypothesis, PC-3 and DU145 cells were examined for clonogenic survival after treatment with orlistat or C75 and the proteasome inhibitor bortezomib. Clonogenic survival of PC-3 and DU145 cells was reduced by bortezomib treatment in a dose-dependent manner (Fig. 1A and B). Suboptimal concentrations of FASN inhibitors were used to reduce cell killing by any of the single agents (data not

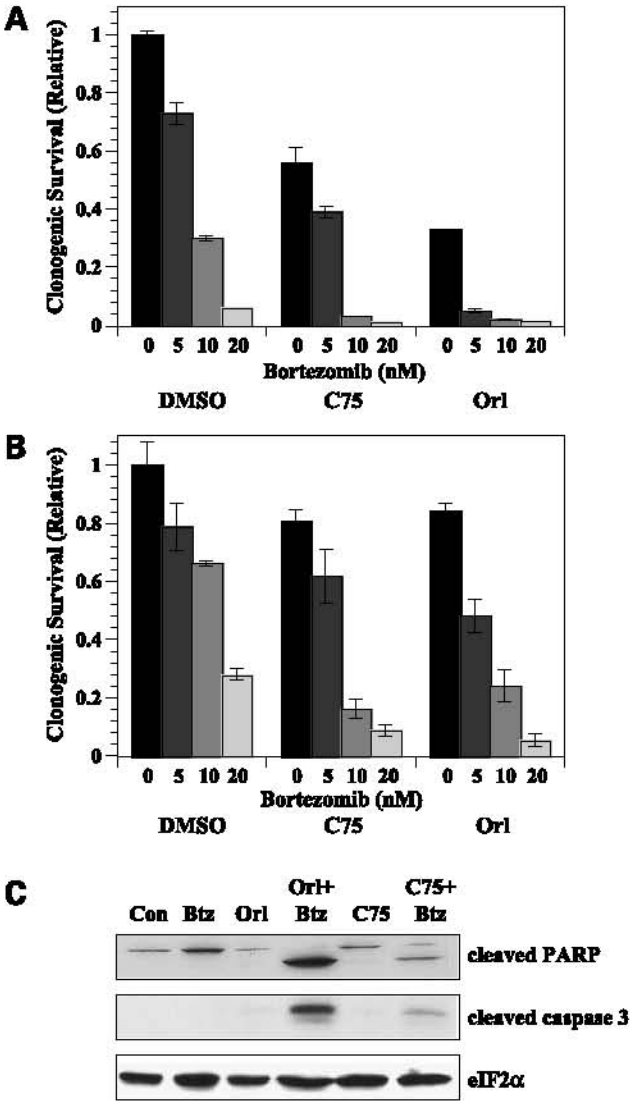

Figure 1. FASN inhibitors combine with bortezomib to increase cell death. Clonogenic survival assays were done on PC-3 (**A**) and DU145 (**B**) cells. Cells were treated with the indicated concentrations of bortezomib in the presence of DMSO, C75 (10 μg/mL), or orlistat (25 μmol/L) for 16 h. Clonogenic survival was determined relative to vehicle-treated controls. Statistical significance was determined by two-tailed Student's *t* test of cells treated with the combination of FASN inhibitors and bortezomib compared with cells treated with FASN inhibitors alone ($P \leq 0.005$). **C**, PC-3 cells treated with bortezomib (5 nmol/L), orlistat (25 μmol/L), C75 (10 μg/mL), or the combination of FASN inhibitors and bortezomib for 18 h and collected for immunoblot analysis using antibodies specific for cleaved PARP, cleaved caspase 3, and total eIF2α. Images represent cropped immunoblots. Full-length scans available in Supplementary Fig. S1.[1]

[1] Supplementary material for this article is available at Molecular Cancer Therapeutics Online (http://mct.aacrjournals.org/).

shown). Clonogenic survival of PC-3 cells treated with orlistat and C75 was reduced by 60% and 30%, respectively ($P < 0.001$; Fig. 1A). In DU145 cells, survival was only reduced by ~20% with each inhibitor. When the FASN inhibitors were combined with bortezomib, clonogenic survival was strikingly diminished compared with cells treated with the single agents ($P \leq 0.005$; Fig. 1A and B). Although isobologram analyses were inconclusive, an analysis of the combination index suggests that combining FASN inhibitors with bortezomib results in synergism (31). Consistent with previous findings, suboptimal concentrations of orlistat and C75 did not result in cleavage of PARP or caspase-3. However, when FASN inhibitors were combined with bortezomib, significant levels of both cleaved PARP and cleaved caspase-3 were detected (Fig. 1C). Combined, the data showed that combining bortezomib and FASN inhibitors resulted in enhanced cell death.

Given the established links between the fatty acid synthesis and proteasome pathways, we asked whether inhibition of FASN would affect the function of the proteasome. PC-3 cells were treated with FASN inhibitors, bortezomib, or FASN inhibitors and bortezomib together followed by immunoblot analysis of ubiquitin-modified proteins. As expected, bortezomib induced accumulation of ubiquitin-modified proteins ($P \leq 0.05$; Fig. 2A and B). Interestingly, PC-3 cells treated with orlistat or C75 also induced a modest but significant accumulation of ubiquitin-modified proteins ($P \leq 0.01$). The cotreatment of FASN inhibitors with bortezomib also appeared to cause an additive accumulation of ubiquitin-modified proteins (Fig. 2A and B), further suggesting that FASN activity contributes to the functionality of the proteasomal pathway. Next, we asked whether bortezomib affected fatty acid synthesis. Bortezomib induced a dose-dependent increase in fatty acid synthesis in PC-3 cells and a modest but significant increase in DU145 cells ($P \leq 0.05$; Fig. 2C). On the other hand, bortezomib had no effect on fatty acid synthesis in FS-4 human fibroblasts. The increased fatty acid synthesis was not associated with increased FASN protein levels (Fig. 2D). Collectively, these data show crosstalk between the FASN and proteasome pathways.

Previous work showed that FASN inhibitors induce ER stress in tumor cells and others have shown that bortezomib induces ER stress (25, 28–30, 32). To characterize the role of the UPR in cells treated with the combination of

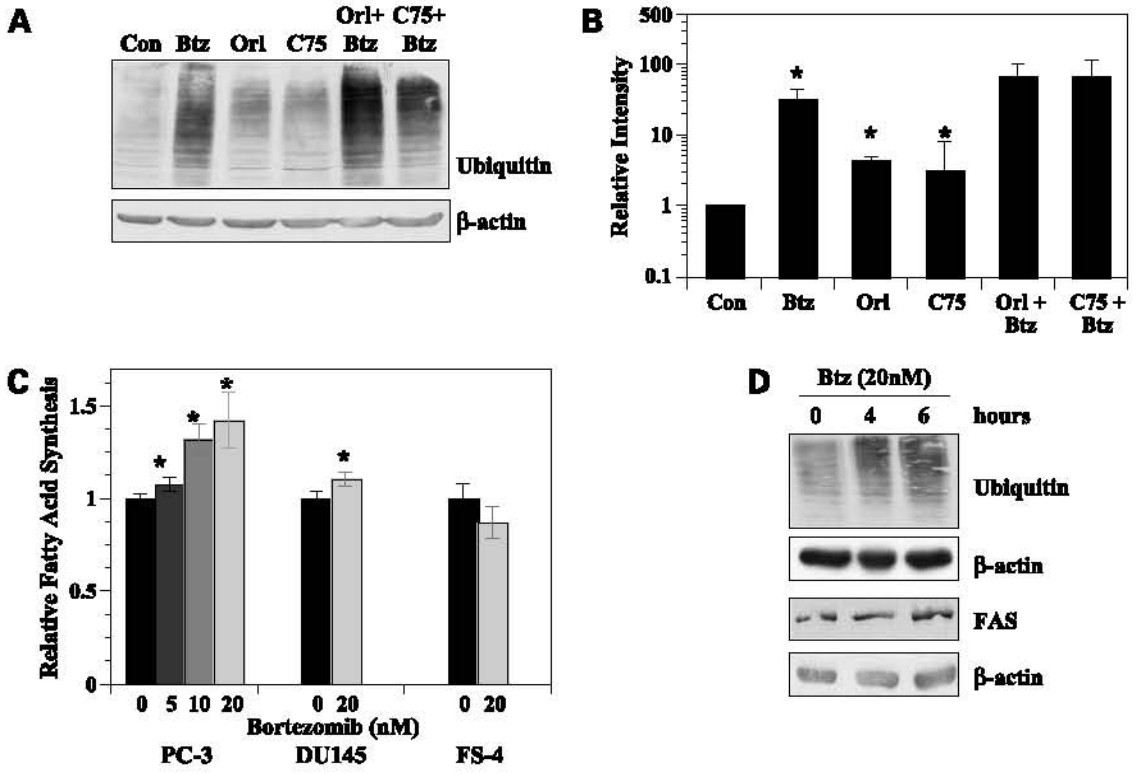

Figure 2. Fatty acid synthesis and proteasome pathways exhibit crosstalk. **A**, PC-3 cells were treated with vehicle, orlistat (25 μmol/L), bortezomib, (5 nmol/L), C75 (9 μg/mL), or the combination of bortezomib and orlistat or C75 for 16 h and subjected to immunoblot analysis with antibodies specific for ubiquitin and β-actin. **B**, three separate experiments of PC-3 cells treated as in **A** were quantified by measuring intensity of the exposure from ubiquitin antibody in each treatment as compared with vehicle-treated lanes using UN-SCAN-IT. *, $P \leq 0.05$, Student's t test. **C**, PC-3 cells, DU145 cells, and FS-4 fibroblasts were incubated with the indicated concentrations of bortezomib for 2 h followed by the addition of [^{14}C]acetate (1 μCi) for 2 h. Cells were collected and washed and lipids were extracted and quantified relative to vehicle-treated control as described in Materials and Methods. *, $P \leq 0.05$, Student's t test. **D**, PC-3 cells were treated with vehicle or bortezomib (20 nmol/L) for 4 or 6 h in duplicate. Cells were collected for immunoblot analysis using antibodies specific to FASN, ubiquitin, or β-actin. Images represent cropped immunoblots. Full-length scans available in Supplementary Fig. S2.

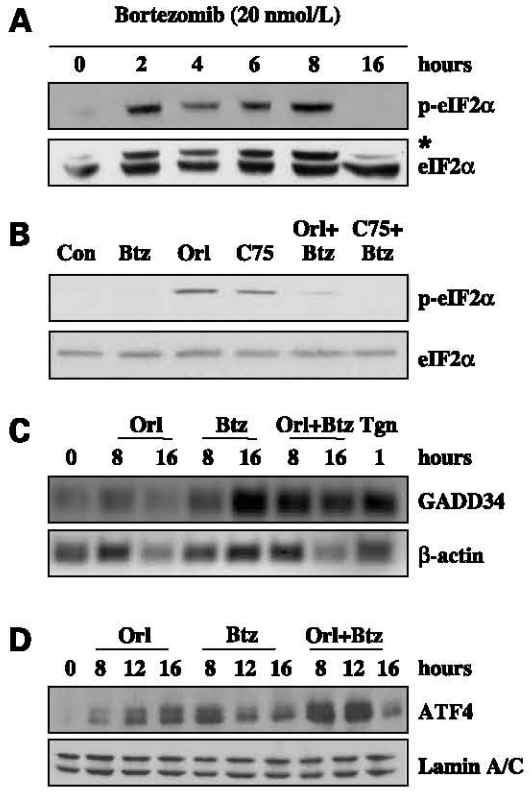

Figure 3. Bortezomib and FASN inhibitors combine to saturate the PERK arm of UPR adaptation signaling. **A,** PC-3 cells were treated with vehicle (DMSO) or 20 nmol/L bortezomib for the indicated times. Samples were resolved by SDS-PAGE and transferred to polyvinylidene difluoride and the membrane was probed with antibodies specific for phospho-eIF2α and total eIF2α. **B,** PC-3 cells were treated with vehicle, bortezomib (5 nmol/L), orlistat (25 μmol/L), C75 (10 μg/mL), or the combination of bortezomib and orlistat or bortezomib and C75 for 16 h and samples were subjected to immunoblot analysis and probed with antibodies specific for phospho-eIF2α and total eIF2α. *Asterisk,* higher molecular weight nonspecific band. **C,** PC-3 cells were treated with vehicle, orlistat (25 μmol/L), bortezomib (20 nmol/L), or the combination of bortezomib and orlistat for the indicated times. Total RNA was collected and semiquantitative reverse transcription-PCR was done using primers specific for GADD34 and β-actin. **D,** PC-3 cells were treated with vehicle, orlistat (25 μmol/L), bortezomib (5 nmol/L), or the combination of bortezomib and orlistat. Nuclear fractions were isolated and prepared for immunoblot analysis and probed with antibodies specific for ATF4 and lamin A/C. Images represent cropped immunoblots. Full-length scans available in Supplementary Fig. S3.

FASN inhibitors and bortezomib, we first examined the phosphorylation status of eIF2α. Bortezomib induced a rapid and transient phosphorylation of eIF2α that diminished by 16 h (Fig. 3A). Consistent with previous findings, phosphorylation of eIF2α was sustained through 16 h in cells treated with FASN inhibitor (25). Disrupting the crosstalk between the proteasome and FASN resulted in non-phospho-eIF2α at 16 h, consistent with the lack of phospho-eIF2α with bortezomib alone at the same time point (Fig. 3B).

In the UPR signaling cascade, growth arrest and DNA damage-inducible protein 34 (GADD34) is induced, mediating dephosphorylation of eIF2α to restore bulk translation (33, 34). To test whether single and combined agents induce *GADD34* expression over the course of 16 h, semiquantitative reverse transcription-PCR was done with oligonucleotides specific for *GADD34*. PC-3 cells treated with orlistat showed slight *GADD34* mRNA at 8 and 16 h compared with vehicle-treated controls (Fig. 3C). Consistent with the time course of eIF2α phosphorylation in bortezomib-treated cells, *GADD34* mRNA expression was minimal at 8 h followed by robust expression at 16 h (Fig. 3C). Inhibiting crosstalk between pathways induced *GADD34* mRNA expression by 8 h to a level higher than seen with bortezomib or orlistat alone that was maintained through 16 h, correlating with the lack of phospho-eIF2α at the same time point (Fig. 3C). Together, these data showed that interrupting crosstalk between the proteasome and FASN resulted in acceleration of the eIF2α-GADD34 feedback loop indicative of increased UPR signaling and suggested that proteotoxicity may contribute to cell death.

Phosphorylation of eIF2α is a primary event in UPR signaling that activates downstream signals including the prosurvival ATF4 (35, 36). Therefore, we tested whether interrupting crosstalk between proteasome and fatty acid synthesis pathways would increase ATF4 expression. Orlistat induced early expression of ATF4 at 8 h that was sustained through the 16 h time point (Fig. 3D), consistent with robust phosphorylation of eIF2α (Fig. 3B) and low levels of *GADD34* (Fig. 3C) in orlistat-treated cells. Bortezomib treatment induced expression of nuclear ATF4 by 8 h, which decreased at 12 and 16 h, consistent with phospho-eIF2α status and *GADD34* expression (Fig. 3). Interfering with the FASN-proteasome crosstalk induced ATF4 expression that was more robust than orlistat- or bortezomib-treated cells at 8 h but decreased by the 16 h time point (Fig. 3D). Correspondingly, *GADD34* levels were high and phospho-eIF2α levels were low at 16 h in combination-treated cells (Fig. 3C). Together, the time courses of eIF2α phosphorylation, *GADD34*, and ATF4 expression indicated that adaptation signals of the PERK arm of the UPR pathway was not only active in cells treated with FASN inhibitors and bortezomib but was saturated when both pathways were inhibited.

We next examined the IRE1-mediated processing of XBP-1 in cells treated with orlistat, bortezomib, or both. Suboptimal concentrations of orlistat and bortezomib induced moderate splicing of XBP-1 mRNA by 8 h (Fig. 4A). Treating cells with both agents caused an earlier and more robust processing of XBP-1 that was complete by 16 h (Fig. 4A). Correspondingly, at these times and concentrations, accumulation of the XBP-1(s) transcription factor only occurred in cells treated with both FASN inhibitor and bortezomib (Fig. 4B and C). Therefore, interfering with FASN and the proteasome simultaneously enhanced the adaptation response through IRE1-mediated processing of XBP-1 in prostate tumor cells.

We next asked whether IRE1-activated signals characteristic of the alarm arm of the UPR pathway were upregulated in cells in which we inhibited fatty acid

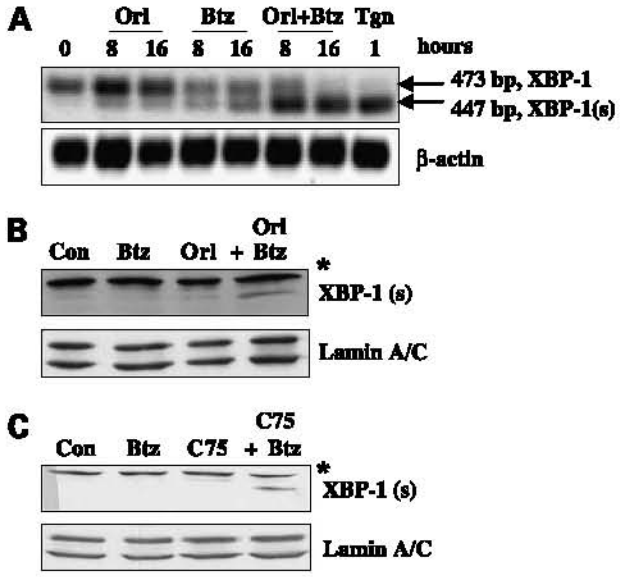

Figure 4. Combining bortezomib with FASN inhibitors enhances IRE1-mediated XBP-1 mRNA processing. **A**, PC-3 cells were treated with vehicle, orlistat (25 μmol/L), bortezomib (5 nmol/L), or the combination of bortezomib and orlistat. Total RNA was collected with TRIzol and reverse transcription-PCR was done with oligonucleotides specific for XBP-1 and β-actin. XBP-1(us) is indicated by the 473 bp product and XBP-1(s) is indicated by the 447 bp fragment. PC-3 cells were treated for 1 h with thapsigargin (1 μmol/L) as a positive control. **B**, PC-3 cells were treated with vehicle, orlistat (25 μmol/L), bortezomib (5 nmol/L), or the combination of bortezomib and orlistat. Nuclear lysates were collected as described in Materials and Methods for immunoblot analysis with antibodies specific for XBP-1 and lamin A/C. Immunoblot indicates the 55 kDa XBP-1(s) protein. *Asterisk,* higher molecular weight nonspecific band. **C**, PC-3 cells were treated with vehicle, bortezomib (5 nmol/L), C75 (9 μg/mL), or the combination of bortezomib and C75. *Asterisk,* higher molecular weight nonspecific band. Images represent cropped immunoblots. Full-length scans available in Supplementary Fig. S4.

synthesis-proteasome crosstalk. The phosphorylation status of JNK was examined by immunoblot (Fig. 5A). Orlistat did not induce JNK phosphorylation, and bortezomib treatment induced only minimal JNK activation at 16 h (Fig. 5A). Treating cells with both agents in combination, though, induced JNK phosphorylation within 4 h that increased through 16 h. Similar results were observed in DU145 cells (data not shown). The CHOP transcription factor can be induced by JNK activation (37, 38). Orlistat only induced moderate CHOP expression at 16 h (Fig. 5B). Similarly, at 12 h, bortezomib induced minimal CHOP expression that slightly increased by 16 h (Fig. 5B). On the other hand, combined inhibition of FASN and the proteasome pathways induced an earlier and more robust CHOP expression (Fig. 5B). A JNK inhibitor was used to verify the role of JNK in mediating CHOP expression. Pharmacologic inhibition of JNK blocked the phosphorylation of JNK and c-Jun (Fig. 6A). More importantly, inhibition of JNK also reduced CHOP expression and cleavage of caspase-3 and PARP (Fig. 6A). Consistent with these findings, trypan blue exclusion assays also showed that JNK inhibition protected cells from cell death induced by the combination of orlistat and bortezomib ($P < 0.01$; Fig. 6B).

We next tested whether CHOP is an effector of JNK signaling that regulates cell death in this scenario. PC-3 cells were transfected with control or *CHOP*-targeted siRNA, and after 48 h, the cells were treated with vehicle, orlistat, or the orlistat-bortezomib combination. The siRNA-mediated knockdown of *CHOP* had no effect on orlistat- or bortezomib-induced cell death (not shown). However, siRNA-mediated knockdown of *CHOP* expression protected cells from the effects of the orlistat-bortezomib combination ($P < 0.01$; Fig. 6C) at a level that was proportional with the reduction in CHOP levels (Fig. 6D). Therefore, it appears that the JNK-CHOP axis is an important mediator of cell death in cells where the UPR is saturated. Collectively, these data show that blocking crosstalk between FASN and the proteasome shifts UPR balance from adaptation phase to the alarm phase, resulting in increased cell death via JNK-mediated CHOP expression.

Discussion

We have shown previously that inhibiting FASN induces ER stress and UPR signaling before cell death occurs and hypothesize that cell death induced by FASN inhibition is dependent on UPR activation (25). The data herein reveal a functional nexus between FASN and the proteasome. The connection of each of these pathways with ER homeostasis provides a unique therapeutic opportunity. Indeed, when inhibitors of both the proteasome and FASN pathways are combined, increased cell death occurs through the IRE1-JNK-CHOP arm of the UPR pathway.

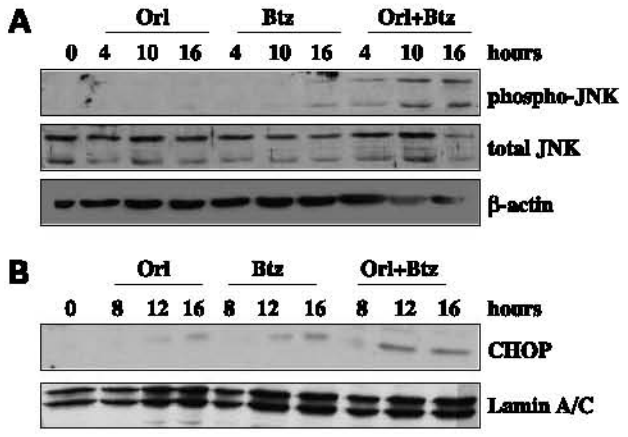

Figure 5. Combining bortezomib and FASN inhibitors induces JNK activation and CHOP expression. **A**, PC-3 cells were treated with vehicle, orlistat (25 μmol/L), bortezomib (20 nmol/L), or the combination of bortezomib and orlistat for the indicated times. Whole-cell lysates were collected for immunoblot analysis of phospho-JNK, total JNK, and β-actin. **B**, PC-3 cells were treated with vehicle, orlistat (25 μmol/L), bortezomib (20 nmol/L), or the combination of bortezomib and orlistat for the indicated times. Nuclear lysates were collected as described in Materials and Methods for immunoblot analysis with antibodies specific for CHOP and lamin A/C. Images represent cropped immunoblots. Full-length scans available in Supplementary Fig. S5.

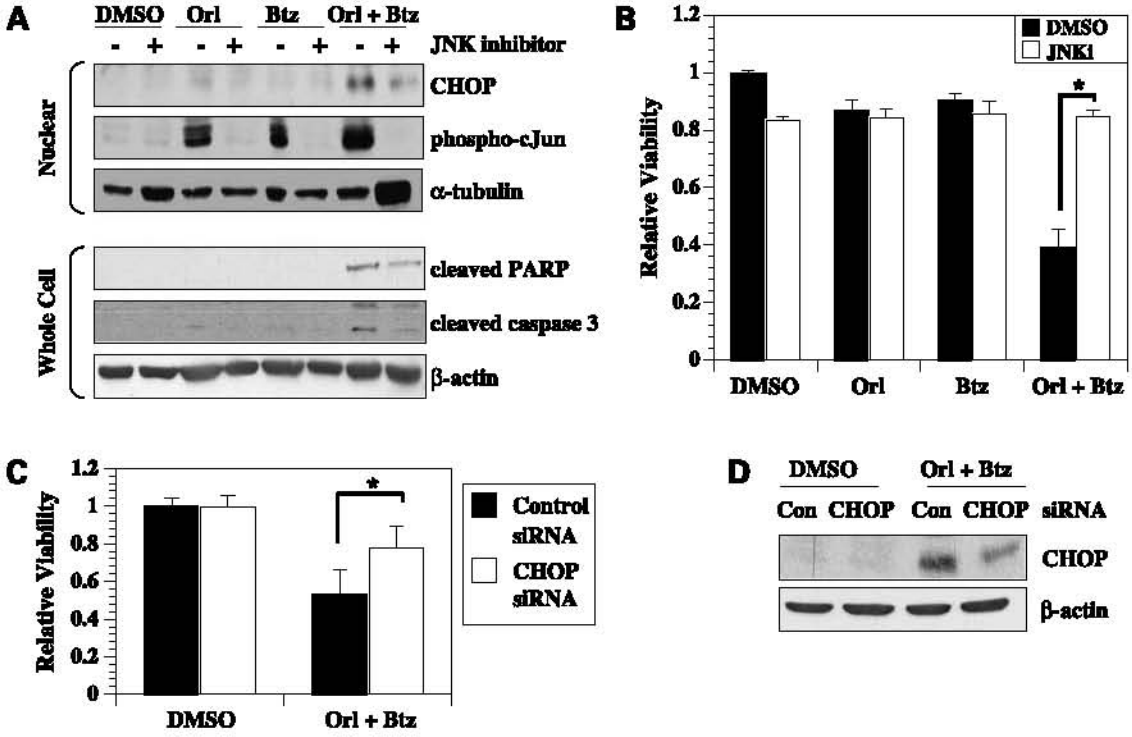

Figure 6. UPR-associated cell death is mediated by JNK activation and CHOP. **A**, PC-3 cells were treated with vehicle, orlistat (50 μmol/L), bortezomib (20 nmol/L), or the combination of bortezomib and orlistat with and without JNK inhibitor (*JNKi*; 20 nmol/L). Nuclear lysates were collected as described in Materials and Methods for immunoblot analysis with antibodies specific for CHOP, phospho-c-Jun, and α-tubulin. Whole-cell lysates were analyzed with antibodies specific for cleaved PARP, cleaved caspase 3, and β-actin. **B**, PC-3 cells were treated with vehicle, orlistat (50 μmol/L), bortezomib (20 nmol/L), or the combination of bortezomib and orlistat with and without JNK inhibitor (20 nmol/L). Cells were collected and counted using a trypan blue exclusion assay and the ratio of viable cells was calculated relative to vehicle-treated cells. *, $P < 0.01$, Student's t test. **C**, PC-3 cells were transfected with a SMARTpool siRNA against CHOP or a control siRNA. After 48 h, cells were treated with vehicle or the combination of bortezomib (20 nmol/L) and orlistat (50 μmol/L) for 18 h. Cells were then collected and counted using trypan blue exclusion and the ratios of viable cells relative to vehicle-treated controls were calculated from three independent experiments. Statistical significance between CHOP siRNA and control siRNA cells treated with orlistat and bortezomib was determined by two-tailed Student's t test ($P < 0.01$). **D**, cells from **C** were analyzed by immunoblot with antibodies specific for CHOP and β-actin. Images represent cropped immunoblots. Full-length scans available in Supplementary Fig. S6.

Accumulating evidence links the proteasome and FASN pathways (21, 23, 24). The data herein suggest that the integrity of the proteasome pathway relies, at least in part, on functional fatty acid synthesis, as FASN inhibitors cause the accumulation of ubiquinated proteins through an undetermined mechanism (Fig. 2). It is possible that either the proteasome overall or a component of the proteasome pathway relies on the fatty acid synthesis pathway for proper function. Interestingly, the ER stressor tunicamycin can also induce the accumulation of ubiquitin-modified proteins and enhances the stability of E3 ligases gp78 and Hrd1 (39). Therefore, it is likely that the proper functioning of proteasome-mediated ER-associated degradation pathway is dependent on global ER function.

Perhaps more interesting is that inhibiting the proteasome alone can increase fatty acid synthesis (Fig. 2C). As the increased activity does not correlate with increased FASN protein levels, the data suggest a mechanism independent of SREBP-1 or FASN protein stabilization as others have shown previously (21, 22). Induction of fatty acid synthesis by bortezomib could be due to several possibilities. Inhibition of the proteasome could affect turnover of a protein that modifies FASN or acetyl-CoA carboxylase. Because of the short time of treatment with bortezomib required to detect the increase of lipogenesis, a previously unidentified post-translational modification may occur to increase activity of either FASN or acetyl-CoA carboxylase. Alternatively, there could be increased incorporation of fatty acid into phospholipid. Previous studies have shown that XBP-1(s) can increase phosphatidylcholine synthesis (40). However, significant splicing of XBP-1 was not observed within the same period in which fatty acid synthesis increased (Fig. 4). Therefore, it is unlikely that XBP-1(s) induces phospholipid synthesis in response to bortezomib treatment. Regardless, the crosstalk between FASN and proteasome pathways is the basis for amplification of UPR signaling and increased cell death when inhibitors of these pathways are combined. Increased UPR signaling in this scenario, particularly that of the alarm arm, supports a growing body of literature describing the ability for the UPR to induce cell death after adaptation signals have been saturated or are ineffective (41–43).

The activation of adaptation and stress signals is critical to the cellular balance between survival and cell death. PERK-dependent phosphorylation of eIF2α can act as a rheostat to fine-tune signals that balance survival and death in a cell experiencing ER stress (44). If a cell is unable to sustain balanced levels of phospho-eIF2α, the cell dies due to proteotoxicity. If the cell has levels of phospho-eIF2α that are too high, the cell cannot translate enough protein to adapt and survive. Compared with the combination of FASN inhibitors with bortezomib and bortezomib alone, FASN inhibitors take the longest amount of time to induce cell death. Correspondingly, FASN inhibitors result in sustained phospho-eIF2α, therefore more cellular protection (Fig. 3). Simultaneous inhibition of the proteasome and fatty acid synthesis pathways induces early and robust GADD34 expression to mediate the dephosphorylation of eIF2α (Fig. 3). Coincidentally, the combined treatment quickly induces cell death perhaps by proteotoxicity associated with decreased eIF2α phosphorylation.

The IRE1 arm of the UPR is another signaling pathway designed to mediate adaptation and alarm signals (41, 43, 45). IRE1 splices XBP-1 mRNA that is then translated to a stable ER stress-specific transcription factor that up-regulates ER chaperones and other adaptation genes (46, 47). We show that FASN inhibitors and bortezomib both induce splicing of XBP-1 but that the combined treatment results in the accumulation of the XBP-1 transcription factor (Fig. 4A-C). Therefore, blockade of FASN-proteasome crosstalk enhances adaptation signaling through the IRE1 arm of the UPR. Inhibiting both pathways also shifts the balance from adaptation to stress signaling downstream of IRE1. Activated IRE1 can also interact with tumor necrosis factor receptor adaptor factor 2 to activate JNK and corresponding alarm signals, including expression of the ER stress proapoptotic protein CHOP (38, 48). Indeed, the combined treatment results in robust activation of JNK as well as enhanced accumulation of CHOP, thereby confirming the hypothesis that increased ER stress shifts the UPR program to cell death. Consistent with other studies, the data presented here indicate that CHOP mediates cell death when FASN-proteasome crosstalk is interrupted (Fig. 6; ref. 49). That JNK and CHOP mediate death in this system is consistent with the notion that IRE1 guides cell fate in response to ER stress (43).

Altogether, the data indicate that rapid and robust UPR activation occurs when FASN and the proteasome are inhibited simultaneously. Although the connection between the proteasome and the ER-associated degradation pathway has been established, the mechanism by which FASN mediates proteasome function remains to be determined. It will be important for future studies to determine the precise connections between these two important tumor support systems. Significant interest and opportunity lies in exploiting the UPR with therapeutic agents to augment tumor cell death. Collectively, these data provide insight into how FASN and the proteasome can be targeted to shift UPR balance from adaptation to stress signaling to affect increased tumor cell death.

Disclosure of Potential Conflicts of Interest

No potential conflicts of interest were disclosed.

References

1. Jayakumar A, Tai MH, Huang WY, et al. Human fatty acid synthase: properties and molecular cloning. Proc Natl Acad Sci U S A 1995;92:8695–9.

2. Wakil SJ, Stoops JK, Joshi VC. Fatty acid synthesis and its regulation. Annu Rev Biochem 1983;52:537–79.

3. Kridel SJ, Lowther WT, Pemble CWt. Fatty acid synthase inhibitors: new directions for oncology. Expert Opin Investig Drugs 2007;16:1817–29.

4. Kuhajda FP. Fatty-acid synthase and human cancer: new perspectives on its role in tumor biology. Nutrition 2000;16:202–8.

5. Kuhajda FP. Fatty acid synthase and cancer: new application of an old pathway. Cancer Res 2006;66:5977–80.

6. Funabashi H, Kawaguchi A, Tomoda H, et al. Binding site of cerulenin in fatty acid synthetase. J Biochem (Tokyo) 1989;105:751–5.

7. Kuhajda FP, Pizer ES, Li JN, et al. Synthesis and antitumor activity of an inhibitor of fatty acid synthase. Proc Natl Acad Sci U S A 2000;97:3450–4.

8. Kridel SJ, Axelrod F, Rozenkrantz N, Smith JW. Orlistat is a novel inhibitor of fatty acid synthase with antitumor activity. Cancer Res 2004;64:2070–5.

9. Alli PM, Pinn ML, Jaffee EM, McFadden JM, Kuhajda FP. Fatty acid synthase inhibitors are chemopreventive for mammary cancer in neu-N transgenic mice. Oncogene 2005;24:39–46.

10. Zhou W, Han WF, Landree LE, et al. Fatty acid synthase inhibition activates AMP-activated protein kinase in SKOV3 human ovarian cancer cells. Cancer Res 2007;67:2964–71.

11. Wang HQ, Altomare DA, Skele KL, et al. Positive feedback regulation between AKT activation and fatty acid synthase expression in ovarian carcinoma cells. Oncogene 2005;24:3574–82.

12. Liu X, Shi Y, Giranda VL, Luo Y. Inhibition of the phosphatidylinositol 3-kinase/Akt pathway sensitizes MDA-MB468 human breast cancer cells to cerulenin-induced apoptosis. Mol Cancer Ther 2006;5:494–501.

13. Van de Sande T, De Schrijver E, Heyns W, Verhoeven G, Swinnen JV. Role of the phosphatidylinositol 3′-kinase/PTEN/Akt kinase pathway in the overexpression of fatty acid synthase in LNCaP prostate cancer cells. Cancer Res 2002;62:642–6.

14. Bandyopadhyay S, Pai SK, Watabe M, et al. FAS expression inversely correlates with PTEN level in prostate cancer and a PI 3-kinase inhibitor synergizes with FAS siRNA to induce apoptosis. Oncogene 2005;24:5389–95.

15. Menendez JA, Vellon L, Mehmi I, et al. Inhibition of fatty acid synthase (FAS) suppresses HER2/neu (erbB-2) oncogene overexpression in cancer cells. Proc Natl Acad Sci U S A 2004;101:10715–20.

16. Menendez JA, Vellon L, Lupu R. Antitumoral actions of the anti-obesity drug orlistat (XenicalTM) in breast cancer cells: blockade of cell cycle progression, promotion of apoptotic cell death and PEA3-mediated transcriptional repression of Her2/neu (erbB-2) oncogene. Ann Oncol 2005;16:1253–67.

17. Menendez JA, Colomer R, Lupu R. Inhibition of tumor-associated fatty acid synthase activity enhances vinorelbine (Navelbine)-induced cytotoxicity and apoptotic cell death in human breast cancer cells. Oncol Rep 2004;12:411–22.

18. Menendez JA, Lupu R, Colomer R. Inhibition of tumor-associated fatty acid synthase hyperactivity induces synergistic chemosensitization of HER -2/neu-overexpressing human breast cancer cells to docetaxel (Taxotere). Breast Cancer Res Treat 2004;84:183–95.

19. Menendez JA, Vellon L, Colomer R, Lupu R. Pharmacological and small interference RNA-mediated inhibition of breast cancer-associated fatty acid synthase (oncogenic antigen-519) synergistically enhances Taxol (paclitaxel)-induced cytotoxicity. Int J Cancer 2005;115:19–35.

20. Liu H, Liu Y, Zhang J-T. A new mechanism of drug resistance in breast cancer cells: fatty acid synthase overexpression-mediated palmitate overproduction. Mol Cancer Ther 2008;7:263–70.

21. Graner E, Tang D, Rossi S, et al. The isopeptidase USP2a regulates the stability of fatty acid synthase in prostate cancer. Cancer Cell 2004;5:253–61.

22. Hirano Y, Yoshida M, Shimizu M, Sato R. Direct demonstration of rapid degradation of nuclear sterol regulatory element-binding proteins by the ubiquitin-proteasome pathway. J Biol Chem 2001;276:36431–7.

23. Knowles LM, Axelrod F, Browne CD, Smith JW. A fatty acid synthase blockade induces tumor cell-cycle arrest by down-regulating Skp2. J Biol Chem 2004;279:30540–5.

24. Knowles LM, Smith JW. Genome-wide changes accompanying knockdown of fatty acid synthase in breast cancer. BMC Genomics 2007;8:168–81.

25. Little JL, Wheeler FB, Fels DR, Koumenis C, Kridel SJ. Inhibition of fatty acid synthase induces endoplasmic reticulum stress in tumor cells. Cancer Res 2007;67:1262–9.

26. Alberts B, Johnson A, Lewis J, et al., editors. Molecular biology of the cell. 4th ed. New York: Garland Science; 2002.

27. Gardner RC, Assinder SJ, Christie G, et al. Characterization of peptidyl boronic acid inhibitors of mammalian 20S and 26S proteasomes and their inhibition of proteasomes in cultured cells. Biochem J 2000;346:447–54.

28. Obeng EA, Carlson LM, Gutman DM, et al. Proteasome inhibitors induce a terminal unfolded protein response in multiple myeloma cells. Blood 2006;107:4907–16.

29. Nawrocki ST, Carew JS, Pino MS, et al. Bortezomib sensitizes pancreatic cancer cells to endoplasmic reticulum stress-mediated apoptosis. Cancer Res 2005;65:11658–66.

30. Fribley A, Zeng Q, Wang C-Y. Proteasome inhibitor PS-341 induces apoptosis through induction of endoplasmic reticulum stress-reactive oxygen species in head and neck squamous cell carcinoma cells. Mol Cell Biol 2004;24:9695–704.

31. Chou T-C, Talalay P. Quantitative analysis of dose-effect relationships: the combined effects of multiple drugs or enzyme inhibitors. Adv Enzyme Regul 1984;22:27–55.

32. Kincaid MM, Cooper AA. ERADicate ER stress or die trying. Antioxid Redox Signal 2007;9:2373–87.

33. Novoa I, Zeng H, Harding HP, Ron D. Feedback inhibition of the unfolded protein response by GADD34-mediated dephosphorylation of eIF2α. J Cell Biol 2001;153:1011–22.

34. Ma Y, Hendershot LM. Delineation of a negative feedback regulatory loop that controls protein translation during endoplasmic reticulum stress. J Biol Chem 2003;278:34864–73.

35. Harding HP, Novoa I, Zhang Y, et al. Regulated translation initiation controls stress-induced gene expression in mammalian cells. Mol Cell 2000;6:1099–108.

36. Lu PD, Harding HP, Ron D. Translation reinitiation at alternative open reading frames regulates gene expression in an integrated stress response. J Cell Biol 2004;167:27–33.

37. Guyton KZ, Xu Q, Holbrook NJ. Induction of the mammalian stress response gene GADD153 by oxidative stress: role of AP-1 element. Biochem J 1996;314:547–54.

38. Urano F, Wang X, Bertolotti A, et al. Coupling of stress in the ER to activation of JNK protein kinases by transmembrane protein kinase IRE1. Science 2000;287:664–6.

39. Shen Y, Ballar P, Apostolou A, Doong H, Fang S. ER stress differentially regulates the stabilities of ERAD ubiquitin ligases and their substrates. Biochem Biophys Res Commun 2007;352:919–24.

40. Sriburi R, Bommiasamy H, Buldak GL, et al. Coordinate regulation of phospholipid biosynthesis and secretory pathway gene expression in XBP-1(S)-induced endoplasmic reticulum biogenesis. J Biol Chem 2007;282:7024–34.

41. Xu C, Bailly-Maitre B, Reed JC. Endoplasmic reticulum stress: cell life and death decisions. J Clin Invest 2005;115:2656–64.

42. Ma Y, Hendershot LM. The role of the unfolded protein response in tumour development: friend or foe? Nat Rev Cancer 2004;4:966–77.

43. Lin JH, Li H, Yasumura D, et al. IRE1 signaling affects cell fate during the unfolded protein response. Science 2007;318:944–9.

44. Novoa I, Zhang Y, Zeng H, et al. Stress-induced gene expression requires programmed recovery from translational repression. EMBO J 2003;22:1180–7.

45. Ron D, Walter P. Signal integration in the endoplasmic reticulum unfolded protein response. Nat Rev Mol Cell Biol 2007;8:519–29.

46. Calfon M, Zeng H, Urano F, et al. IRE1 couples endoplasmic reticulum load to secretory capacity by processing the XBP-1 mRNA. Nature 2002;415:92–6.

47. Lee A-H, Iwakoshi NN, Glimcher LH. XBP-1 regulates a subset of endoplasmic reticulum resident chaperone genes in the unfolded protein response. Mol Cell Biol 2003;23:7448–59.

48. Wang XZ, Harding HP, Zhang Y, et al. Cloning of mammalian Ire1 reveals diversity in the ER stress responses. EMBO J 1998;17:5708–17.

49. Zinszner H, Kuroda M, Wang X, et al. CHOP is implicated in programmed cell death in response to impaired function of the endoplasmic reticulum. Genes Dev 1998;12:982–95.